Immunomodulatory mechanisms in the pathogenesis of *Cryptococcus neoformans* infection

By
Alison Joan Eastman

A dissertation submitted in partial fulfillment
of the requirements for the degree of
Doctor of Philosophy
(Immunology)
in the University of Michigan
2016

Doctoral committee:

Associate Professor Michal A. Olszewski, CHAIR
Professor David M. Aronoff
Associate Professor Irina Grigorova
Associate Professor Yonqun He
Assistant Professor Ilona Kryczek
Professor Bethany Moore
Professor Theodore J. Standiford

DEDICATION

For my mother and grandmother, who were denied these opportunities.

And for my brother, who made me who I am— I finally win.

ACKNOWLEDGMENTS

This work would not be possible without the support, encouragement, and trust of my mentor, Dr. Michal Olszewski, the incredible guidance of Dr. Beth Moore, director of the Graduate Program in Immunology, and my committee. Zarinah Aquil, our program coordinator, has solved every administrative problem I've thrown at her, and more that I didn't even know existed: thank you. I would like to thank my husband, Clayton Wheeler, for his understanding, patience, and unwavering support, and the incredible friends and colleagues here at Michigan and abroad for celebrating or commiserating whenever the occasion arose. For technical assistance at the Ann Arbor VA, I would like to acknowledge Nicole Potchen and Jacob Carolan, my two extremely intelligent and motivated undergraduate mentees, and the lab manager and student researchers of the Olszewski lab, who make it possible for us to collect so much data from each single mouse: Antoni Malachowski, Jeremy Dayrit, Guolei Zhao, Ana Pamela Torres Ocampo, Miekyn Cotton, Kanav Gupta, Zachary Hadd, Enze Xing, Daphne Cheng, Jay Akolkar, and Eric Cho. For experimental guidance, I would like to acknowledge Drs. Lori Neal, Yafeng Qiu, Michael Davis, Benjamin Murdock, Karen Cavassani, Aaron denDekker, Matthew Schaller, Seagal Teitz-Tennenbaum, Gary Huffnagle, and Nick Lukacs. Finally, I would like to thank the research community at the University of Michigan for the honor of conducting my thesis work in such a supportive and collaborative environment.

TABLE OF CONTENTS

LIST OF FIGURES

LIST OF TABLES

Chapter 1 Introduction[1]

Foreword

The central role of dendritic cells (DCs) in the generation of antifungal immunity is increasingly appreciated in fungal immunology, and infections caused by the pathogenic yeast *Cryptococcus* is no exception. The interplay between innate immunity that initially detects the pathogen and adaptive immunity that is essential to combat the infection hinges on DCs (1-7). The function of DCs as antigen presenting cells is to 1) gather antigens; 2) discriminate between danger and non-danger; 3) process the antigen for presentation, and 4) to prime T-cell responses that are specific to the genre of the original danger signal (i.e. virus, fungi, tissue damage, etc.) (Reviewed in (8)). In addition to initiation of adaptive immunity, there is increasing evidence of a role for DCs in the effector responses in the infected tissues, by both continued restimulation of the effector T cells as well as the direct effector functions: phagocytosis and intracellular killing of fungal pathogens (9-11).

In this introduction, we first provide a brief overview of *Cryptococcus neoformans,* the related species *Cryptococcus gattii,* and the generation of protective immunity

---

[1] Excerpts of this chapter taken from:

Eastman AJ, Osterholzer JJ, Olszewski MA. Role of dendritic cell-pathogen interactions in the immune response to pulmonary cryptococcal infection. Future Microbiol. 2015;10(11):1837-57. doi: 10.2217/fmb.15.92. PubMed PMID: 26597428.

to cryptococcosis. We then systematically identify critical evidence demonstrating that dendritic cells (DCs) are the architects of anticryptococcal immunity, from their initial testing and surveying of the local micro-environment, to their capacity to initiate naive T cell responses within regional lymph nodes, and lastly, to the ability of recruited DC to orchestrate effective adaptive immunity directly within infected tissues. In parallel, we will highlight cryptococcal virulence factors and alterations in the host cytokine milieu that can modulate DC responses and impair host defenses.

Pathogens and epidemiology

Two related cryptococcal species, *Cryptococcus neoformans* (*C.neo*) and *Cryptococcus gattii* (*C. gattii*) are etiological agents of cryptococcosis in humans and animals: an invasive mycosis capable of disseminating to the central nervous system (CNS) with oftentimes-lethal effects. The global burden of cryptococcal infections is substantial; one million new cases are diagnosed each year associated with a staggering mortality rate of over 60% despite antifungal therapy (12). Inhalation of desiccated yeast cells or spores from various environmental sources is thought to be the major gateway for cryptococcal infections (13, 14). The fungi propagate within the host as encapsulated budding yeasts (15, 16). Protective immunity against these highly adaptable opportunistic pathogens requires the successful interplay between intact innate and adaptive immune responses. Thus, patients with impaired T-cell defenses such as those with AIDS (17) and transplant recipients (18) are especially susceptible.

Although most infected patients have a clearly identifiable immunocompromising condition, in the United States, up to 25% of

cryptococcosis cases occur in patients without any previously identified immunodeficiency (19). Some of these infections are caused by *C. gattii* (20-22), whereas others result from a previously unrecognized cause of immunosuppression, as illustrated by recent studies identifying the presence of high titers of anti-granulocyte macrophage colony stimulating factor (GM-CSF) autoantibodies in the serum and CNS in a subset of infected patients (23-25) (reviewed in (26)). The rapidly expanding development and use of newer immune modulating agents may also increase susceptibility to cryptococcal infections, as best illustrated by the increased incidence of infection in patients treated with anti-TNFα antibody therapy (27-31). The identification of these new risk factors for primary infection, increasing concerns about recurrent or latent disease (32-35), and the limited efficacy of current antifungal therapies, motivate new studies focused on protective immunity to cryptococci and mechanisms of cryptococcal persistence in the host. A major goal of these investigations is to translate these findings into therapeutic strategies that augment host immunity while minimizing damage associated with non-protective immune responses.

The first key: an overview of host defenses against *C. neoformans*

The immune response to cryptococci may be divided into two phases: the afferent phase where the immune system begins to activate, and the efferent phase where cells are recruited to the lung to combat the infection. The afferent phase occurs early during cryptococcosis (i.e. the initial interactions between *C.neo* and resident innate immune cells) and is characterized by a subset of cells, primarily DC, trafficking to lymphoid organs to sensitize antigen-specific lymphocytes. Resident lung macrophages and DCs initiate this immune response

by recognizing and ingesting the yeasts (36). The fungus is able to grow within and damage the phagolysosome of macrophages (37), while DCs are better able to both phagocytose and kill *C.neo* (10, 11, 38). Antigen processing occurs in the DCs as *C.neo* enters the endosomal/lysosomal pathway (10, 38, 39), which coincides with the beginning of DC activation/maturation. Activated DCs upregulate MHC class II (MHCII), costimulatory molecules (CD40, CD80, and/or CD86), and chemokine receptor CCR7, responsible for homing of DC to the lung-draining lymph nodes. In these nodes DCs present *C.neo* antigen to T-cells, activate antigen specific T-helper subset promoting their expansion and initiating their polarization (40). Perturbations to the afferent phase response, mediated by macrophages and DC, may result in death of the host due to acute inflammation that damages the lung architecture (41).

The efferent phase occurs later during cryptococcosis and is characterized by the recruitment of additional non-resident cells, such as monocyte populations from the bone marrow and antigen-sensitized T cells from the node, while other lymphocytes and myeloid cells collectively execute adaptive immunity. In this phase, the lung-resident macrophages that initially phagocytosed and sequestered– but did not eliminate– the fungi await activation signals from antigen-sensitized T cells arriving from regional lymph nodes (38, 42). The T cell-derived activation signals for the phagocytes are critically dependent upon interactions between the newly arrived T cells and non-resident monocyte-derived $CD11b^{+}$ DC in the lung environment (43, 44). If these interactions yield robust Th1 and Th17 immune responses, then fungal burden reaches a peak within the first few weeks of infection and then begins to decline (9, 45). In

contrast, non-protective responses such as Th2 immunity, dysregulated immunity, or responses that develop in the absence of T cells result in persistently elevated pulmonary fungal burdens, progressive fungal expansion with dissemination to the spleen and CNS (3, 46-49). Severe impairments in the efferent responses, carried out by $CD4^+$ and $CD8^+$ T cells (50-53), result in uncontrolled pulmonary growth and dissemination leading to fatal meningoencephalitis in humans (17, 35, 54, 55) and mouse models (53, 56-59). DCs, as the bridge between innate and adaptive immunity (reviewed in (60)), are the lynchpin linking these afferent and efferent responses. The factors influencing the outcome of DC:T cell interactions will be further detailed in the following sections.

The second key: DCs in the context of murine models and human disease

Much of the information provided in the preceding overview of host defense was obtained using murine models of cryptococcal infection. In the more detailed information about DC phenotype and function to follow, it will be helpful to understand that different mouse models of cryptococcosis can be employed to mimic distinct clinical patterns observed in human patients. These can be modeled by selecting the appropriate strain of *Cryptococcus*, the magnitude of inoculum, or the route of infection. These strategies can also be combined with manipulations of host molecular or cellular components, including the genetic background of the mouse. For example, the highly pathogenic strain H99 is almost uniformly lethal in all mouse strains (reviewed in (61)); thus, manipulation of its virulence factors sheds light on the contributions of various microbial factors on host immunity (see below). Conversely, infection with less

virulent strains of *Cryptococcus* (JEC21, 52D) into resistant (CBA, BALB/c) or susceptible (C57BL/6) strains of mice facilitates investigations into the cellular and molecular mechanisms determining whether infections are cleared, persist in a contained state, or lethally progress.

Observations in human patients have directed murine modeling of cryptococcosis, which has identified T cells, and their associated cytokine responses, as important "downstream" determinants of adaptive immune responses against the organism. Both $CD4^+$ and $CD8^+$ T cells contribute to adaptive immunity, as studies in mice lacking either or both cytotoxic and helper T cells show significant impairment in anti-cryptococcal host defenses (51-53, 59, 62, 63). Mice with both T cell subsets, but deficient in components of the IFNγ or TLR9 signaling pathways, succumb to infection with a milder strain of *C.neo* earlier and/or at greater numbers than their wild type counterparts (64-68). These observations indicate that T cells alone are necessary but not sufficient to mount a protective immune response. Hallmarks of protective T-cell-mediated immunity to *C.neo* include: a) robust production of Th1 and Th17 cytokines, particularly, IFNγ, TNFα, and IL-17A; b) the presence of classically activated (M1) macrophages and DCs (DC1); and c) progressive clearance of infection and limited dissemination of the microbe (3, 45, 47, 48, 64, 66, 69-75). Conversely, non-protective immunity to *C.neo* infection in mice is identified by: a) increased Th2 cytokine production, particularly IL-10, IL-4, IL-5, and IL-13; b) the presence of alternatively activated macrophages (M2) with resultant YM-1/2 crystal deposition; c) eosinophilia and high serum IgE; and d) progressive growth of the microbe in the lungs followed by multi-organ dissemination (3, 32, 76-80). Non-

protective immune responses may result in either a progressive infection and lethal dissemination (17, 18, 55), or a low-level persistent lung infection where the microbe is contained but not cleared by the immune system and may re-activate upon loss of immune function (32-35). Thus, the importance of murine models in identifying these unique T cell mediated immunophenotypes led to many of the additional investigations (identified throughout this review) that have dissected and delineated the role of DC in orchestrating these responses.

This introduction incorporates data about DC from both human and murine studies. Similar to mice, human T cell responses to *C. neoformans*– rather than being uniformly polarized– are typically of mixed polarization (*i.e.* not completely Th1 or Th2 as is often observed in extreme polarization models developed in mice), and determined by the net balance between several potentially competing cytokine profiles. Broad studies of these cytokine profiles demonstrate that low levels of Th1 cytokines (IFN γ and TNF α) are associated with a poor outcome in patients with cryptococcosis (81, 82), consistent with findings using murine models (3, 45, 57, 64, 66, 73, 83-85). In addition, limited evidence suggests that infected patients displaying features of a strong Th2 bias also do poorly (86, 87). Whether DC are involved in skewing these T cell profiles in human patients is uncertain and not well studied. However, one recent study demonstrated that a particularly virulent strain of *C. gattii* that infects immunocompetent individuals will suppress the host DC's TNFα production (88) which may help explain in increased risk of cryptococcosis in patients receiving TNFα blocking monoclonal antibody therapy for autoimmune disorders (27-31). In addition, recent reports have identified autoantibodies

against GM-CSF, an important DC growth and differentiation factor, in a subset of patients with cryptococcosis who had not previously been identified as immunodeficient (23, 24). Collectively, the literature supports that murine models recapitulate many features of human host defenses against *C. neo*. This introduction will proceed to illustrate the integral role of DC in the immune responses against the organism.

The master key: subsets and nomenclature of dendritic cells

During infection, the composition of the host DC population changes dramatically as resident DC migrate to peripheral lymphoid organs and additional DCs, derived from recruited DC precursors, accumulate at the site of infection (see Table 1-1 and Figure 1-1). We refer to conventional DCs (cDCs) simply as DC, and the findings discussed do not represent plasmacytoid DC unless explicitly stated otherwise. Two separate subsets of DC residing in uninfected mouse lungs are identified and distinguished based on surface expression of CD103 and CD11b molecules: $CD103^+/CD11b^-$ DC and $CD103^-/CD11b^+$ DC (for all subsets described here, see Table 1-1 for the equivalent human DC subset markers). Both subsets express CD11c, MHCII, and feature low levels of autofluorescence by flow cytometry (89-91). These DC are distinct from resident alveolar macrophages, which are large, autofluorescent, $CD11c^+/CD11b^-$, $MHCII^{low}$ cells residing in alveolar spaces (44, 57, 90, 92-94).

Table 1. Summary of DC subsets in afferent and efferent immune responses to pulmonary cryptococcosis discussed in this review.				
Surface markers	**Common name**	**Equivalent human subset**	**Importance to *C.neo* immunity**	**Reference**
Lung-resident populations				
$CD11b^{+}/CD11c^{+}/CD103^{-}$	Conventional DCs	$CD1c^{+}$/Dectin1^{+}/Dectin2^{+}	Initial fungal containment and T-cell priming	Osterholzer 2009 I&I, Traynor 2002, Collin 2013
$CD11b^{-}/CD11c^{+}/CD103^{+}$	$CD103^{+}$DCs	$CD141^{+}/CLEC9A^{+}/SCR1^{+}$	Unclear	Osterholzer 2009 JI, Collin 2013
$CD11b^{-}/CD11c^{+}$/ autofluorescence^{hi}/ FSC^{hi}	Alveolar macrophages	$CD11c^{+}$/ autofluorescence^{hi}/ $CD206^{+}/SSC^{hi}/FSC^{hi}$	Initial fungal containment	Osterholzer 2009 I&I, Shao 2005, Mody 1991, Feldmesser 2000, Jambo 2014
Recruited populations				
$CD11b^{+}/CD11c^{+}/Ly6c^{hi}$/ autofluorescene^{lo}	Inflammatory DCs	$CD1c^{+}/CD16^{-}$	T-cell restimulation	Lin 2008, Collin 2013, Osterholzer 2011
$CD11b^{+}/CD11c^{+}/Ly6c^{hi}$/ autofluorescence^{hi}	Exudate macrophages	$CD14^{+}/CD16^{+/-}/CCR2^{+}$	Phagocytosis	Lin 2008, Osterholzer 2011, Kawakami 1999
$CD11b^{int}/CD11c^{int}$/TNF-α^{+}/ $iNOS^{+}$/autofluorescence^{lo}	Tip-DCs	$CD11c^{+}/CD206^{+}/CD14^{+/-}$/ $CD163^{+/-}CD209^{+/-}$	Unclear	Osterholzer 2009 JI, Serbina 2003, Boltjes 2014
Node populations				
$CD11b^{-}/CD11c^{int}/CD4^{+}/CD8^{-}$/ $Dec205^{-}$	$CD4^{+}/CD8^{-}$/ $Dec205^{-}$	$CD11c^{lo}/CD141^{+}$/ $CD11b^{-}/XCR1^{+}$	Unclear	Henri 2001, Shortman 2002
$CD11b^{-}/CD11c^{int}/CD4^{-}/CD8^{-}$/ $Dec205^{-}$	$CD4^{-}/CD8^{-}$/ $Dec205^{-}$		Unclear	Henri 2001, Shortman 2002
$CD11b^{-}/CD11c^{int}/CD4^{-}/CD8^{+}$/ $Dec205^{+}$	$CD4^{-}/CD8^{+}$/ $Dec205^{+}$	$CD11c^{lo}/CD141^{+}/CD11b^{-}$/ $XCR1^{+}$	Unclear	Henri 2001, Shortman 2002
Other populations				
$CD11b^{lo}/CD11c^{+}/CD8^{lo}$/ $Dec205^{lo}$	Langerhans DCs	$CD141^{+}/CLEC9A^{+}/XCR1^{+}$	Unclear	Bauman 2000, Collin 2013
$CD11b^{-}/CD11c^{+}/B220^{+}/Gr1^{+}$	Plasmacytoid DCs	$CD303^{+}/CD304^{+}/CD123^{+}$	Unclear	Bauman 2000, Hole 2014, Collin 2013

Table 1-1 Summary of DC subsets in afferent and efferent immune responses to pulmonary cryptococcosis.

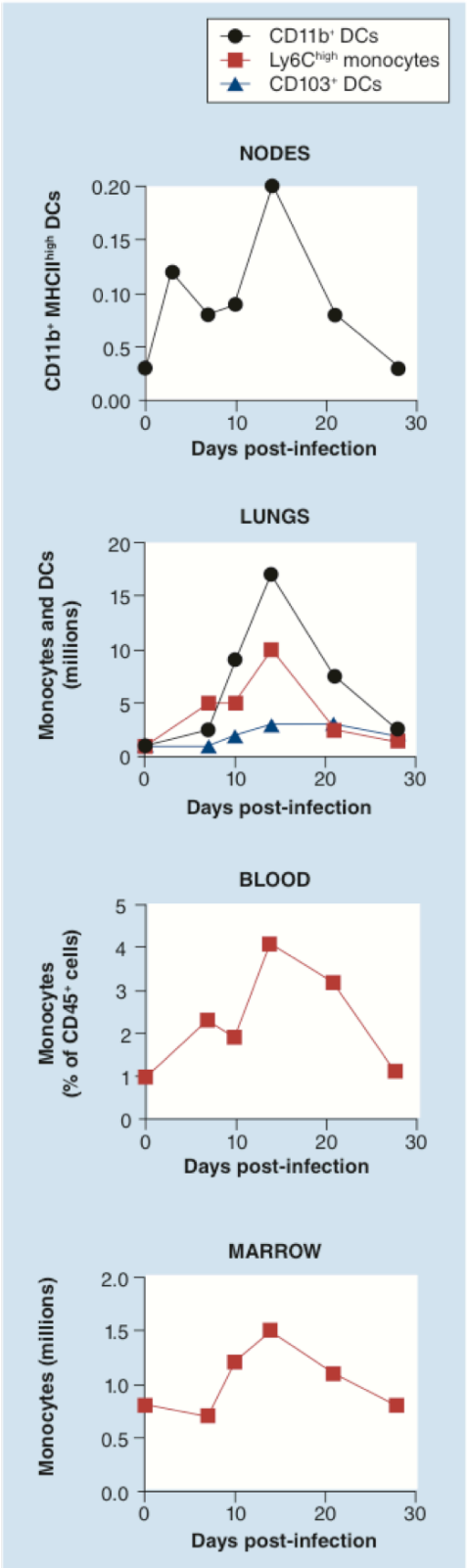

Figure 1-1 Mobilization and trafficking of myeloid cells in different compartments during cryptococcosis.

An increase in DC numbers in the regional thoracic lymph nodes 1 day post infection (dpi; top panel) suggests the immediate migration of resident DC from the lung. A second peak at 10 dpi coincides with a marked accumulation of Ly-6C^{high} monocytes and monocyte-derived CD11b^{+} DC in the lung (2nd panel), some of which may migrate to the node. The observed peak of Ly-6C^{high} monocytes in the lung (2nd panel) coincides with similar peaks in the blood (3rd panel) and bone marrow (4th panel) suggests inter-compartmental "communication" between lung, blood, and marrow to meet the need for additional lung DC in response to cryptococcal infection. Data were generated from published ((44) and (92)) and unpublished *in vivo* studies from the Osterholzer and Olszewski labs.

Cryptococcal infection triggers the rapid and substantial recruitment of Ly-6C^{high} CD11b^{+} inflammatory monocytes arriving from the bone marrow to subsequently differentiate into CD11b^{+} monocyte-derived DC and exudate macrophages (ExM). The latter two populations are CD11c^{+}, CD11b^{+}, and MHCII^{+} but ExM can be distinguished from the DC by their larger size, higher autofluorescence, and lower MHCII expression (44, 90, 92, 95). The differentiation of these CD11b^{+} DC from Ly-6C^{high} monocytes and their CCR2 dependent accumulation suggests these DC are related to and likely encompass a subset of TNFα-iNOS producing DCs (TIP-DCs) that have been shown to be important effector microbicidal cells in *Listeria monocytogenes* (96) and *Histoplasma capsulatum* infections (43, 44, 92, 97-100). Additional subsets of DCs found in the lymph nodes express distinct combinations of CD4, CD8, and the endocytic receptor Dec205; the CD4^{+}8^{-}DEC-205^{-}, the CD4^{-}8^{-}DEC-205^{-} and the CD4^{-}8^{+}DEC-205^{+} subsets are node resident DCs, and these can be distinguished from other DCs that have trafficked to the lymph node by expressing lower amounts of costimulatory molecules, lacking CD11b expression and lacking CCR7 expression (101, 102). Within the lymph node, Langerhans DCs may play a role, and are defined as DEC205^{low}/FSC^{high}/CD8α^{low}/CD11b^{low} (40, 91).

DCs as gatekeepers: pathogen recognition and DC activation

All fundamental DC functions during microbial infections, including cryptococcosis, are initiated with recognition of pathogens (Figure 1-2). This

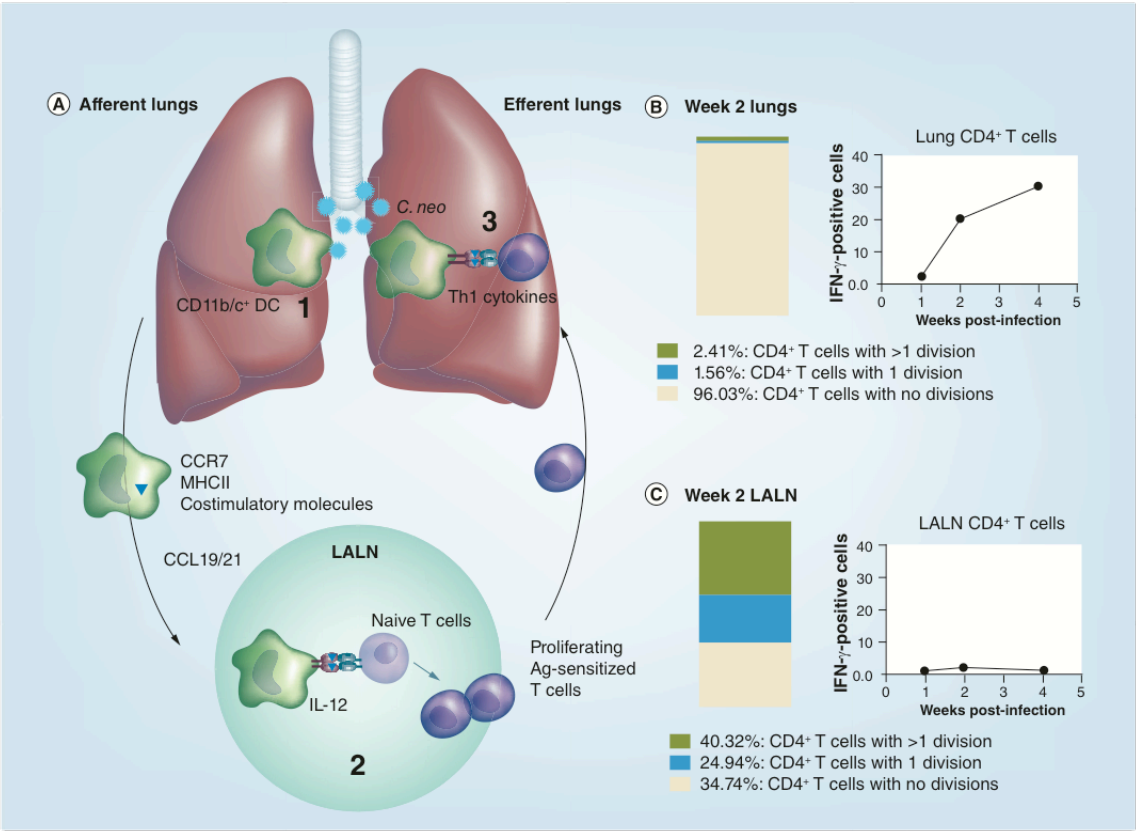

Figure 1-2 Key interactions of immune cells and *C.neo* during cryptococcal infection.

A) 1. DCs recognize and phagocytose *C.neo* in an infected lung and process the antigen, triggering DC maturation and migration to the lung-associated lymph nodes (LALN) through CCR7-CCL19/21 interactions (afferent phase immune response). 2. In the LALN, naïve T cells interact with mature DCs. DCs present antigen on MHCII, express costimulatory molecules (CD40/CD80/CD86), and secrete pro-Th1 cytokines such as IL-12. Cognate T cells become Ag-sensitized and proliferate. They do not yet produce cytokines. 3. Ag-sensitized T cells traffic to the lungs (efferent phase immune response), and they interact once again with DCs in the lung. They do not proliferate at this stage, but they do begin to secrete cytokines, directing the immune cells in the lungs. B) CD4+ T cells within the lungs do not proliferate, but do make cytokines such as IFNγ. C) CD4+ T cells within the LALN are actively proliferating, but do not upregulate cytokine production until they get to the lungs. (B) and (C) are adapted from Lindell *et al.* 2006.

occurs via a system of receptors defined as pattern recognition receptors (PRRs). PRRs are intra- and extracellular molecules designed to detect a matching set of microbial pathogen associated molecular patterns (PAMPS) or damage associated molecular patterns (DAMPS) released by injured tissues. The PRRs trigger signaling cascades that result in DC activation and subsequent interactions that orchestrate behavior of other cells of the immune system. Specifically, PRR signaling is crucial for: a) antigen uptake; b) discrimination between relevant and non-relevant antigens; c) processing of antigens for presentation; d) activation/maturation; and e) generation of signals for priming and execution of the adaptive immune response by DCs. Major types of PRRs of particular or emerging importance to cryptococcal infection are the Toll-like receptors (TLRs), Nod-like receptors (NLRs), scavenger receptors, C-type Lectin receptors (CLRs), and the functionally-related complement receptors (discussed in (103)). While these receptors are intimately tied to DC activation, microbes frequently employ counterstrategies to evade detection by these receptors or co-opt them to manipulate host responses.

PRRs: TLRs, NLRs, and dectins

TLRs are expressed on the cell surface and in endosomes or phagosomes that recognize various types of PAMPs. TLR2 and TLR4 are active during cryptococcal infection and bind cryptococcal polysaccharides with the help of CD14 and CD11/18 (104, 105). LPS, the canonical TLR4 ligand, can be found in the polysaccharide capsule of *C.neo*, likely due to the ubiquity of LPS and the stickiness of the capsule (reviewed in (106)). However, despite its involvement in the initial immune response, studies in TLR4-deficient mice show that it is

ultimately dispensable to anti-cryptococcal immunity (107, 108). Studies show that the necessity for TLR2 ranges from completely unnecessary (108), to slightly beneficial (107), to conferring an obvious survival advantage (109), which may be confounded by each study utilizing different cryptococcal strains (and thus inconsistent capsule thicknesses, which likely influences TLR2 stimulation), inoculum doses, and infection routes. In contrast, TLR9 is of great importance to the generation of protective immunity to *C.neo* (65, 67, 68, 110, 111). Defective immunity in response to *C.neo* in the absence of TLR9 can be attributed to failed DC activation and impaired myeloid cell recruitment from the bone marrow (65). Cryptococcal DNA is a critically important TLR9 ligand, as demonstrated by Nakamura *et al.* 2008 and Tanaka *et al.* 2012 (68, 112). CpG DNA, the canonical TLR9 ligand, is taken up by DCs and directed to the lysosome where it interacts with TLR9 (113). In side-by-side *in vitro* experiments, fluorescently-labeled CpG or cryptococcal DNA from acapsular mutants displayed similar trafficking patterns in bone marrow-derived DCs (BMDCs) via fluorescence microscopy, and elicited similar production of pro-inflammatory cytokines and surface expression of costimulatory molecules from BMDC (68). Similarly, MyD88, as the adaptor molecule for canonical signaling through TLRs 2, 4, and 9 (114-116) and also IL1R, is required for mounting effective immune responses against cryptococcal infection; MyD88 deficiency during cryptococcal infection induces equivalent defects as TLR9 deficiency (65, 67, 107, 109, 111). This response is characterized by diminished Th1 elements, elevated Th2 elements, and reduced numbers of $CD4^+$ and $CD8^+$ T cells in lungs, nodes, and spleen, and alternative activation of macrophages (67).

Little is published about NLRs during cryptococcal infection. Recent work from Cordero *et al.* shows that acapsular mutants of *C.neo* activate the NLRP3 inflammasome in peritoneal and bone-marrow derived macrophages, and NLRP3 activation resulted in decreased cryptococcal replication and escape from macrophages *in vitro* (117). Further investigations with other C.*neo* strains in mice, and more corresponding data from human studies, are needed to clarify the role of NLR and the downstream inflammasome activation in the generation of protective responses to *C. neo*.

Dectin-1, required for β-glucan recognition and immunity against *C. albicans* and *A. fumigatus*, is not required for anti-cryptococcal immune responses (118). Consistent with this finding, a recent study shows that Dectin-2 deficient mice have similar fungal burden as infected WT mice (119). However, infected Dectin-2-deficient mice display numerous Th2 hallmarks: increased IL-4, IL-5, and IL-13, increased mucin, lower TNFα and IL-12 production, and decreased costimulatory molecule expression (119). This phenotype is most often associated with impairments in cryptococcal clearance, yet none were observed in this study. Thus while dectin-2 signaling has clearly some effects on the phenotype of the immune response its net effect on fungal clearance appears to be neutral.

Scavenger and mannose receptors and immune modulation in cryptococcosis

Numerous scavenger receptors aid macrophages and DCs in priming protective immune responses to *C.neo*. Using an *in vitro* shRNA screen of mouse macrophages during cryptococcal stimulation, Means *et al.* demonstrated that the scavenger receptors CD36, SCARF1 and SCARB2 promote IL-1β generation and are protective during cryptococcal immune responses (120). Conversely, studies

using Scavenger Receptor A (SRA)-deficient mice demonstrated that SRA signaling contributed to non-protective immunity via decreased DC and $CD4^+$ T-cell accumulation, decreased DC1 polarization, and an increase in the hallmarks of non-protective immune responses including eosinophilia and IL-10 production (121). This suggests that *C.neo* exploits SRA to modulate the host response, promoting responses that favor survival and persistence of the microbe. The roles of other SR family members in the development of protective immunity to cryptococcal infection remain to be elucidated.

The mannose receptor (CD206) represents a double-edged sword for anti-cryptococcal immunity: it is necessary for the generation of protective immunity to *C.neo* (122), but its overexpression is also a hallmark of alternative activation in macrophages and DCs (reviewed in Gordon 2003 (123)), which contribute to non-protective immunity to *C.neo* (79). CD206 on the surface of macrophages and DCs binds cryptococcal mannoprotein (MP) on the cell wall of acapsular *C.neo* (10, 124); the addition of zymosan or glucan particles to macrophages in culture can bind competitively to CD206 and prevent uptake of *C.neo* (124). BMDCs derived from CD206-deficient mice did not stimulate robust T-cell expansion or activation (relative to WT mouse-derived BMDCs) (122). However, uptake of *C.neo* was unhindered in CD206-deficient BMDCs relative to WT BMDCs, suggesting that another phagocytic receptor may be compensating for the loss of CD206 in *C.neo* uptake (122). Stimulation of macrophages and BMDCs through CD206 induced TNFα mRNA and protein production (10, 124), but in other models, it inhibits IL-12 production and promotes IL-10 production (125, 126). Thus the effects of CD206 signaling appear complex and it is possible that high

CD206 expression, linked with alternative activation of phagocytes, promotes the intracellular survival, and not killing, of *C.neo* (127). Together, these studies show that CD206 may contribute to both protective and non-protective responses, depending on other signals that occur during DC-*C.neo* interactions. More work to clarify the role of CD206 in T-cell activation and CD206 signaling pathways is necessary to more fully understand its complex role in protective immune responses to *C.neo*.

The fungus strikes back: cryptococcal virulence factors influence dendritic cells

Several cryptococcal virulence factors interfere with the development of protective immune responses in the infected host. The majority of these effects are linked to their interference with antigen presenting cells (APCs) of myeloid lineage including DC, macrophages, and their monocyte precursors (Figure 1-3). These cells share many functional and metabolic pathways, and thus the virulence-associated genes not surprisingly affect these mononuclear APCs in a similar fashion. Functional pathways commonly affected by fungal virulence factors include those associated with pathogen uptake and degradation, APC cell activation/maturation, classical versus alternative polarization, cytokine production, and crosstalk of APC with the antigen specific T-cells. As a consequence of cryptococcal interference with these pathways, *C.neo* not only directly alters innate functions of DCs and other APCs, but also induces profound down-stream effects on the adaptive/efferent arm of the immune response. For example, cryptococcal laccase (128-130), virulence-associated DEAD-box protein (VAD1) (131, 132), cryptococcal Hsp70 homologue Ssa1 (133),

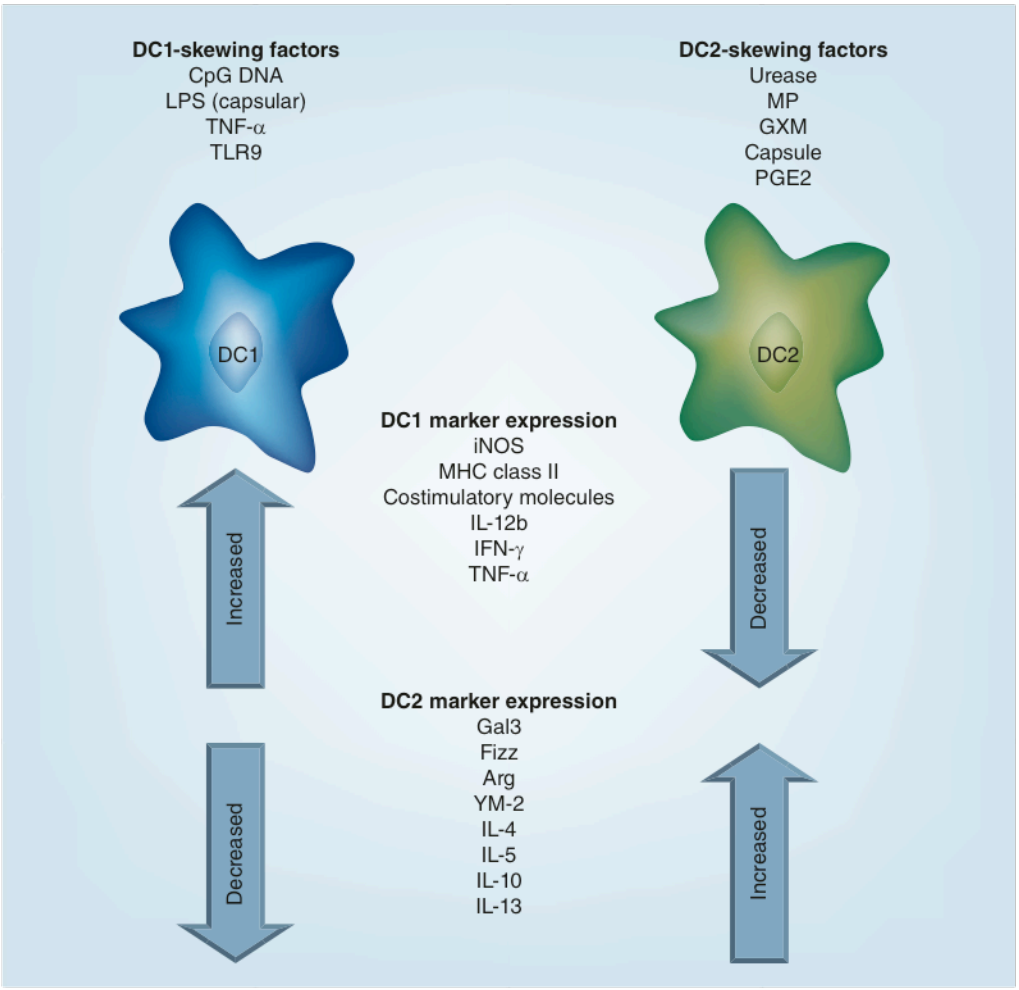

Figure 1-3 Host and pathogen-derived factors can skew DCs to DC1 or DC2 polarization.

Activated DCs are capable of becoming DC1 cells, which promote protective Th1 T cell responses in *C.neo*-infected mice, or DC2 cells, which promote non-protective Th2 T cell responses in *C.neo*-infected mice. Note that this schematic is over-simplified as many DC, particularly in human disease, exist on a spectrum between DC1 and DC2. The relative strength of DC1 and DC2 pathways is influenced by factors derived both from the host and the pathogen and it is the relative balance between these pathways that determines the net DC phenotype . DC1 express high iNOS, MHC Class II, costimulatory molecules, and pro-Th1 cytokines whereas levels of Arginase, Fizz1, and other DC2 markers are low. Conversely, DC2 express a reciprocal pattern and are more associated with pro-Th2 cytokine expression.

and phosphatidylinositol 4-kinase (PIK1), a ubiquitin-like protein (RUB1), and a cation ATPase transporter (ENA1) (134) were shown to interfere with the innate APC pathways upstream of their effects on the development of adaptive immunity. While future studies are needed to dissect specific interactions of these factors with DC, some cryptococcal components have been already shown to modulate maturation and polarization of DC and their monocyte precursors. Among these factors are capsular polysaccharides, mannoproteins, and cryptococcal urease, laccase, and Ssa1.

Polysaccharide capsule and GXM

The *C.neo* polysaccharide capsule is a major virulence factor that inhibits phagocytosis, as illustrated by acapsular mutant strains of *C.neo* being avirulent and readily ingested by phagocytes in mice (135-138). The addition of capsular material to co-cultures of myeloid cells with acapsular *C.neo* prevents phagocytosis of the acapsular *C.neo* (139). The polysaccharide capsule, comprised primarily (80%) of glucuronoxylomannan (GXM) (140-147), exerts effects on dendritic cell activation in both human and murine monocytic cells. *In vitro* exposure of murine $CD11c^+$ splenic DC to *C.neo* polysaccharide capsule decreases their secretion of TNFα and chemokine ligands (CCL3, CXCL10, CCL4), and impairs CCR7 expression (148).

Monocytes encountering acapsular *C.neo in vitro* upregulate MHC II and costimulatory molecules similar to those induced by treatment with LPS (44, 149); in contrast, these effects are not observed when monocytes are exposed to encapsulated organisms (150, 151). In work performed with human tissue, the

addition of purified capsule component GXM to human monocytes treated with acapsular *C.neo* modulated their function as evidenced by their: a) decreased TNFα and IL-1β production (152); b) increased IL-10 secretion (150): c) decreased surface expression of MHCI and MHCII; and d) impaired phagocytosis of acapsular *C.neo* (151). However, when human monocytes were incubated with encapsulated *C.neo* treated with anti-GXM, the human monocytes were nonetheless unable to upregulate MHCII or costimulatory molecules (151), suggesting that another, as of yet unidentified component(s) of the capsule, can suppress MHCII expression. The cryptococcal polysaccharide capsule is thus an extremely important and incompletely understood virulence trait with important effects on DC activation.

Mannoprotein

Cryptococcal mannoprotein (MP, in two isoforms, MP1 and MP2) promotes $CD4^+$ T cell stimulation (153, 154), although it was initially unknown which phagocyte was primarily responsible for presenting it to T cells. Early studies showed that MP induced replication in human PBMCs (155) and enhanced IL-12 secretion from human monocytes (156). Later work showed that multiple lectin receptors on DCs were responsible for MP uptake via MMR (157), and that uptake induced IL-2 production from $CD11c^+$ splenic DCs (158) (reviewed in (159)). However, the effects of MP on DC maturation differ with stimulant duration, model system, and the presence or absence of other immunostimulatory molecules. MP1 and MP2 were shown to induce DC maturation over 48 hours at concentrations between 5 and 20 μg/mL via

upregulation of costimulatory molecules, MHCI and MHCII, and down-regulation of phagocytic receptors comparable to LPS in human PBMCs differentiated to DCs using IL-4 and GM-CSF (157). In another study, a mixed population of MP1 and MP2 at a concentration of 50 μg/mL for 24 hours maintained DC immaturity in murine BMDCs differentiated with GM-CSF and IL-4 when compared to LPS stimulation (84). Finally, the addition of TLR receptor ligands CpG DNA, dsRNA, and others (discussed above) to MP preparations *in vitro* resulted in greatly enhanced DC activation (160). Thus, the context in which DCs encounter MP may be a deciding factor in whether its effects are immunostimulatory or immunosuppressive.

Urease, laccase, and Ssa1

The cryptococcal virulence factor urease, an extracellular enzyme that hydrolyzes urea, promotes CNS dissemination and facilitates microvascular sequestration of *C.neo* in the brain (161). The cryptococcal virulence factor laccase, necessary for melanin production and inflammatory mediators such as prostaglandins, is also necessary for CNS dissemination (128-130, 162-164). In some strains of *C.neo*, the cryptococcal HSP70 homologue Ssa1 (a major antigen for the antibody response, and often found in cryptococcal capsule) controls the expression of laccase, and thus all the hallmarks of laccase-dependent virulence (165). Ssa1 is also a virulence factor in its own right: independent of its control of laccase in some strains, but it is unknown what its role is during the innate and adaptive response (133). Mice infected intratracheally with either a urease-deficient strain or laccase-deficient strain of *C.neo* have fewer hallmarks of non-protective Th2 immunity: lower pulmonary fungal burden, less extrapulmonary

dissemination, dramatically less eosinophil recruitment, and less YM-1 crystal deposition (49, 130). Furthermore, the urease-deficient strain accumulated fewer immature DC in the lung-associated lymph nodes (LALN) compared to wild-type *C.neo* (44), which was consistent with the hypothesis that urease promoted development of non-protective immunity by interfering with maturation of DC in the *C.neo* infected lungs. These findings were also consistent with other mouse studies showing a strong association between immature DC phenotype and the development of non-protective Th2 immune responses to *C.neo* (47, 84). As we will discuss in the next section, the critical role of DC in anti-cryptococcal defenses is being strengthened by the accumulating evidence linking impaired DC numbers and activation with higher fungal burdens in the lung and increased risk of lethal CNS dissemination.

Host factors that influence dendritic cells

Pro-DC1 and pro-DC2: IFN γ and IL-4

IFN γ activates DCs to become classically activated (DC1), thus priming Th1/Th17 immune responses (reviewed in (166)) , while IL-4 activates DCs to become alternatively activated (DC2), thus priming Th2 immune responses (167).

Throughout the *in vitro* experiments in this dissertation, we will use IFN γ as the pro-DC1 stimulus and IL-4 as the pro-DC2 stimulus, as these are the predominant pro-DC1 or pro-DC2 cytokines found during pulmonary cryptococcal infection (3, 7, 57, 66, 72, 78, 80, 97, 168-170), and thus are the biologically relevant stimuli for our modeling of DC activation during *C.neo* infection (as opposed to more standard pro-DC1 activatiors, such as LPS). While

IL-4 is generally considered to be non-protective in cryptococcal infections, we cannot ignore recent studies showing that IL-4 receptor signaling can temporarily promote *C.neo* control during the very early, but not later, phases of cryptococcal infection in mice (119, 171). However, with our strain of *C.neo* (primarily 52D), in our mouse background (primarily CBA/J, with some Balb/c), and at the relevant time points in our extensively characterized model (3, 7, 14, and 28 dpi) (45, 84, 85), IL-4 is correlated to DC2 activation and nonprotective Th2 immune responses; thus we feel justified in its usage as pro-DC2 cytokine *in vitro*.

GM-CSF in human cryptococcosis patients

Granulocyte macrophage colony stimulating factor (GM-CSF) is a cytokine instrumental in generating DCs (reviewed in (172))**.** As noted above, GM-CSF is increasingly appreciated as a necessary factor in anticryptococcal immunity as evidenced by anti-GM-CSF autoantibodies, such as those found in patients who either have or go on to develop pulmonary alveolar proteinosis, correlating to higher rates of cryptococcosis with either *C.neo* or *C. gattii* (23). Furthermore, the presence of anti-GM-CSF autoantibodies results in higher rates of dissemination of *C. gattii* to the CNS in human patients (24). The data generated in mice and rats are consistent with the requirement of GM-CSF for generation of protective response; Chen *et al.* showed that both mice and rats deficient in GM-CSF have a significantly higher pulmonary fungal burden at the efferent phase of the immune response and in association with some impairment in T cell numbers and cytokine responses (25, 173). Of note, TNFα production in infected GM-CSF-deficient mice was significantly reduced relative to wild type mice (25).

Importance of TNFa in human patients and in mouse models of cryptococcal infection

Several different lines of evidence point to TNFα as a crucial cytokine in the host response to *C.neo*. Along with IFN γ , TNFα is the major protective biomarker in *C.neo* infected patients (81, 82). Furthermore, human patients that are receiving TNFα blocking antibody therapy (Infliximab, Etanercept, Adalimumab) and who are otherwise immunocompetent, are at increased risk of *C.neo* infection (30, 83). The resistance of CBA/J mice to strain 52D can be overcome by TNFα depletion (45, 73, 84, 85). Conversely, C57BL/6 mice (susceptible) given an adenoviral vector expressing TNFα prior to intratracheal cryptococcal infection increased their number of accumulated monocytes, decreased the numbers of accumulated eosinophils, displayed progressive clearance of the infection similar to CBA/J mice, and increased the hallmarks of Th1 response relative to mice that were infected with *Cryptococcus* that received a control adenoviral vector (174). In addition to host-specific effects on TNFα-production, different strains of *C.neo* also vary in the amount of TNFα elicited from immune cells derived from the same strain of mice. Strains of *C.neo* that have been induced to express high melanin via culture in asparagine salts agar induce baseline levels of TNFα production from cultured alveolar macrophages *in vitro*, while *in vivo*, naturally occurring high-melanin-producing strains of *C.neo* yield levels of TNFα comparable to uninfected mice in BAL fluids (175, 176). Similar effects were observed with *C. gattii* strains that cause invasive disease in patients with no known immunodeficiencies. Infection resulted in down-regulation of the host TNFα response and skewed the adaptive immune response away from

Th1/Th17 (88, 177). Thus, the removal or addition of TNFα is sufficient to fundamentally alter whether *C.neo* is or isn't cleared.

TNFα and DCs during C. neoformans *infection*

Studies using murine models consistently identify the first 7 days of infection while the afferent immune response develops as the period in which TNF α signaling has the most profound effect on the generation of protective immunity against *C. neo*. (45). Transient depletion of TNFα before day 7 post-infection by injection of TNFα blocking antibodies induces profound, long-term effects on anti-cryptococcal immunity, while short-term depletions of TNFα after day 7 of infection do not prevent development of protective immunity (45). In other studies, administration of exogenous human TNFα to mice during days 1-3 post-infection was sufficient to extend survival times by over 30% (73). The temporal relationship between TNF α production (or blockade) and the afferent immune response provides important evidence that TNF α is critically associated with priming of the immune response and that DCs, as primers of the immune response, may represent the cell subset most significantly affected by TNF α signaling. While early studies did not distinguish between macrophages, DCs, and monocytes (45), they noted a dramatic decrease in mononuclear phagocyte accumulation during TNFα depletion, which resolved upon recovery of TNFα levels (45, 84, 85). Further experiments showed a correlation between the phenotype observed when mice were depleted of TNFα and the phenotype observed when infected mice had received adoptively transferred immature dendritic cells pulsed with cryptococcal mannoprotein prior to infection. Mice

receiving adoptively transferred immature DC developed non-protective Th2 immunity in subsequently infected recipient mice relative to infected mice that received LPS- and MP-pulsed mature DC (84). Thus, DC maturation and/or polarization are of the utmost importance in generation of protective immunity to *C.neo*.

"Training" of dendritic cells against *C. neoformans*

A series of novel paradigm-shifting studies demonstrated that epigenetic modifications substantially influence patterns of DC and macrophage activation and gene expression (reviewed in (178)). Epigenetic modifications are biochemical modifications (methylation, acetylation, phosphorylation, among others) added to DNA or histones that stably regulate gene expression by altering a gene's accessibility to the cell's transcriptional machinery (reviewed in (179)). These modifications can be either activating or suppressive. Histone acetylation is typically activating, while DNA hypermethylation in promoter-region CG islands is transcriptionally repressive. Histone methylation can be either activating or repressive depending on the residue of the histone tail that receives the methyl group(s). Histone methylation marks are deposited by histone methyltransferases (reviewed in (180)) and removed by histone demethylases. DNA methyltransferases add methyl groups to DNA, while demethylation is induced by cytidine deaminases or Tet proteins, (reviewed in (181)). Many of the signaling pathways, protein complexes, and enzymes that affect DC and macrophage polarization through epigenetic modification are beginning to be elucidated. The studies enumerated below provide evidence that these pathways can modulate DC responses to cryptococcal infection.

TNFα signals through MAPK and NFκB pathways (reviewed in (182)), and epigenetic modification of key immune genes is known to occur through both the MAPK (183, 184) and NFκB (185) signaling pathways. Exciting new work from Diermeier *et al.* has shown that TNFα signaling directly changes chromatin structure around NFκB-associated gene regions (186). MAPK signaling has been shown to be required for IL-1β production in DCs (184) and MHCII expression in macrophages (187). NFκB signaling has been shown to epigenetically regulate the promoter of the chemokine eotaxin (185), and NFκB signaling has been linked to activities of the histone methyltransferase MLL1, which forms a multi-protein complex instrumental for IL-12p40 epigenetic regulation in DCs (188) and at numerous other promoters in myeloid cells (189). Our studies showing that cryptococcal clearance is impaired by TNFα signaling blockade during the first week post-infection highlight the critical importance of early TNFα signaling in the transition between innate and adaptive immune responses mediated by DCs to the organism. Our yet unpublished results suggest that this transition may be highly influenced by TNFα-induced epigenetic modifications to key DC1 and DC2 genes. Taken together, these studies suggest that TNFα signaling can epigenetically modify DCs at critical regions of DC1 and DC2 genes during cryptococcal infection, and is a potential mechanism behind the long-term effects of short-term TNFα depletion in cryptococcal infection.

Epigenetic modifications induced by TLR signaling may also contribute to the paramount importance of PAMP/TLR signaling in cryptococcal infection. TLRs signaling through the MyD88 adaptor protein use the NFκB and MAPK pathways, similar to TNFα signaling (above), and affect the epigenetic regulation

of inflammatory genes in monocytes (190-192). In work by Weinmann *et al.*, chromatin remodeling and subsequent transcription factor binding to the promoter region of IL-12p40 in murine macrophages depended upon TLR stimulation (193, 194). Further, *Mycobacterium tuberculosis* induced IL-12 production from DCs specifically through ligation of TLR9, while *M.tb* stimulation of macrophages, which occurs through TLR2, caused minimal IL-12 production. This was due to chromatin remodeling around the IL-12p40 promoter stimulated by TLR9, but not TLR2, signaling (195). As discussed above, CpG DNA signaling through TLR9 critically contributes to IL-12 production in mouse models of cryptococcosis (110), and the loss of TLR9 impairs DC responses during cryptococcal infection (65). Thus, TLR signaling may epigenetically regulate pro-Th1 gene expression in DC response to *C.neo*.

Summary

Protective immunity to *C.neo* requires robust T cell responses, and this is preceded by the production of key protective pro-inflammatory cytokines TNFα, IL-12, GM-CSF, and IFNγ. These responses are primed by classically activated DCs in the node and in the infected lung tissue where effector DC also play a role in phagocytosis and killing of *C.neo*. DCs in cryptococcal infection must overcome alternative activation or immaturity, which is promoted by a vast repertoire of cryptococcal factors. It is possible that epigenetic training of DC during cryptococcal infection aids DCs in maintaining DC1 programming in the infected lungs, lymph nodes, and any sites of dissemination in order to prime effective T cell responses.

This dissertation investigates how both *C.neo* and host factors can modulate the afferent immune response, and under what circumstances these factors impact the developing efferent immune response. The overarching hypothesis is that crosstalk between host defense signals and fungal factors during the afferent immune response to *C.neo* by modulating DC activation and/or polarization directly impacts the developing adaptive response to become either protective or non-protective. This dissertation will primarily focus on the roles of a specific cryptococcal factor, the heat shock protein 70 homologue Ssa1, on the microbial side, and the cytokine TNFα on the host side, to gain better insights on the mechanisms by which hosts can develop protective responses.

Chapter 2 Cryptococcal HSP70 homologue Ssa1 contributes to pulmonary expansion of C. neoformans during the afferent phase of the immune response by promoting macrophage M2 polarization[2]

Abstract

Numerous virulence factors expressed by *C. neoformans* (*C.neo*) modulate host defenses by promoting non-protective Th2-biased adaptive immune responses. Prior studies demonstrate that the HSP70 homologue, Ssa1, significantly contributes to serotype-D *C.neo* virulence through the induction of laccase, a Th2-skewing and CNS-tropic factor. In the current study, we sought to determine whether Ssa1 modulates host defenses in mice infected with a highly virulent serotype A (serA) strain of *C.neo* (H99). To investigate this, we assessed pulmonary fungal growth, CNS dissemination, and survival in mice infected with either H99, an *SSA1*-deleted H99 strain (*Δssa1*), and a complement strain with restored *SSA1* expression (*Δssa1::SSA1*). Mice infected with the *Δssa1* strain

[2] Excerpts of this chapter taken from:

Eastman AJ, He X, Qiu Y, Davis MJ, Vedula P, Lyons DM, Park YD, Hardison SE, Malachowski AN, Osterholzer JJ, Wormley FL Jr, Williamson PR, Olszewski MA. Cryptococcal heat shock protein 70 homolog Ssa1 contributes to pulmonary expansion of Cryptococcus neoformans during the afferent phase of the immune response by promoting macrophage M2 polarization. J Immunol. 2015 Jun 15;194(12):5999-6010. doi: 10.4049/jimmunol.1402719. Epub 2015 May 13. PubMed PMID: 25972480; PubMed Central PMCID: PMC4458402.

displayed substantial reductions in lung fungal burden during the innate phase (days 3 and 7) of the host response whereas less pronounced reductions were observed during the adaptive phase (day 14) and mouse survival increased only by 5 days. Surprisingly, laccase activity assays revealed that *Δssa1* was not laccase-deficient, demonstrating that H99 does not require Ssa1 for laccase expression, which explains the CNS tropism we still observed in the Ssa1-deficient strain. Lastly, our immunophenotyping studies showed that Ssa1 directly promotes early M2 skewing of lung mononuclear phagocytes during the innate, but not the adaptive phase of the immune response. We conclude that Ssa1's virulence mechanism in H99 is distinct and laccase-independent. Ssa1 directly interferes with early macrophage polarization, limiting innate control of *C. neo*, but ultimately has no effect on cryptococcal control by adaptive immunity.

Introduction

In this chapter, we investigate the impact of cryptococcal Ssa1 on the afferent and efferent immune response to highly virulent *C.neo* strain H99. Many *C.neo* virulence factors act on the immune response directly, but few affect the early containment of *C. neoformans*, and instead promote extensive fungal growth during the efferent phase of the immune response that coincides with robust Th2 polarization (49, 130). For example, the cryptococcal virulence factors urease and laccase promote undesirable Th2 polarization and corresponding M2 macrophage polarization (49, 130, 196). Another group of virulence-associated genes including a phosphatidylinositol 4-kinase (*PIK1*), a ubiquitin-like protein (*RUB1*), and a cation ATPase transporter (*ENA1*), promote cryptococcal survival

in the host's tissues and do, in fact, contribute to early fungal growth. However, the overall level of virulence conferred by each of these factors correlates with their effects on the adaptive immune response polarization and subsequent macrophage polarization status during the efferent phase of host response (134), and not highly immunomodulatory at the afferent phase.

The mammalian heat shock protein 70 (Hsp70) functions both as intracellular chaperone and as an extracellular protein that can be detected by the innate immune system. Some pathogens express Hsp70 homologues that unfavorably modulate the host immune response, including *Mycobacterium tuberculosis (M.tb)* (197) and *Candida albicans (C. albicans)* (198, 199). These microbial Hsp70 have been linked to suppression of dendritic cells and induction of the non-protective pro-M2 cytokine IL-10. Cryptococcal Hsp70 homologue, Ssa1, is secreted as a component of extracellular vesicles destined for the capsule (200). Accordingly, Ssa1 is an immunodominant antigen for antibody production in both mice and humans (201-204). While microbial Hsp70 proteins show strong effects on the innate immune system and thus are likely to affect macrophages, cryptococcal Ssa1 also serves another role as a DNA-binding protein in *C.neo* that is a co-activator of cryptococcal laccase expression in serotype D (serD) *C.neo* JEC21 (165). However, it is unknown whether Ssa1 plays a similar role in the more prevalent and typically more virulent serotype A of *C.neo* and whether, in addition to its ability to regulate laccase expression, Ssa1 could interfere with the early control of *C.neo*.

In this chapter, we study the putative *C.neo* virulence factor Ssa1 utilizing a serotype A (serA) strain of *C.neo* that lacks Ssa1, *Δssa1* in comparison to the

highly virulent wild-type (WT) serotype A parent strain, H99. We will first assess differences in the broad immune responses to H99 and *Δssa1* by measuring pulmonary and disseminated *C.neo* and immunophenotyping of the infected lungs. We will then assess macrophage polarization during the afferent immune response, because HSP70 and its homologues expressed by pathogens can modulate macrophage activation. The sub-hypothesis for this chapter is that the loss of Ssa1 will result in greater ability of the afferent immune response to control *C.neo* infection, and that this will result in the development of protective immunity to infection with *Δssa1*.

Results

Cryptococcal Ssa1 expression contributes to pulmonary virulence of C. neoformans *serotype A in a mouse model*

The Hsp70 homologue Ssa1 has been shown to be required for cryptococcal laccase expression and thus to contribute significantly to the virulence composite of *C.neo* serD strain JEC21 (165). However, the function of virulence-associated genes between serD and the more commonly isolated serA may differ when it comes to clinical impact (205, 206). In this study, we sought to determine the role of Ssa1 in the virulence of *C.neo* serA using the wildtype strain H99 and its mutants with targeted manipulations of the *SSA1* gene: (*Δssa1*) the deletant strain, and *Δssa1* complemented with the functional *SSA1* gene (*Δssa1*::*SSA1*). Deletant and complement strains were generated using an analogous protocol as described previously for serD (165). Both deletion and restoration of the *SSA1* gene were confirmed by PCR and Southern blot analysis (data not shown). The

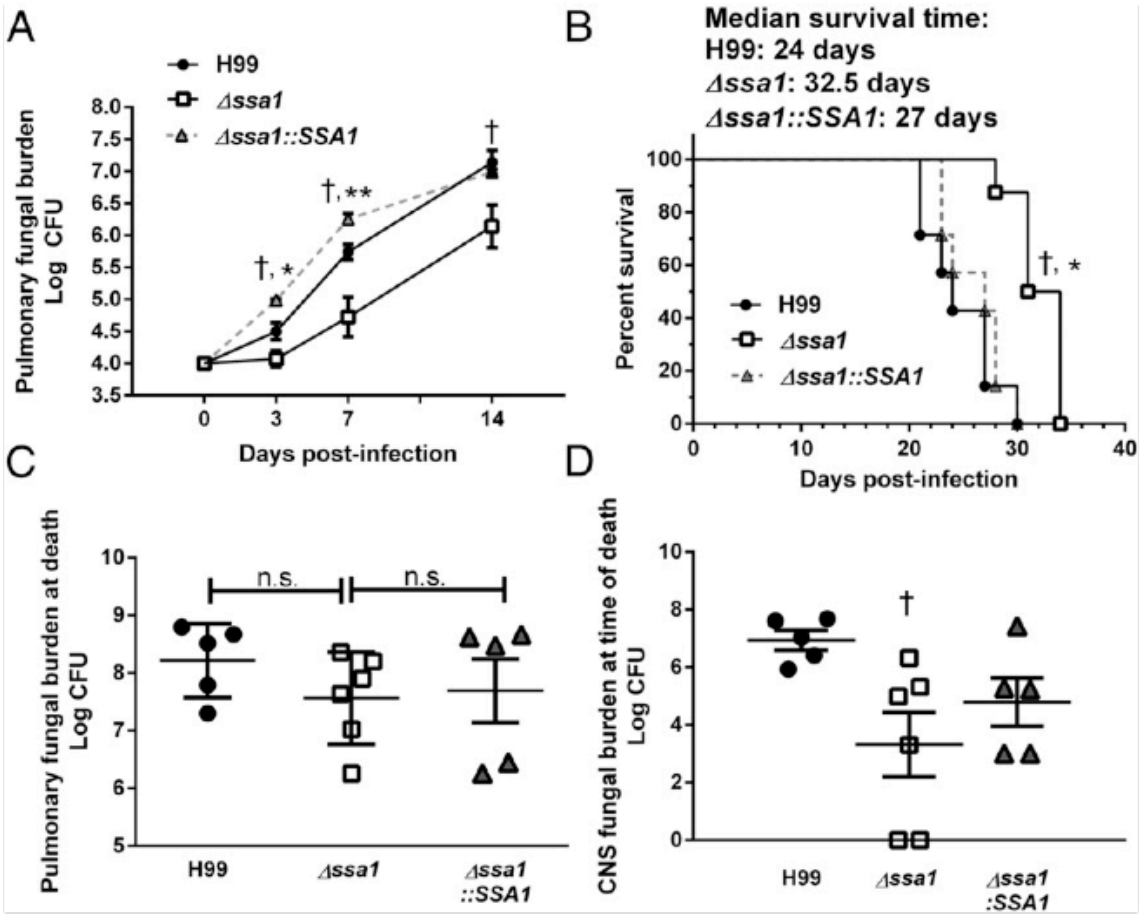

Figure 2-1 Cryptococcal *SSA1* gene deletion delays fungal growth in the lungs and the CNS dissemination, and improves survival of infected mice.

(A) Mice were infected with 10^4 cells of wild type (WT) *C. neoformans* H99 (serotype A), *SSA1*-gene deleted mutant *Δssa1*, or complement strain *Δssa1*::*SSA1* on an H99 background. Pulmonary fungal burdens were quantified on 3, 7, or 14 days post infection (dpi). Mice infected with *Δssa1* had significantly reduced pulmonary fungal burden relative to H99 at 3, 7, and 14 dpi and had significantly reduced pulmonary fungal burden relative to *Δssa1*::*SSA1* at 3 and 7dpi. Note the faster growth rates of the WT and complement strains at 0-7 dpi, and parallel growth rates for all 3 strains beyond day 7. Data represent pooled average CFU per lung or brain from separate matched experiments; n=13 mice per group per time point for H99 and *Δssa1* and n=4 for *Δssa1*::*SSA1*. (B) Survival study was performed on 7-8 mice per group. Infection with *Δssa1* conferred a modest but significant survival advantage compared to H99 and *Δssa1*::*SSA1*. (C, D) Post-mortem CFU assay was performed on homogenized lung (C) and brain (D) from mice in the survival study. Pulmonary fungal burden did not differ significantly between any strains at the time of death, while fungal burden in the brain was significantly decreased in *Δssa1*-infected mice. († $p < 0.01$ relative to H99, * $p < 0.05$ relative to *Δssa1*::*SSA1*, ** $p < 0.01$ relative to *Δssa1*::*SSA1*).

deletant and complement strains of H99 did not exhibit demonstrable growth differences from the parent strain H99 organism *in vitro*. Subsequently, BALB/c mice were infected intratracheally with 10^4 CFU of wild type *C.neo* H99, *Δssa1*, or *Δssa1::SSA1*, and pulmonary fungal growth was assessed in the lungs at 3, 7, and 14 days post infection (dpi). Substantial decreases in fungal load were observed at 3 and 7 dpi in the lungs of mice infected with *Δssa1* compared to both *Δssa1::SSA1*- and H99-infected mice; however, beyond day 7 *Δssa1* acquires strong logarithmic growth rate displayed by both Ssa1-expressing strains (Figure 2-1A), consistent with Ssa1 expression promoting early growth of *C.neo* in the infected lungs during the afferent phase of the immune response.

To further assess the virulence properties of the *Δssa1* strain, we performed a comparative survival study in mice infected with H99, *Δssa1* and *Δssa1::SSA1*. Mice infected with H99 or *Δssa1::SSA1* succumbed to infection by 31 and 30 dpi, respectively, while mice infected with *Δssa1* survived up to 35 dpi (Figure 2-1B). The median survival time for mice infected with H99 and*Δssa1::SSA1* was 24 and 27 days respectively. In contrast, the median survival for mice infected with *Δssa1* displayed a small but statistically significant extension of survival out to 32.5 days. Interestingly, the fungal burden from the lungs at the time of death was not significantly different between the H99 and *Δssa1*-infected mice (Figure 2-1C), indicating that *SSA1* deletion resulted in only a modest attenuation of H99 virulence.

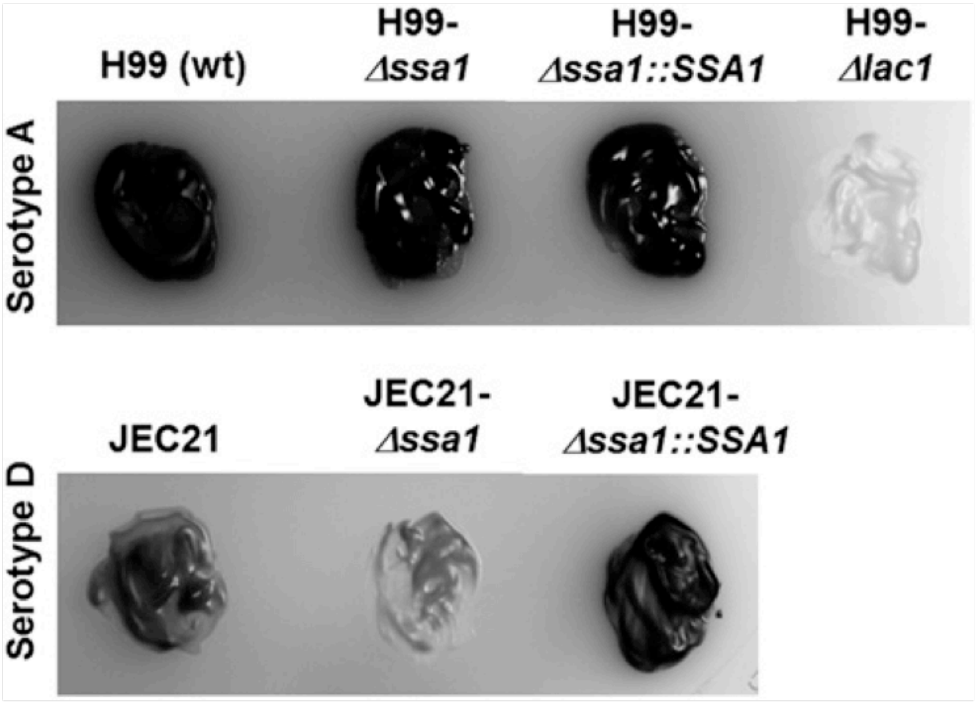

Figure 2-2 Cryptococcal *SSA1* deletion suppresses laccase activity in a serotype D JEC21-*Δssa1* mutant but not in a serotype A *Δssa1* mutant.

Laccase activity was determined by melanization of *C. neoformans* colonies cultured for 48 h in YPD media at 37°C, then plated on asparagine salts agar with norepinephrine, and incubated at room temperature for 5 days. Note strong melanin pigmentation displayed by WT serotype A strain H99, the *Δssa1* mutant in an H99 background, and the corresponding *Δssa1*::*SSA1* complemented serotype A, and the absence of pigmentation in the laccase-deficient mutant (*Δlac*) in an H99 background. Also note the pigmentation in the serotype D WT strain JEC21 and corresponding *Δssa1*::*SSA1* but the minimal pigmentation displayed by the *Δssa1* strain on JEC21 background.

Ssa1 expression in serotype A is not required for brain dissemination or laccase expression

Since H99 is highly neurotropic, we harvested brain tissue to assess microbial dissemination to the central nervous system (CNS) post-mortem during the survival study. As expected, H99 disseminated in high titers into the brain in 100% of the infected mice, as did the complemented strain *Δssa1::SSA1*. Surprisingly, the *Δssa1* mutant also disseminated to the brain in all the infected mice, albeit in reduced numbers relative to H99 (Figure 2-1D). This contrasted with our previously published work with the*Δlac1* strains in both JEC21 and H99 backgrounds, which consistently demonstrated that laccase-deficient *C.neo* did not disseminate into the CNS (128, 130). Thus, the current data strongly suggested that the *Δssa1* strain was capable of expressing laccase.

To test this hypothesis, we re-isolated *Δssa1* from the brains of mice that succumbed to infection and tested them for completeness of the *SSA1* deletion and for laccase activity. We found complete deletion of the *SSA1* transcript by qPCR both in the original*Δssa1* strain used for infection and in the*Δssa1* isolated from the brains of mice from the survival study (data not shown), showing that the H99-*Δssa1* mutant did not revert to WT H99 in the infected mice. As a readout for laccase activity, we assessed melanin synthesis by serotype A strains H99, *Δssa1*, *Δssa1::SSA1*, and *Δlac1* (Figure 2-2, top panel, left to right) and by the serotype D strains JEC21 WT (JEC21-WT), *SSA1*-deficient (JEC21-*Δssa1*), and complement (JEC21-*Δssa1::SSA1)* (Figure 2-2, bottom panel, left to right) in cultures on asparagine-norepinephrine agar. In serotype A, H99, *Δssa1*, and

Δssa1::SSA1 strains displayed robust melanin pigmentation consistent with laccase activity, while the *Δlac1* strain lacked any pigmentation (Figure 2-2, top panel, left to right). In serotype D, the JEC21-WT strain displayed modest pigmentation, while the JEC1-*Δssa1* strain completely lacked pigmentation (Figure 2-2, bottom panel, middle) consistent with published studies (165), showing that laccase expression in JEC21 (a serD strain) requires Ssa1 while laccase expression in H99 (a serA strain) does not require Ssa1. Thus, apart from the differential role of Ssa1 in laccase regulation between strain H99 (serA) and JEC1 (serD), we demonstrated Ssa1's role as a virulence factor independent of its role in laccase expression in the H99 strain.

Cryptococcal Ssa1 expression accelerates but does not significantly alter the development of lung and brain pathologies

Next, we sought to determine the effect of cryptococcal Ssa1 expression on lung pathology and the extent of the inflammatory response via histopathological examination of lungs from mice infected with H99 or the *Δssa1* strain at 21 dpi. H99 and *Δssa1*-infected mice showed similar leukocyte accumulation in the alveolar spaces of lungs at 21 dpi (Figure 2-3A and B). Both strains induced severe lung pathology by 21 dpi, with organisms growing in widespread areas of the lungs. Inflammatory infiltrates were present in the infected areas, but many fungi resided within the alveolar space unaccompanied by inflammatory cells, indicating that both strains can evade the inflammatory response. We also noted areas of dissemination of the *Δssa1* organisms to uninfected lung areas,

consistent with the somewhat delayed kinetics of fungal growth but overall progressive nature of pulmonary infection with *Δssa1*.

To further establish that *Δssa1* was capable of invading the brain and inducing CNS pathology, we performed histological analysis of brain sections of mice infected with H99 or *Δssa1*. Our data demonstrate that at the time of death, *Δssa1* induced CNS pathology similar to that of the H99. Both H99 and *Δssa1* induced similarly-sized CNS lesions with evidence of modest inflammatory infiltrates at the periphery surrounding large central areas occupied mostly by *C.neo* and debris (Figure 2-3C and D).

Cryptococcal Ssa1 expression affects pulmonary leukocyte populations during the innate but not the adaptive phase of the immune response in the infected lungs

Collectively, data from our assessment of fungal burden, CNS dissemination, survival, and histopathology suggested that cryptococcal Ssa1 expressed by SerA *C.neo* affected the innate phase of the immune response more prominently than the adaptive phase. To determine the effect of Ssa1 on host defenses, we quantified and further characterized leukocyte populations in the lungs of mice infected with H99 or *Δssa1* at 3, 7, and 14 dpi. Leukocytes from enzymatically-dispersed lungs were evaluated by differential cell counts. Both H99- and *Δssa1*-infected mice accumulated similar numbers of leukocytes at 3 and 14 dpi, but the *Δssa1* strain showed slight but significant decreases of leukocyte numbers at 7 dpi (Figure 2-4A), indicating that cryptococcal *SSA1* expression may contribute to the magnitude of the inflammatory response at the peak of innate inflammation. A leukocyte subset analysis (performed by visual inspection of

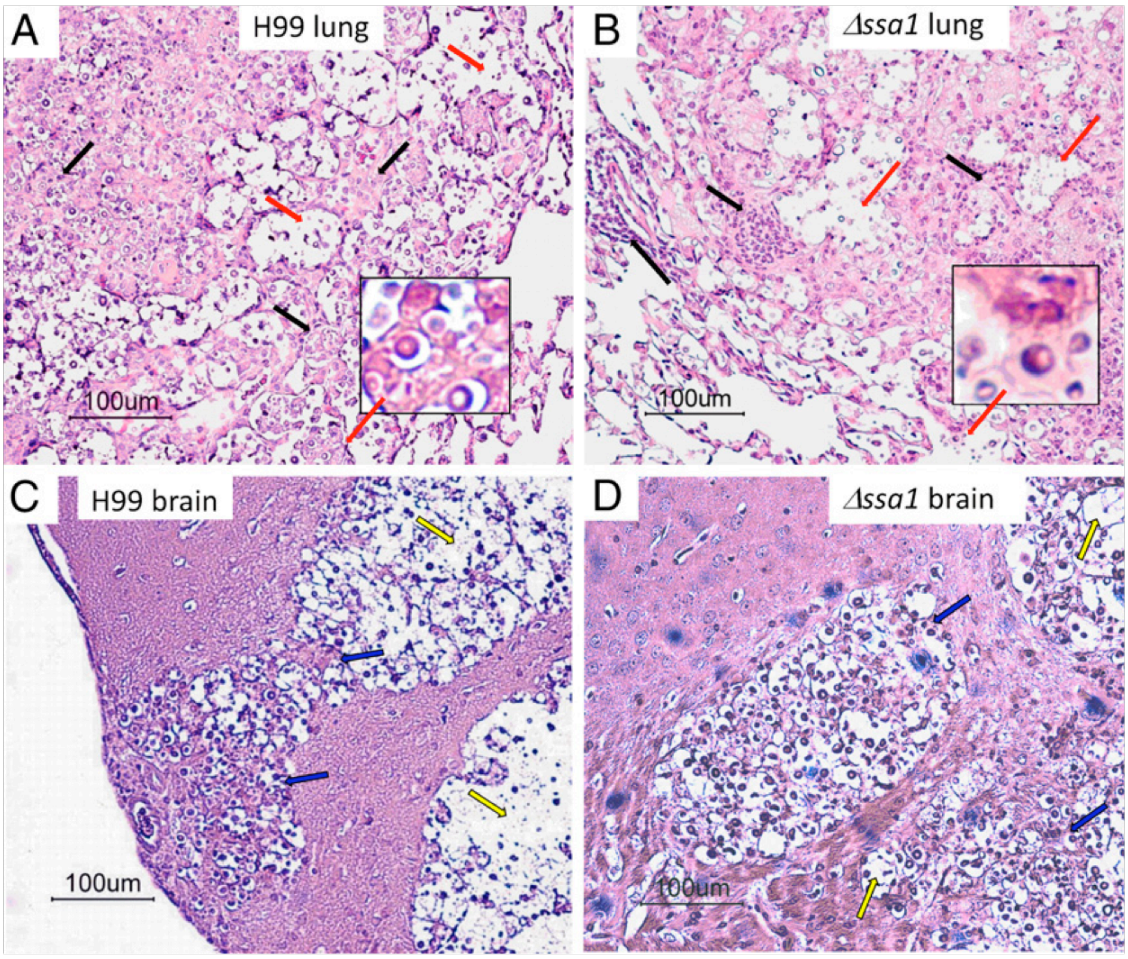

Figure 2-3 Deletion of cryptococcal *SSA1* results in delayed but similar type of lung and CNS pathology.

Lungs and brains of mice infected with H99 (A, C, respectively) and *Δssa1* (B, D, respectively) strains were isolated at week 3. Tissues were preserved in formalin, processed for histology, and cut and stained with mucicarmine to visualize *C. neoformans*. Lungs were counterstained with H&E. Representative images taken at 20x magnification with 100x magnification insets for lung histology images. A and B) Inflammatory infiltrates (black arrows) are present in both H99 and *Δssa1* strains. Note the cryptococci (red arrows, 100x) residing in the alveolar space and the presence of inflammatory cell infiltrates in H99- and *Δssa1*-infected lungs. C and D) Cryptococcal mucoid cysts infiltrating and displacing brain tissue. Note the infiltrating inflammatory cells at the periphery and cocci and cell debris in the middle of the cysts (blue arrows), where normal brain tissue has eroded (yellow arrows) in both H99 and *Δssa1* strains.

cytospins) identified changes in frequencies of pulmonary leukocytes, specifically at the early time points. Relative to H99 infected mice, the *Δssa1*-infected lungs accumulated a higher proportion of mononuclear phagocytes (Figure 2-4B) and a much lesser proportion of granulocytes (eosinophils and neutrophils) (Figure 2-4C-D), indicating that cryptococcal Ssa1 contributed to the development of innate inflammation, especially its granulocytic component. In contrast, no changes in magnitude or frequency of pulmonary leukocyte subsets were observed on day 14, providing a clue that the adaptive response did not significantly differ between the H99- and *Δssa1*-infected mice. Thus, deletion of cryptococcal gene *SSA1* altered the composition of lung leukocyte populations during the innate but not adaptive phase of the immune response.

Cryptococcal Ssa1 promotes M2 macrophage polarization during the innate but not adaptive phase of the immune response to cryptococcal infection

Pulmonary control of *C.neo* depends on macrophage polarization status: M1 (classical activation) is protective and M2 (alternative activation) is non-protective. Thus, we next sought to determine whether the early Ssa1-induced impairment in pulmonary fungal clearance was linked to differential M1/M2 polarization. First, we assessed early M1/M2 macrophage polarization markers in H99 and *Δssa1*-infected lungs using immunohistochemistry. Due to low levels of inflammation during the first days of infection (unpublished observations), lung sections were analyzed at 8 dpi, a time point that still largely represents an innate/afferent phase of the immune response. In lung sections obtained from mice infected with H99, we observed clusters of cells highly expressing Arg1 and mannose receptor (CD206), but very few cells positive for inducible nitric oxide

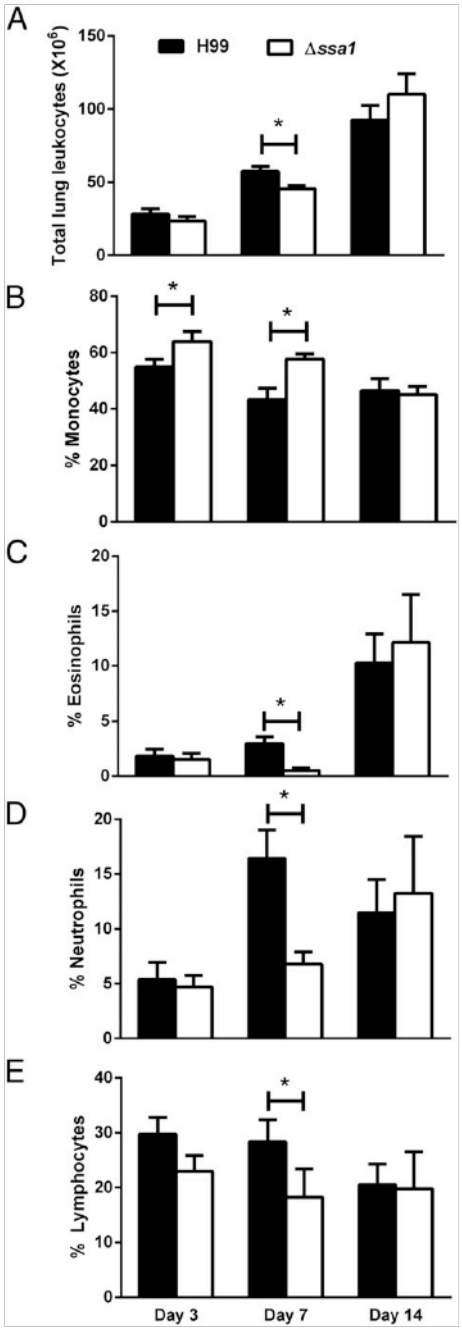

Figure 2-4 Deletion of cryptococcal SSA1 resulted in a similar magnitude but distinct polarization of early but not late inflammatory responses in the infected lungs.

Lung leukocytes were isolated and characterized by microscopy at 3, 7, and 14 dpi from *C. neoformans*-infected lungs. Total leukocyte numbers in the lungs were equivalent in H99 versus *Δssa1*-infected lungs with the exception of a small but significant decrease on day 7 in the *Δssa1*-infected lungs (A). Monocytes (B), eosinophils (C), neutrophils (D) and lymphocytes (E) were identified by morphology and staining characteristics. Monocyte frequency was significantly increased at 3 and 7 dpi in *Δssa1*-infected mice, while eosinophil and neutrophil frequency was significantly decreased at 7 dpi in *Δssa1*-infected mice relative to H99-infected mice, and lymphocyte frequency never differed significantly between the two strains at any time points. N=5-11 mice per time point per strain, representing 3 separate matched experiments. *$p < 0.05$ compared to H99.

synthase (iNOS) (Figure 2-5), consistent with presence of M2 macrophages in the H99-infected lungs. In contrast, we observed fewer CD206 and Arg1-positve cells and higher number of cells expressing iNOS in lung sections obtained from mice infected with *Δssa1,* suggesting more predominant M1 polarization in the absence of cryptococcal Ssa1.

To evaluate these differences more quantitatively and to evaluate the M1/M2 status of pulmonary mononuclear phagocytes at the earlier and later time points, we next performed flow cytometry analysis on leukocytes populations obtained from H99- and *Δssa1*-infected lungs at 3 and 14 dpi. We measured expression of MHC class II (high expression consistent with M1 polarization) and CD206 and Galectin 3 (high expression consistent with M2 polarization) on $CD11c^+$ populations of lung leukocytes which, following exclusion of T cells, B cells, neutrophils, and eosinophils (Figure 2-6A, also see Materials and Methods) (41, 44, 92) are highly enriched for resident alveolar macrophages as well as monocyte-derived exudate macrophages and dendritic cells. These cell subsets represent fully differentiated mononuclear phagocytes, which are all capable of M1/M2-type polarization as well as killing of *C.neo*. Results showed significant differences in the expression levels of all of these markers by $CD11c^+$ myeloid cells between H99 and *Δssa1*-infected lungs at 3 dpi. Surface expression of MHC class II (MHC II) was increased (Figure 2-6B) while surface expression of CD206 and Galectin 3 (Gal3) was decreased (Figure 2-6 C-D) at 3 dpi in *Δssa1*-infected lungs compared to those infected with H99, consistent with enhanced M1 polarization in *Δssa1*-infected lungs and more pronounced M2 polarization in

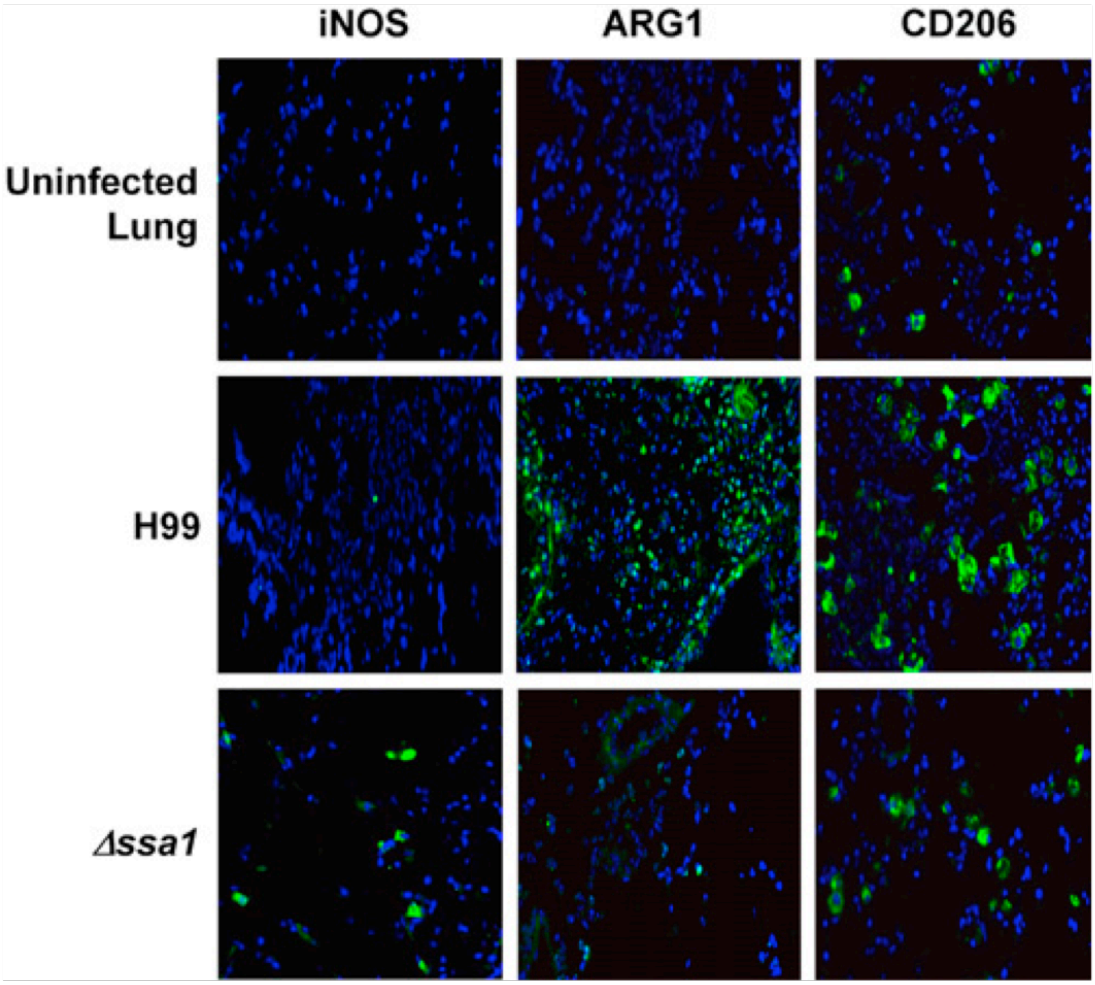

Figure 2-5 Cryptococcal *SSA1* expression promotes the induction of crucial M2 proteins ARG1 and CD206 while preventing induction of M1 protein iNOS in the lungs.

Defrosted lung sections taken at 8 dpi were stained with DAPI (blue) to show nuclei, and antibodies for M1 activation marker iNOS (left panel), M2 activation marker Arginase (Arg1, middle panel) and M2 activation marker mannose receptor (CD206, right panel). Secondary FITC conjugated antibodies (green) were used to visualize immunoreactive proteins. Note the significant induction of Arg1 and CD206 and the absence of iNOS staining in H99-infected lung sections. In contrast, iNOS protein can be detected in *Δssa1*-infected sections, while the M2 markers Arg1 and CD206 show strikingly less immunoreactivity in *Δssa1*-infected lungs. Sections were imaged at 40X magnification.

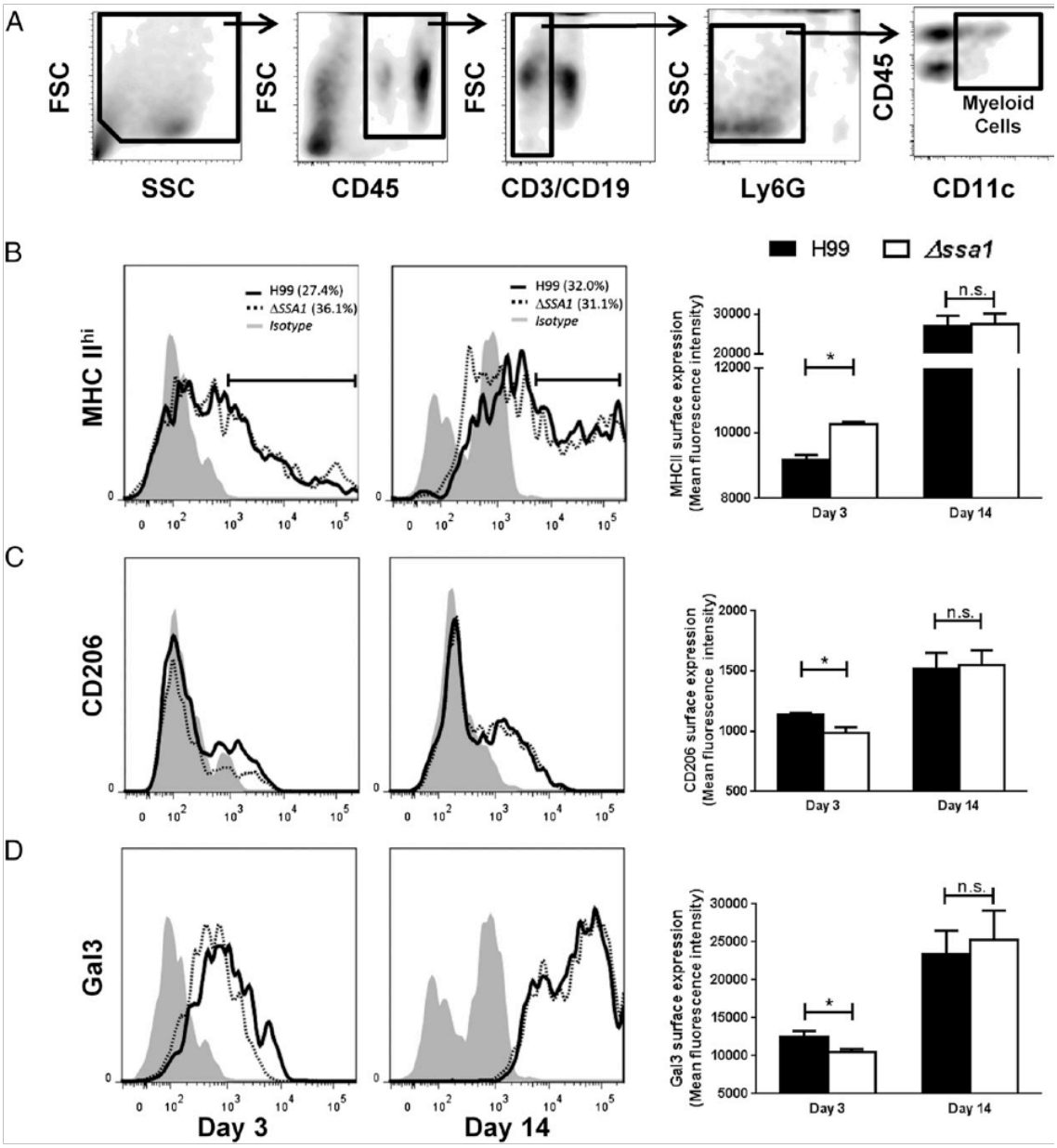

Figure 2-6 Cryptococcal Ssa1 increases surface expression of M2 activation markers and decreases surface expression of MHCII during the innate but not adaptive phase of the immune response in the infected lungs.

Flow cytometric analysis of leukocyte populations from infected mouse lungs used the gating scheme in (A) to sequentially gate out debris, non-immune cells, lymphocytes, and granulocytes and then we selected the $CD11c^{+}$ subset of this population. M1 activation marker MHC class II (B) and M2 activation markers Gal3 (C) and CD206 (D) surface expression was assessed at 3 and 14 dpi. Note the significant increase in MHCII and decrease in CD206 and Gal3 surface staining in *Δ*ssa1-infected mice at 3 dpi, but a resolution of these differences by 14 dpi. Representative histograms were selected from two separate, matched

experiments. N = 5 per treatment per time point. Combined mean fluorescence intensity plots represent high-expressing cells (MHC II) or positively staining cells (CD206 and Gal3), and reflect the cumulative phenotype. * $p < 0.05$ using Student's t-test.

H99-infected lungs on 8 dpi. In contrast, the surface expression levels of these markers in H99 and *Δssa1*-infected groups were equivalent at 14 dpi (Figure 2-6B-D), demonstrating similar M1/M2 polarization profiles of these mononuclear cells during the adaptive phase of the immune response in the presence and absence of cryptococcal Ssa1.

To further assess and verify our findings, additional M1/M2 markers and M1/M2-associated cytokines were analyzed by quantifying mRNA expression in adherence-purified macrophages from lungs of mice at 3 and 14 dpi with H99 and *Δssa1*. At 3 dpi, macrophages from *Δssa1*-infected lungs induced significantly more transcript for M1 activation gene iNOS (Figure 2-7A) and less transcript for M2 activation genes Arg1 (Figure 2-7B), Gal3 (Figure 2-7D), CD206 (Figure 2-7E) and FIZZ (not shown) at 3 dpi than did those infected with H99. Further, the iNOS:Arg expression ratio was M1-skewed, with *Δssa1*-infected lung macrophages having a higher expression ratio, compared to a lower expression ratio (indicating a less M1- and more M2-polarized phenotype) in the H99-infected lung macrophages. Consistent with our flow cytometry readouts, at 14 dpi none of these genes were differentially expressed, nor were gene expression ratios differentially skewed between H99 and *Δssa1*- infected groups. Collectively, these data indicate that cryptococcal *SSA1* expression by SerA promotes M2 polarization during the innate, but not the adaptive, phase of the immune response to cryptococcal infection.

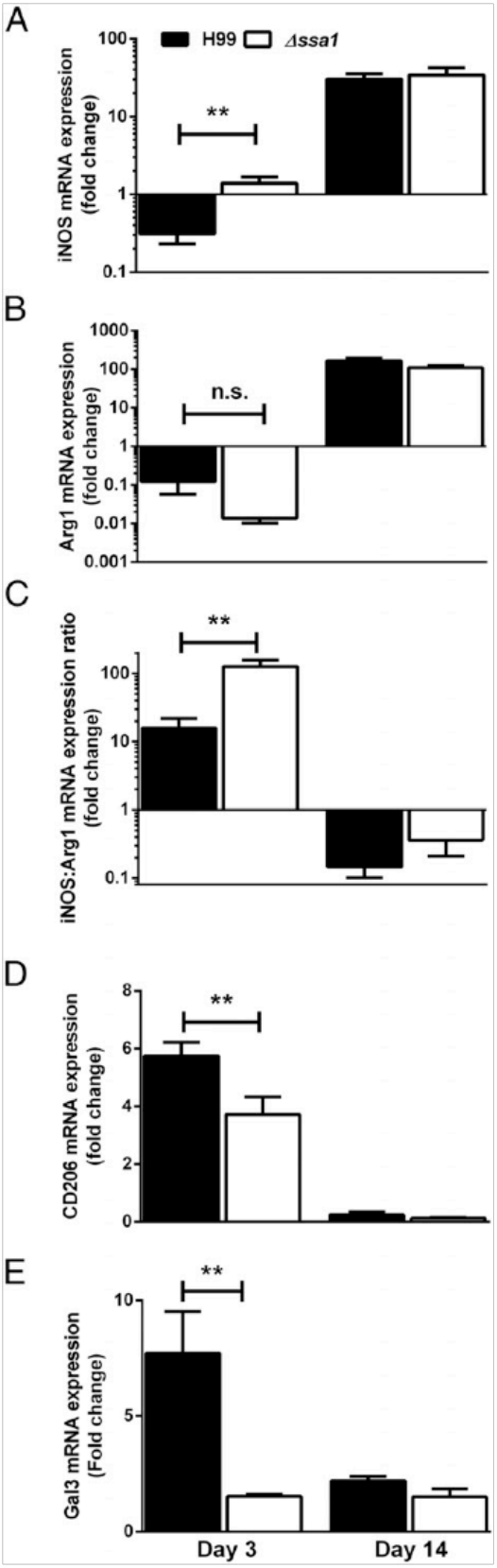

Figure 2-7 Cryptococcal Ssa1 increases induction of macrophage M2 activation markers and decreases induction of M1 activation marker iNOS during the early but not the late phase of lung infection in mice.

Macrophages were isolated from infected mouse lung leukocyte preparations by adherence selection. iNOS (A), Arg1 (B), the iNOS/Arg1 expression ratio (C), CD206 (D) and Gal3 (E) mRNA transcript levels were assessed by qPCR. Note the increase in iNOS in *Δssa1*-infected mouse macrophages relative to H99-infected mouse macrophages at day 3 but not at day 14. Arg1 is not significantly different between the macrophages at day 3. However, a paired iNOS/Arg1 ratio (C) where an individual mouse's macrophage iNOS mRNA fold change was divided by its own Arg1 mRNA fold change yielded highly significant M1-skewed signature in macrophages from *Δssa*-infected mice but a far lower ratio in H99-infected mouse macrophages at day 3, but not at day 14, where both *Δssa1*- and H99-infected mice had M2-skewed macrophages. Also note the decrease in expression of both M2 activation markers CD206 and Gal3 in *Δssa1*- infected mice relative to H99-infected mice at day 3, but not at day 14. N = 8 from 2 separate experiments. * $p < 0.05$, ** $p < 0.01$ using Student's t-test.

Cryptococcal SSA1 expression modulates innate but not adaptive phase pulmonary type 2 cytokine responses in infected lungs

We next investigated the cytokine mRNA expression levels by leukocytes obtained from the lungs of H99- and *Δssa1*-infected mice. Cryptococcal *SSA1* deletion resulted in decreased expression of non-protective Th2 cytokines IL-4 and IL13 at day 3 but not day 14 (Figure 2-8A and B), indicating that cryptococcal Ssa1 acted as an early inducer of type 2 cytokine production. The expression of protective Th1-driving IFNγ was not significantly different between the groups (Figure 2-8C). However, the IL-4:IFNγ ratio, shown to be a good indicator of type 1 versus type 2 response balance, was decreased in the absence of Ssa1 at 3 dpi (Figure 2-8D), demonstrating that the early cytokine balance of type 1/type 2 cytokines was shifted towards type 2 in the presence of cryptococcal Ssa1. Consistent with the similar outcomes of lung pathology and leukocyte populations at the later time point, we did not observe differences in Th1/Th2 polarizing cytokine expression by leukocytes from H99 versus *Δssa1*-infected lungs on day 14 (Figure 2-8A-D). Thus, cryptococcal Ssa1 expression modulates innate but not adaptive phase pulmonary type 2 cytokine responses in the infected lung.

Cryptococcal SSA1 expression promotes alternative activation markers and down-regulates classical activation markers during C. neoformans*-macrophage interaction* in vitro

To determine if *SSA1* expression is sufficient to directly promote M2 polarization of macrophages, we assessed the M1/M2 polarization response of bone marrow-

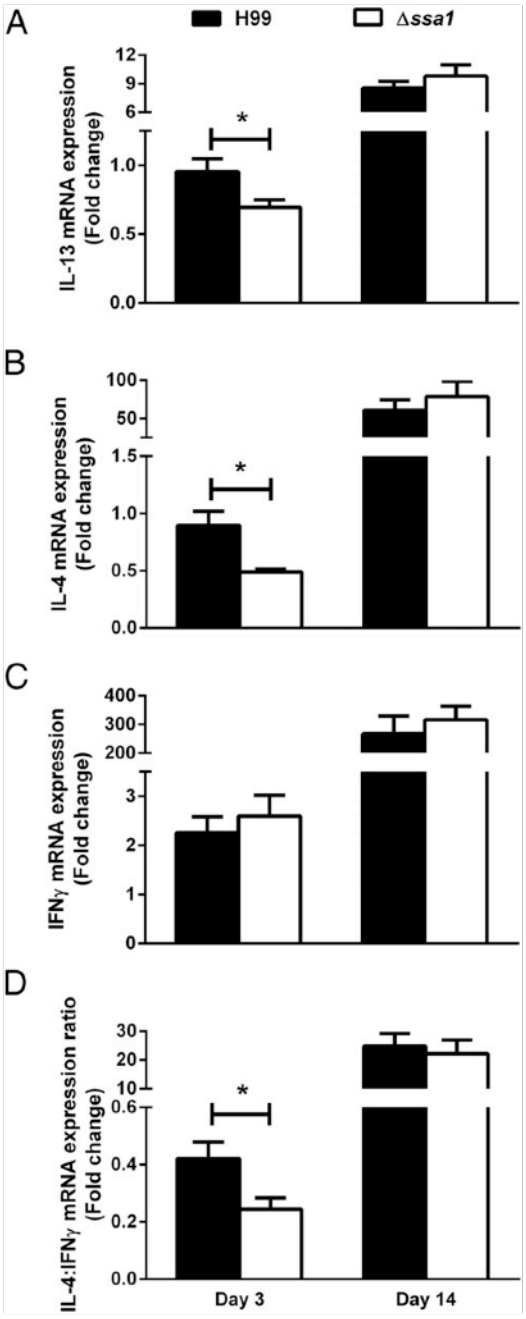

Figure 2-8 Cryptococcal *SSA1* expression results in increased pro-Th2 cytokine induction and increased IL4:IFNγ regulation ratio in pulmonary leukocytes from infected mice during innate phase of the immune response to *C. neoformans*.

Leukocyte preparations from H99 and *Δssa1*- infected mouse lungs were processed for mRNA quantification of IL-13 (A), IL-4 (B), IFNγ (C) and for the IL-4:IFNγ induction ratio (D) at 3 and 14 dpi. Note the decrease in non-protective cytokines IL-4 and IL-13, along with the decreased IL-4:IFNγ induction ratio in the leukocytes obtained from *Δssa1*-infected mice relative to the H99-infected mice at day 3, followed by progressive but no longer differential cytokine induction in the lungs of *Δssa1*- and H99-infected mice on day 14. N = 5/time point/group from 2 separate experiments. * $p < 0.05$ using Student's t-test.

derived macrophages (BMM) following direct stimulation with *C.neo* H99 or *Δssa1 in vitro*. BMMs were harvested after stimulation with H99 or *Δssa1* for 24h and analyzed for expression of M1 and M2-associated genes by qPCR. Expression of M1 activation marker iNOS was increased, while expression of M2 activation markers Gal3 and CD206 (Figure 2-9B) as well as Fizz1 (data not shown) was decreased in macrophages stimulated with *Δssa1* compared to those stimulated with H99 (Figure 2-9) as early as 24h post-treatment. Further, the iNOS:Arg expression ratio, a broadly accepted readout of M1/M2 polarization balance, was heavily skewed towards M1 in the *Δssa1*-treated macrophages compared to those stimulated with H99. Thus, these findings demonstrate that cryptococcal Ssa1 directly promotes M2 polarization *in vitro*.

Despite the ability of Ssa1 to directly modulate macrophage polarization, the virulence factor on its own does not significantly affect the efferent immune response that eventually develops. The efferent response is reliant on DCs as the antigen presenting cells that traffic to the lymph node and prime T cells. In order to reconcile our findings of Ssa1-induced M2 polarization with the few observed changes in the adaptive immune response to *Δssa1*, we assessed the activation of DCs during infection with H99 versus *Δssa1*. Using the same markers of M1/M2 polarization as in Figure 2-6— MHCII, CD206, and Gal3 surface expression— we found no significant differences in $CD11b^{+}/CD11c^{+}$ DC polarization at 3 or 14 dpi between H99 and *Δssa1*-infected mice (Figure 2-10), which is in contrast to the Ssa1-induced changes in macrophage polarization at 3 dpi detailed in Figure 2-6. Furthermore, while lung leukocyte culture supernatants yielded early Th1/Th2 polarization differences, there were no differences in TNFα levels at the

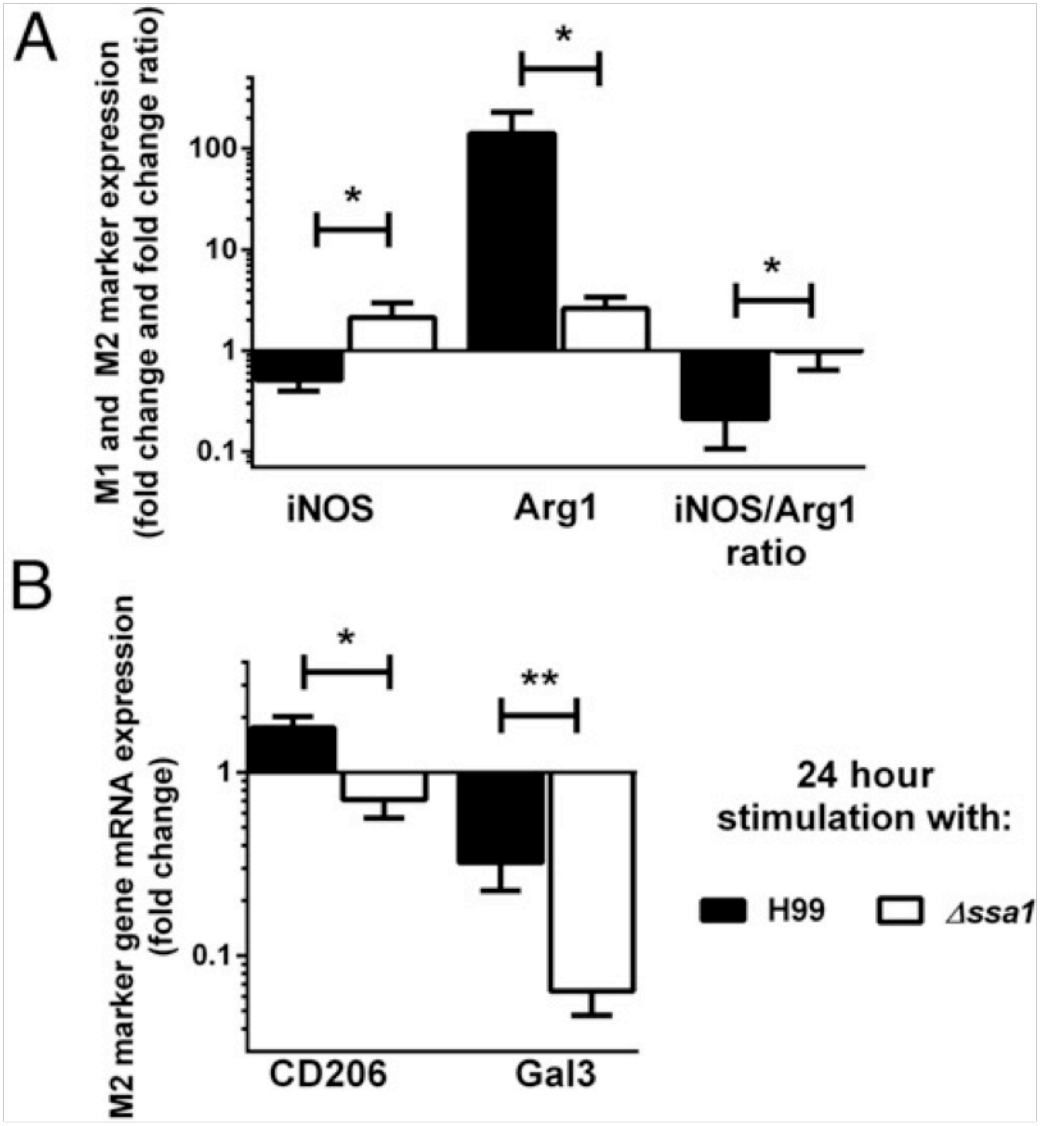

Figure 2-9 ***In vitro*** **stimulation with an** ***SSA1*****-expressing cryptococcus is sufficient to decrease M1 and increase M2 activation markers in bone marrow derived macrophages.**

mRNA was extracted from bone marrow-derived macrophages stimulated with live H99 or *Δssa1 C.neo* for 24 hours and qPCR was performed for M1 activation marker iNOS (A) and M2 activation markers Arg1 (A), CD206 (B) and Gal3 (B). iNOS/Arg1 expression ratio (A) was also prepared. Note the increase in iNOS expression and iNOS/Arg1 ratio and the decreases in Arg1, CD206, and Gal3 expression in the *Δssa1*-infected macrophages relative to the H99-infected macrophages. N=6-9 from three separate experiments. * $p < 0.05$, ** $p < 0.01$ using Student's t-test.

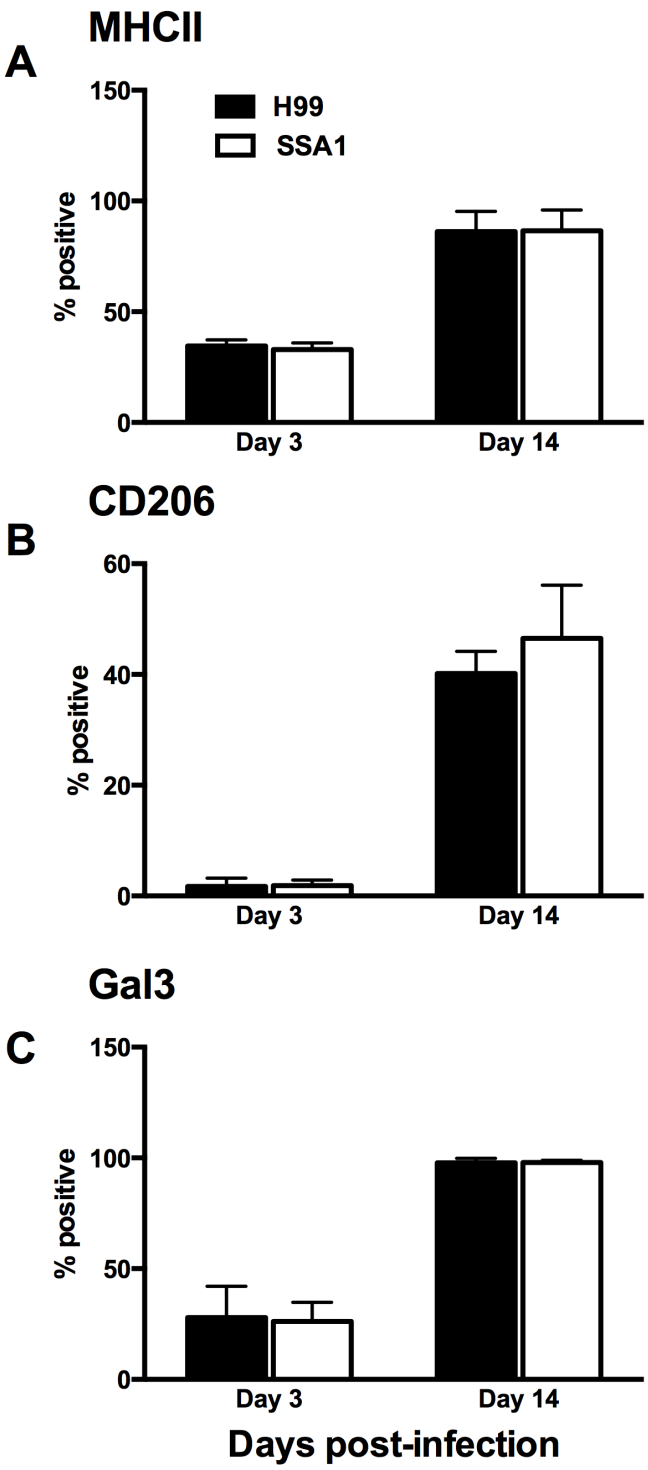

Figure 2-10 Ssa1 does not affect dendritic cell polarization *in vivo* at early or late times post-infection.

Dendritic cells were sorted from myeloid cells via expression via CD11b expression. This specific DC subset was then analyzed by flow cytometry for expression of DC1 marker MHCII (A) and DC2 markers CD206 (B) and Gal3 (C) at 3 and 14 dpi. There were no significant differences in surface expression observed in any of these parameters. N = 10 from two separate, matched experiments. Statistical analysis was performed by two-way ANOVA.

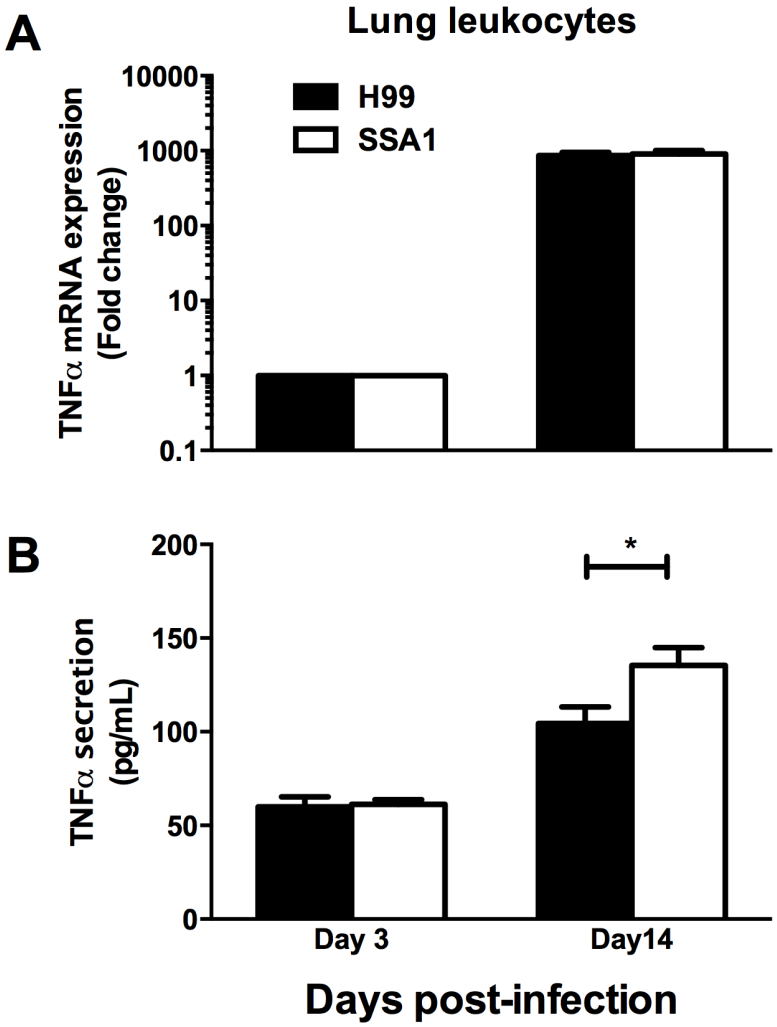

Figure 2-11 Ssa1 deletion does not alter TNF α secretion by lung leukocytes early during infection.

Lung leukocytes were isolated from enzymatically-digested lungs, plated, and cultured to assess production of TNFα by RT-qPCR (A) and ELISA (B). TNF α production was modestly increased in *Δssa1*-infected mice at 14 dpi at the protein level, but not at the transcriptional level. N = 10 from two separate, matched experiments. Statistical analysis was performed by 2-way ANOVA and student's t-test.

mRNA or protein levels at 3 dpi (Figure 2-11). Thus, Ssa1-mediated effects on antigen presenting cells do not extend to DCs— the cell type responsible for priming of T cell responses— or to early TNFα production within the lung environment, both of which are implicated in the development of protective immunity.

Discussion

Here, we demonstrate that the cryptococcal Hsp70 homologue Ssa1 plays a unique role as a virulence factor that interferes with the innate immune response by promoting early M2 activation of pulmonary macrophages, thereby interfering with the first line of defense against cryptococcal infection. This is the first demonstration of a cryptococcal (fungal) virulence factor that works in this fashion (i.e. that significantly modulates innate host defenses, while leaving the development of the adaptive immunity intact). Our studies also reveal that in contrast with previously known functions of Ssa1 in *C.neo* serotype D, Ssa1 does not regulate cryptococcal laccase expression in strain H99 (serotype A strain). This finding of differential regulation of cryptococcal virulence components between strains of serotypes A and D provides evidence that the divergence between these strains stretches well beyond initially-noted differences in these serotypes' capsular composition. As a whole, this work significantly advances our understanding of cryptococcal factors' interactions with the mechanisms of host defenses in the infected host.

Our studies identified Ssa1 as a cryptococcal factor that promotes early alternative activation of pulmonary macrophages and other $CD11c^{+}$

mononuclear phagocytes during the innate phase of the immune response to cryptococcal infection. This conclusion is based on the following observations obtained by infecting mice with Ssa1-deficient SerA *C.neo* (relative to mice infected with WT H99): 1) a significant early reduction in pulmonary fungal burden; 2) repression of alternative activation-associated genes and surface expression of M2 markers by macrophages and the entire population of $CD11c^{+}$ mononuclear cells; 3) increased abundance of iNOS protein expression and $MHCII^{hi}$ cells in the lungs during the innate phase of the immune response. The subsequent *in vitro* data show that deletion of cryptococcal *SSA1* resulted in down-regulation of M2 markers and up-regulation of M1 markers when bone marrow derived macrophages were stimulated with *C.neo Δssa1* versus H99. These data indicate that cryptococcal Ssa1 in serotype A strain H99 directly affects macrophage polarization pathways, promoting M2 and suppressing M1 pathways in infected macrophages. To our knowledge, this is the first cryptococcal factor known to affect macrophage polarization this early during the infection and in such a direct fashion.

The unique timing of the effects that Ssa1 induces in the host sets it apart from other virulence factors studied in similar systems (49, 128, 130, 161, 196). Observed differences in macrophage polarization state in the presence and absence of Ssa1 during *C.neo* infection (expression of M2 markers CD206, Arg1, and Gal3 and M1 markers iNOS and MHC class II at both the mRNA and the protein level) were significant on days 3 and 7 post-infection. However, by day 14 these differences in macrophage polarization in H99-WT and H99- Δ*ssa1* infected lungs resolved completely (Figures 6, 7, and 8), consistent with the

similar phenotypes of the adaptive immune response polarization (Fig. 5). Consequently, the fungal growth rate in the lungs is not inhibited beyond the early time points and we observe only a temporary delay in pulmonary fungal burdens, CNS dissemination, and infected mouse mortality in the absence of cryptococcal *SSA1* expression. Together, these data demonstrate that Ssa1 is a virulence factor that selectively interferes with the innate immune response without significant effects on generation of the adaptive immune response.

This mechanism of the immunomodulatory effects of Ssa1 contrasts with previously reported effects of other virulence factors that modulate the immune responses. These factors, such as urease (49, 161, 196), phospholipase (128, 207), and laccase (130) promote the development of non-protective Th2 immunity and subsequent M2 polarization and confer a fungal growth advantage late during the infection. It is also in contrast with other factors, such as *PIK1*, *RUB1*, *ENA1* (134), and *VAD1* (132), which confer growth advantages during both the innate and adaptive phase of the immune response but nevertheless predominantly modulate the cytokine environment during the efferent phase of the immune response in *C.neo* -infected lungs. In contrast, Ssa1 directly modulates macrophage- *C.neo* interactions only during the innate phase, with little to no effect on the development of adaptive immunity. In an attempt to specifically address the mechanism of Ssa1-dependent effects on macrophages, our laboratory has performed studies using mice deficient in the SRA receptor, which we originally thought to be the major receptor for the Ssa1 protein (121). Through our investigation, we have found that it is possible that some effects of Ssa1 on macrophages could be induced by SRA; however, the data were not very

clear, hinting that multiple receptors and signaling pathways were likely to be involved.

Our novel findings regarding the virulence effects of cryptococcal Ssa1 also have other important implications for understanding cryptococcal interactions with the host's immune system. First, significant modulation of the innate immune response and early fungal load by a virulence factor is not always sufficient to induce downstream changes in the phenotype of the adaptive immune response. Second, our findings show that the direct effect of a virulence factor on macrophage polarization can eventually be overcome by the extrinsic effects of cytokines induced by the cells of the adaptive immune system. Potential mechanisms for this counter-intuitive finding could include a) contribution of other virulence factors that do not affect innate control but are known to skew the adaptive immune response, such as laccase and urease (49, 129, 130, 165), which are expressed by *Δssa1*, or b) possible differential effects of Ssa1 on dendritic cells, responsible for priming and perpetuating the adaptive response. Together, these data further support our view that cytokine environment manipulation could be a promising therapeutic strategy that may override many aspects of cryptococcal virulence and host deficiencies leading to improper M1/M2 polarization status within the infected host.

The present study also highlights a critical difference in Ssa1's contribution to the virulence composite between two strains that belong to serA and serD, which is linked to their differential regulation of cryptococcal laccase expression. We initiated our work based on an assumption that *SSA1* deletion in H99 would deprive the fungus of virulence properties associated directly with Ssa1 as well

as the virulence properties of laccase. This was based on studies in *C.neo* JEC21 (serD), which demonstrated that Ssa1 is required for laccase expression (165). Laccase is an enzyme required for melanin production in *C.neo* (162-164) and a virulence factor essential for cryptococcal CNS colonization (128, 130). Accordingly, the *Δssa1* strain on a JEC21 background showed a profound suppression of melanin production and a profound defect in CNS invasion (165). The *SSA1* deletion in strain H99 did not reproduce these effects, as H99-*Δssa1* successfully disseminated from lungs into the CNS, induced CNS pathology, and expressed comparable melanin pigmentation to the parent H99 strain (Figure 2-1, Figure 2-2, Figure 2-3). Likewise, *SSA1* deletion in H99 did not induce the immunological consequences of laccase deletion, which were predominantly observed during the efferent phase of the immune response (130). These differences in the regulation of laccase expression between H99 (serA strain) and JEC21 (serD strain) allowed us to define a laccase-independent role of Ssa1 as a standalone virulence factor and also elucidated a novel and crucial difference in virulence gene regulation between *C.neo* strains. In addition to previously-observed differences in regulation of cryptococcal cytochrome c oxidase subunit 1 (COX1) (205), our data underscores major differences in gene regulation among *C.neo* strains. While it is yet unknown how this impacts the spectra of host susceptibilities and pathogenicity of serotypes A and D, our studies provide evidence of differential regulation of crucial virulence-associated genes between representative strains of these serotypes. If the observed differences in virulence gene regulation between strains H99 (serA) and JEC21 (serD) proved to be consistent between all or most serotype A and D strains, our findings would help to explain differential epidemiology between serotypes, similarly to what has

been found for two cryptococcal species- *C.neo* and *C. gatti*- in recent studies (24, 208).

Finally, while our studies focused on *C.neo,* we believe they have broader implications for host interactions with pathogen-derived Hsp70. Other pathogens have been shown to employ Hsp70 as virulence factor/modulator of innate responses including *M.tb* (197, 209), *Toxoplasma gondi* (210, 211) and *Candida* sp. (198). While the mechanism of the Ssa1-induced effects on the host and on pathogen's virulence appear to be different in each group of pathogens, these previously published studies combined with our present work support the broader importance of Hsp70 family proteins as standalone virulence factors and immune response modulators.

In this chapter, we showed that Ssa1 could modulate macrophage polarization, but had no effect on DCs or on certain key afferent-phase cytokines, such as TNF α. We hypothesize that Ssa1 ultimately had no effect on the efferent response because it failed to modulate DC activation, which is the cell type primarily responsible for priming and restimulating CD4 T cells in the lymph node and the lungs (9, 40, 49). In other models, classically activated DCs (DC1) prime Th1/Th17 responses, which, in *C.neo*, are protective responses. It is unclear why Ssa1 can modulate afferent-phase macrophages but not afferent-phase dendritic cells, but this may be due to possible differential receptor expression between DCs and macrophages (such as SRA), or the well-characterized ability of DCs to phagocytose and kill *C.neo* more effectively than macrophages, which could effectively inactivate the cryptococcal Ssa1 before it can successfully signal and modulate phagocyte activation. Because DCs are responsible for activating CD4

T cells during *C.neo* infection, the next chapters will focus more exclusively on DC activation.

In summary, our findings provide novel insights regarding the immunomodulatory role of cryptococcal Ssa1 and we identify important gene regulation differences between serotypes A and D. We have shown that Ssa1 promotes early M2 macrophage polarization and that this form of immune modulation improves fungal growth during the innate phase of the immune response. Yet our data also emphasizes that the immunophenotype of the adaptive immune response ultimately defines the outcome of infection. Furthermore, our studies reveal that immune modulation and the propensity for CNS dissemination mediated by Ssa1 may vary between serotypes and depends on whether or not laccase expression is induced.

Chapter 3 TNFα is required for generation of lasting DC1 phenotype throughout *Cryptococcus neoformans* pulmonary infection[3]

Abstract

A Th1/Th17 response is required to clear *Cryptococcus neoformans* (*C.neo*), a fungal pathogen infecting immunocompromised patients, including those on anti-TNFα antibody (αTNFα) therapy. To determine the mechanisms by which early TNFα signaling promotes the generation and stability of a protective Th1/Th17 response, CBA/J mice received a single dose of αTNFα or isotype control antibody followed by infection with *C.neo* 24067. We found that the robust Th1/Th17 responses in control mice were replaced by non-protective responses with many Th2 features and fluctuating cytokine levels in the αTNFα-treated and infected group, in which the DC1 signature in $CD11c^+$ cells was suppressed through 28 days of infection. We modeled the effects of TNFα on DC phenotypes *in vitro* using bone marrow-derived DCs stimulated with IFNγ with or without TNFα, then challenged with IL-4 to assess plasticity of DC1 and DC2

[3] Excerpts of this chapter taken from:

Eastman, A.J., J. Xu, N. Potchen, A. denDekker, L. M. Neal, G. Zhou, A. Malachowski, S. Kunkel, J. J. Osterholzer, and M. A. Olszewski. TNF α is necessary for long lasting protective immunity to fungal infection through epigenetic stabilization of classically activated dendritic cells and bone marrow dendritic cell precursors. In submission at Science Immunology.

markers at the mRNA and protein level. DCs were plastic to their cytokine environments, as assessed by the expression of iNOS, Fizz1, MHCII, CD206, IL-12b, and IL-13, but the addition of TNFα reduced the plasticity. This TNFα-mediated training was observed in the presence of antigen as well, and correlated to our *in vivo* findings. Using TNFα receptor 1 and 2 inhibitors *in vitro*, we found that this training is dependent on both TNFR1 and TNFR2 in an additive manner. We conclude that TNFα is necessary to train DCs during *C.neo* infection, thus resulting in priming and perpetuation of protective Th1/Th17 immunity, and that in the absence of TNFα, this training does not occur, resulting in a non-protective Th2 immune response.

Introduction

In the previous chapter, we found that despite early modulation of host macrophage polarization, the presence or absence of cryptococcal Ssa1 does not impact the phenotype of the efferent immune response to *C.neo*. DCs– and not macrophages– are thought to be the primary drivers of the developing adaptive immune response to *C.neo* (9, 40, 49), and Ssa1 did not modulate DC activation or polarization, as shown in Figure 2-10. Further, the pulmonary expression of a major DC function mediator, TNFα, was unchanged by expression of Ssa1. Thus, we next proceed to a different model of afferent immune modulation during *C.neo* infection where afferent-phase TNFα is depleted (but, importantly, recovers during the late afferent-early efferent phase) and results in nonprotective efferent immune responses. Neither a) the full immunophenotype,

nor b) the mechanism behind long-term immune modulation, resulting from transient TNF α depletion is known.

The necessity for TNFα early during cryptococcal infection has been well documented (45, 81, 84, 85, 88). CBA/J mice, which normally clear *C.neo* from the lungs within 4 weeks and limit extrapulmonary dissemination, have a persistent and/or progressive infection when TNFα has been depleted by a single injection of TNFα blocking antibody at the time of infection (45, 84, 85). C57BL/6 mice, which are normally unable to clear *C.neo* from the lungs and have a persistent infection, are able to clear *C.neo* when co-infected with an adenoviral vector expressing TNFα (174). Immunocompromised patients with cryptococcosis that produce less TNFα tend to succumb to *C.neo* infection earlier than those that can mount a robust TNFα response (81). Patients receiving anti-TNFα monoclonal antibody therapy for autoimmune disorders are also at increased risk for cryptococcosis (28-30); they are also more susceptible to other infectious agents such as *Histoplasma capsulatum* and *Mycobacterium tuberculosis* (27, 31). The mechanism underlying patients' increased susceptibility to these infections is unclear, but studies by Herring *et all.* (84) and Milam *et al.* (174) of TNFα linked early TNFα expression with DC activation. Furthermore, a particular strain of *Cryptococcus* capable of suppressing host TNFα, causes outbreaks in the Pacific Northwest of the United States in humans without known underlying immunological defects (88). The precise mechanism behind the necessity for TNFα in generating protective immunity is unknown.

DCs are responsible for priming the immune response to *C.neo* in the lymph nodes, and also for re-stimulating antigen-specific T cells in the lungs (reviewed

in (212)). Upon maturation, DCs begin to present more antigen via MHC class II (MHCII), upregulate co-stimulatory molecule expression, downregulate surface expression of many phagocytic receptors, upregulate CCR7, and traffic to local lymph nodes (38, 44, 213). DCs can be classically activated (DC1, characterized by high expression of iNOS, IL-12, MHCII, and costimulatory molecules) wherein they prime Th1/Th17 responses, or alternatively activated (DC2, characterized by high expression of arginase, Fizz1, Gal3, IL-13, and CD206), wherein they prime Th2 responses (reviewed in (213)). DC1 activation has been proposed as a mechanism behind protective immunity to *C.neo* (84), but has not been conclusively shown in the lungs.

There are two canonical receptors for TNFα, TNFα receptor 1 (TNFR1) and TNF α receptor 2 (TNFR2). Both TNFRs can be expressed on the same cell at various stages of immune cell development and are capable of crosstalk (214), although TNFR1 tends to predominate in circulating human peripheral blood monocytes (215). However, both receptors are capable of signaling through NFκB and the MAPK pathways. In other models, such as during oral Salmonella infection, DC maturation is dependent upon TNFR1 (216); further, a more recent study ties DC maturation to TNFR1 as well, but prolonged DC survival to both receptors (217). While much is known about the necessity for TNFα signaling during *C.neo* infection, the dominant TNFR, if any, remains unknown.

In this chapter, we assess the cellular mechanism behind the requirement for TNFα during the afferent immune response to *C.neo* infection. We begin by carefully immunophenotyping CD4 T cells during the efferent response, followed by assessing the activation and polarization of the DC subsets in the

lungs, which are responsible for priming and restimulating T cells during *C.neo* infection. We then model the activation and polarization of DCs *in vitro* in the presence or absence of TNF α and known DC polarization-skewing cytokine factors, and determine which TNFR is necessary for generation of long-term protective immune responses. The subhypothesis for this chapter is that transient TNF α depletion interferes with DC-mediated activation of T cell-mediated immunity during *C.neo* infection, in a TNFR2-mediated manner.

Results

TNFα signaling promotes stability of Th1 polarization during pulmonary C.neo *infection*

To dissect the mechanisms by which early TNFα signaling affects host defenses to *C. neoformans*, isotype antibody-treated and anti-TNFα antibody-treated CBA/J mice were infected intratracheally with a clinical isolate of *C. neo* (the low pathogenic strain 52D, which allows for prolonged analysis of immune responses in the host). First, we determined pulmonary fungal burdens and measured fungal dissemination by evaluating spleen CFU. Consistent with published work, we found that transient depletion of TNFα prevented fungal clearance at 14 and 28 days post-infection (dpi) resulting in a 3-log increase in fungal load by 28 dpi (Figure 3-1A). *C.neo* disseminated to the spleen in each treatment group, but the dissemination in control mice was minimal and transient; without TNFα, *C.neo* disseminated to the spleen in a progressive manner through 28 dpi (Figure 3-1B). We confirmed that TNFα levels begin to recover in TNFα-depleted mice after 7 dpi (Figure 3-1E), thus demonstrating that single dose of anti-TNFα

treatment at the time of infection yielded lasting dysfunction in pulmonary and systemic control of *C.neo* infection.

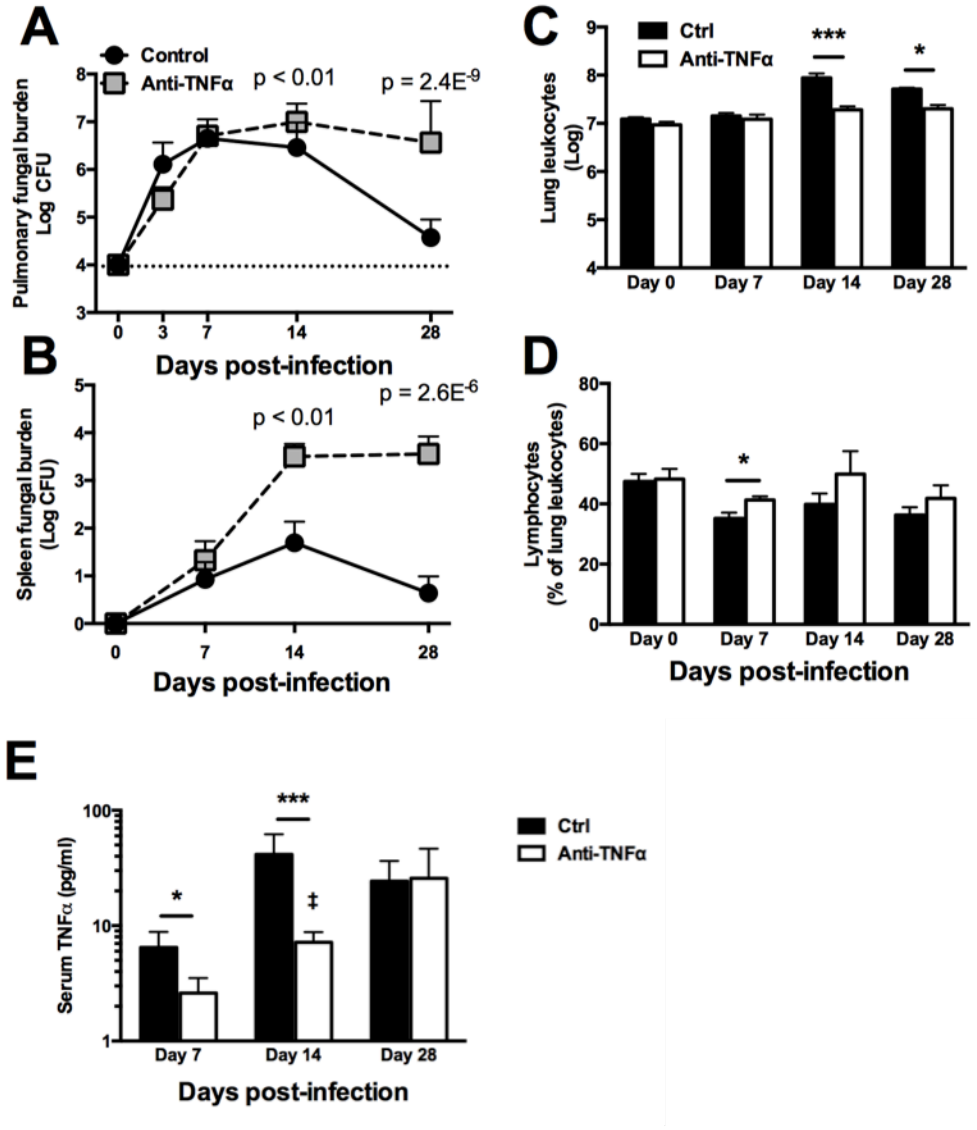

Figure 3-1 Afferent phase TNFα yields protective Th1/Th17 responses throughout infection.

(A and B) Pulmonary fungal burden (A) and splenic fungal burden (B) were evaluated at 3, 7, 14, and 28 days post-infection (dpi). N = 26-32 from five separate, matched experiments. (C and D) Lung leukocytes recovered after enzymatic lung digest were enumerated by light microscopy (C), cytospun onto slides, diff-quick stained, and lymphocytes counted (D). N = 26-32 from five separate, matched experiments. Statistical analysis was performed using student's t-test or ANOVA as appropriate. Non-parametric data was log-transformed. *p< 0.05; **p<0.01; ***p<0.001. (E) Cytometric bead array for TNFα was performed on serum from whole blood of infected mice. N = 36-48 from 3-4

separate, matched experiments. Nonparametric data was log transformed and two way ANOVA and student's t-test were performed. * $p < 0.05$; *** $p < 0.001$; ‡ statistically significant difference between TNFα serum levels in Anti-TNFα mice at 14 dpi compared to 7 dpi.

We next evaluated the effect of early TNFα signaling on magnitude of cellular response in the infected lungs. We observed that leukocyte recruitment at 14 and 28 dpi was diminished in anti-TNFα-treated mice (Figure 3-1C), indicating that early TNFα signaling has a lasting effect on magnitude of inflammatory response. There was small but statistically significant increase in the frequency of lymphocytes in TNFα-depleted mice at 14 dpi, but no other differences in frequencies of leukocyte subsets in the infected lungs throughout 28-days of infection (Figure 3-1D), suggesting that the decrease in pulmonary leukocyte accumulation in TNFα-depleted mice was not restricted to a specific subset. Since $CD4^+$ T cells are required for proper protective immunity to *C.neo*, we assessed the proportion of $CD4^+$ T cells in the lung leukocyte populations by flow cytometry. TNFα-depleted mice had a reduced proportion of $CD4^+$ T cells within their total leukocyte population at 14 and 28 dpi (Figure 3-2A). We next assessed $CD4^+$ T cell activation and found fewer cells expressing CD44 and more cells expressing CD62L in TNFα-depleted mice relative to control mice at 14 and 28 dpi, implying that $CD4^+$ T cells from TNFα-depleted mice were less activated (Figure 3-2B). Thus, early TNFα signaling was required for optimal recruitment of pulmonary leukocytes, including $CD4^+$ T cells with an activated effector phenotype.

To further evaluate the effect of early TNFα signaling on $CD4^+$ T cell polarization, we first measured cytokine expression by $CD4^+$ T cells via intracellular flow cytometry. We found that CD4+ T cells from TNFα-depleted mice made less of the protective cytokines IFNγ and IL-17 and more of the non-protective IL-13 at

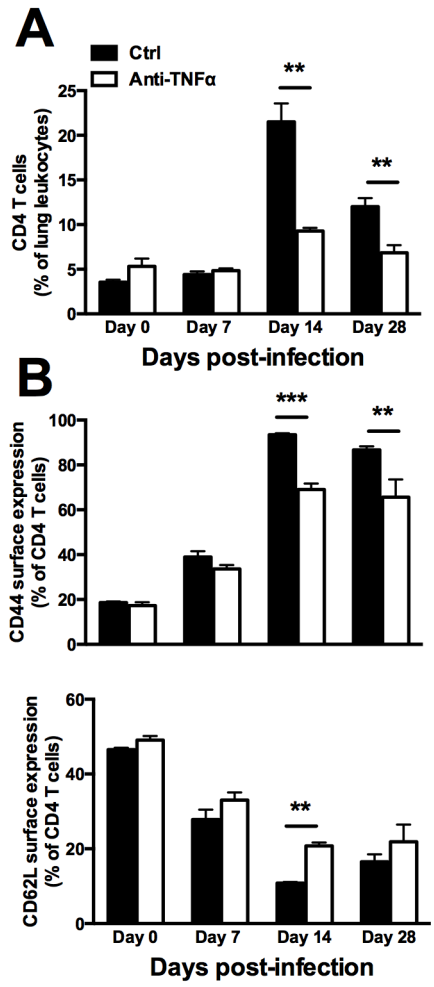

Figure 3-2 TNF α is required for CD4 T cell recruitment and activation.

CD4 T cells were identified by flow cytometry by sequentially gating live cells/CD45$^+$/CD3$^+$/CD8$^-$/CD4$^+$. The frequency of CD4 T cells (A) and their activation state (B) was determined by CD62L and CD44 surface staining. N = 8 from two separate, matched experiments. Representative histogram overlays are presented with bar graphs representing average percent positive. Statistical analysis was performed using 2-way ANOVA. * $p < 0.05$; ** $p < 0.01$; ***$p < 0.001$.

14 dpi as assessed by intracellular flow cytometry (Figure 3-3). Interestingly, despite a largely Th2 biased polarization, more $CD4^+$ T cells from TNFα-depleted mice made TNFα than did in the control mice. These data provided evidence that early TNFα signaling is required for optimal Th1 polarization of $CD4^+$ T cells and its depletion alters the Th1/Th2 balance of T cells recruited to *C. neo*-infected lungs.

We next broadly assessed the transcriptional profile of $CD4^+$ T cells isolated from dispersed lungs by MACS via qPCR arrays, which revealed that $CD4^+$ T cells from TNFα-depleted mice showed strong upregulation of Th2 transcription factors and Th2-related genes and lower amounts of Th1 transcription factors and related genes than control mice at all time points post-infection (Figure 3-4A). Thus, early TNF α is necessary for protective $CD4^+$ T cell-mediated immunity to *C.neo*.

TNFα is required for DC1 polarization in vivo

Because polarization of lung $CD4^+$ T cells following transient TNFα depletion was dysregulated, we next assessed the number, maturation, and polarization of DCs in the lungs. There was a small but statistically significant decrease in frequency of total monocytes in TNFα-depleted mice occurring at 14 dpi (Figure 3-5A). Due to the differences in total leukocyte numbers (Figure 3-1C), there were significant decreases in the number of monocytes in the lungs of TNFα-depleted, infected mice at 14 and 28 dpi (Figure 3-5B). To broadly characterize the polarization of differentiated lung DCs, we isolated RNA from $CD11c^+$ cells

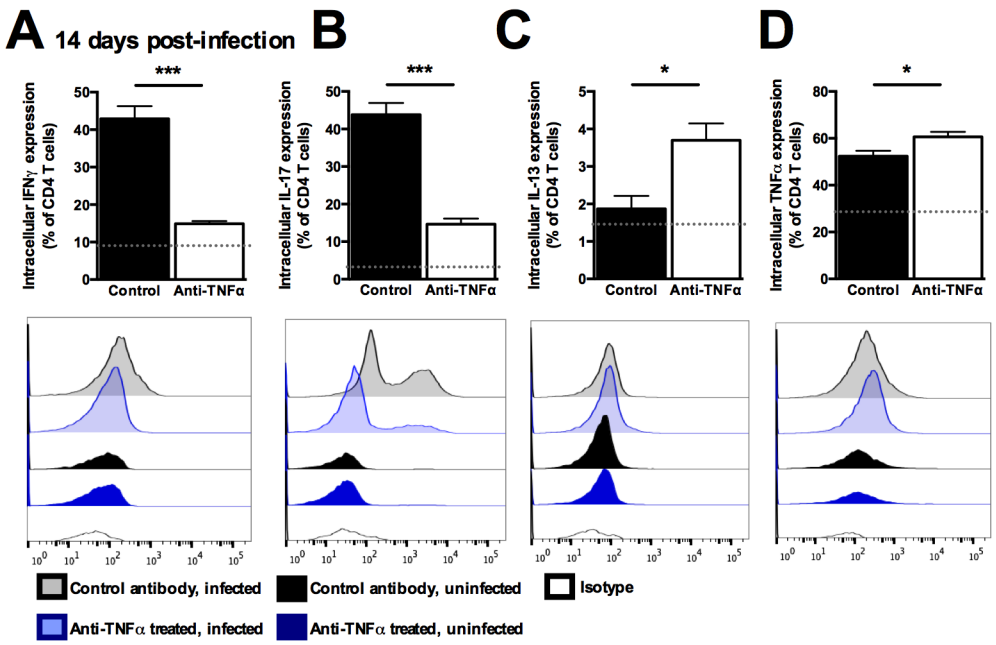

Figure 3-3 TNF α results in Th1/Th17 polarization of CD4 T cells during *C.neo* infection.

Mice were infected and a subset was depleted of TNF α as described above. Intracellular flow cytometry performed on enzymatically-digested lung at 14 dpi. T cells were sequentially gated on live cells/$CD45^+$/$CD3^+$/$CD8^-$/$CD4^+$, and then for expression of IFNγ (A), IL-17 (B), IL-13 (C) and TNFα (D). Statistical analysis was performed using student's t-test. * $p < 0.05$; ***$p < 0.001$.

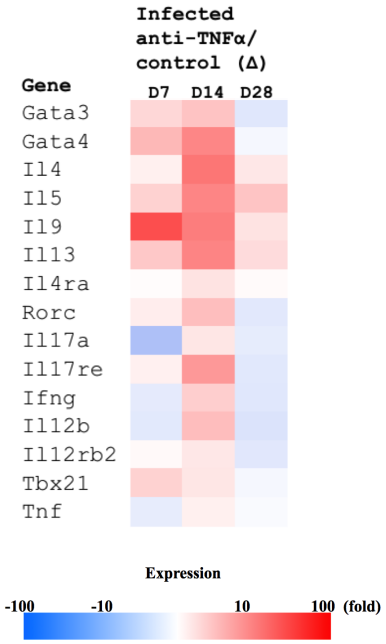

Figure 3-4 Afferent phase TNFα results in long lasting Th2 phenotype in the lungs.

Magnetically sorted $CD4^+$ cells isolated from mouse lung at 7, 14, and 28 dpi. CT values are presented as a heatmap of gene expression in TNFα-depleted infected mice relative to control-treated infected mice. N = 4-7 from separate, matched experiments.

magnetically separated from infected mouse lung and performed qPCR for iNOS and Arginase. The ratio of iNOS:Arginase mRNA expression was highly skewed towards iNOS production in control mice, but in TNFα-depleted mice, it was significantly skewed towards Arginase expression (Figure 3-5C). This motivated temporal analysis of the transcriptional profile of crucial DC1/DC2 genes expressed by the pulmonary CD11c cells. Results show that DCs from TNFα-depleted mice suppressed mRNA for DC1-associated cytokines, chemokines, and receptors compared to those in control mice throughout the studied time points (Figure 3-6). Analysis of DC1/2 marker expression on gated DC populations from TNFα-depleted mice revealed significantly lower surface expression of MHCII and costimulatory molecule CD86 and significantly higher surface expression of DC2 polarization markers CD206 and Mac2 compared to those in control mice at 7 dpi (Figure 3-7). This suppression of MHCII and CD86 and elevation of CD206 and Mac2 surface expression remained consistent through all studied time-points (data not shown). Thus, DCs were able to sustain their polarization throughout infection and, importantly, DCs from TNFα-depleted mice maintained suppressed DC1 and enhanced DC2 profiles well after TNFα levels recovered.

TNFα and IFNγ train DCs to maintain DC1 programming and suppress DC2 gene activation

This sustained downregulation of DC1 genes after transient TNFα depletion, even when TNFα levels have recovered, suggested that during the initial week of infection, TNFα was required to stabilize a DC1 transcriptional profile. We addressed this hypothesis using an *in vitro* model in which bone-marrow derived

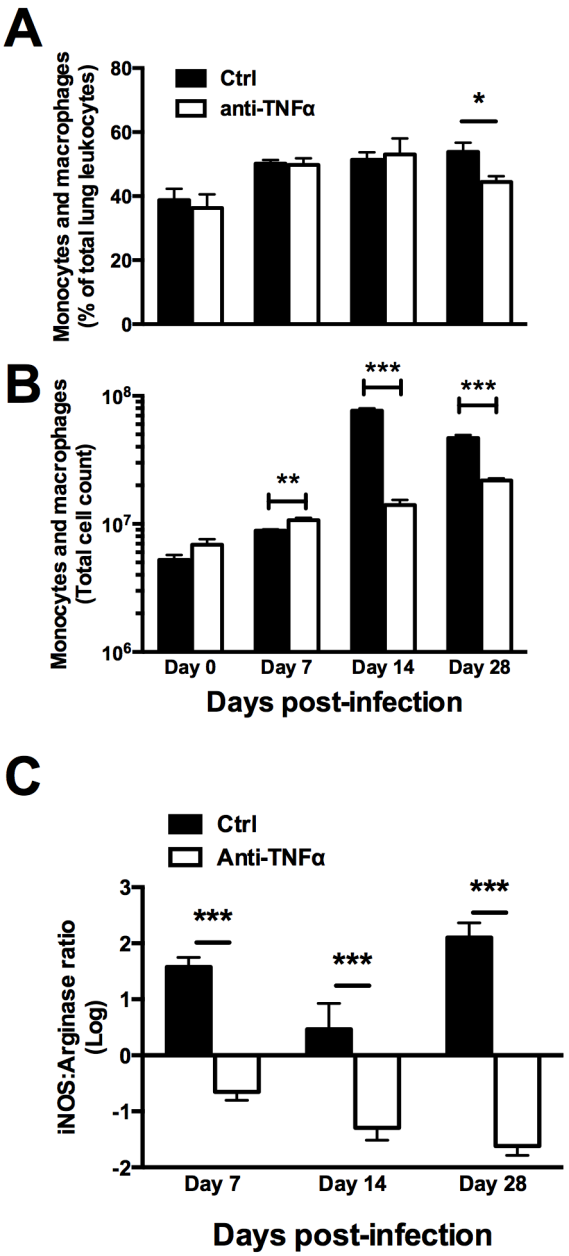

Figure 3-5 TNF α results in variable mononuclear phagocyte accumulation, but strong classical activation phenotype throughout infection.

Leukocytes from enzymatically-digested lungs were cytospun onto charged microscope slides, fixed and stained with a diff-quick kit, and then cell populations were enumerated by light microscopy. Monocyte frequencies (A) and total numbers (B) were calculated. $CD11c^+$ cells were isolated from lung leukocyte preparations by magnetic bead separation, and the ratio of iNOS to Arginase mRNA expression was calculated (C). N = 4-7 from two separate, matched experiments.

Statistical significance was determined by unpaired two-way ANOVA with multiple comparisons test or Student's t-test where appropriate. * $p < 0.05$; ** $p < 0.01$; ***$p < 0.001$.

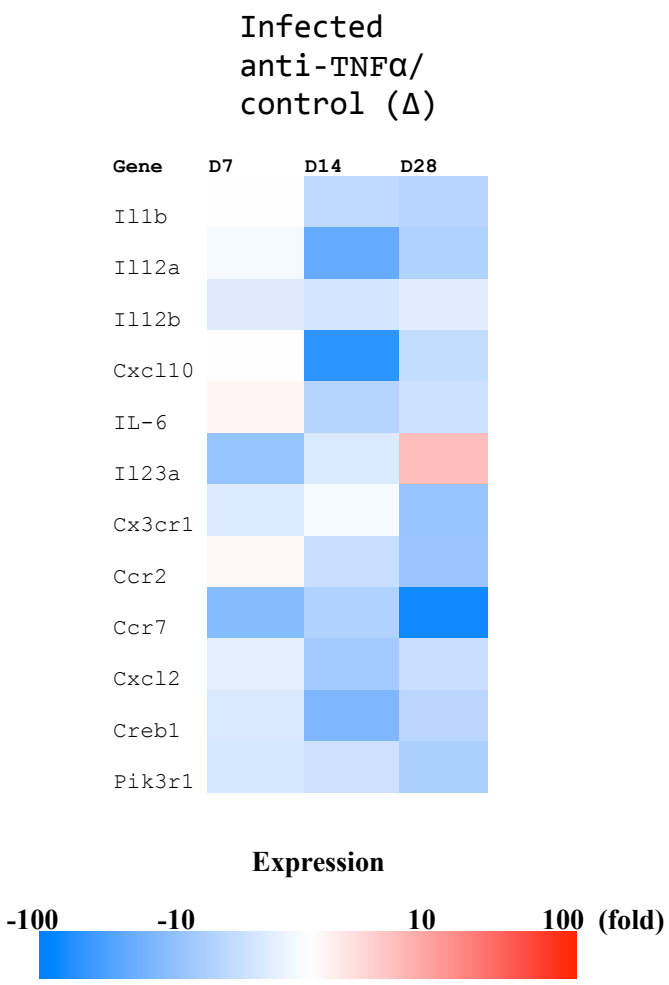

Figure 3-6 Depletion of TNFα disrupts long-term stable DC1 phenotype.

Magnetically sorted CD11c^{+} cells isolated from mouse lung at 7, 14, and 28 dpi. CT values are presented as a heatmap of gene expression in TNFα-depleted infected mice relative to control-treated infected mice. N = 4-7 from two separate, matched experiments. CT values are presented as a heatmap of gene expression in TNFα-depleted infected mice relative to control-treated infected mice. N = 4-7 from two separate, matched experiments.

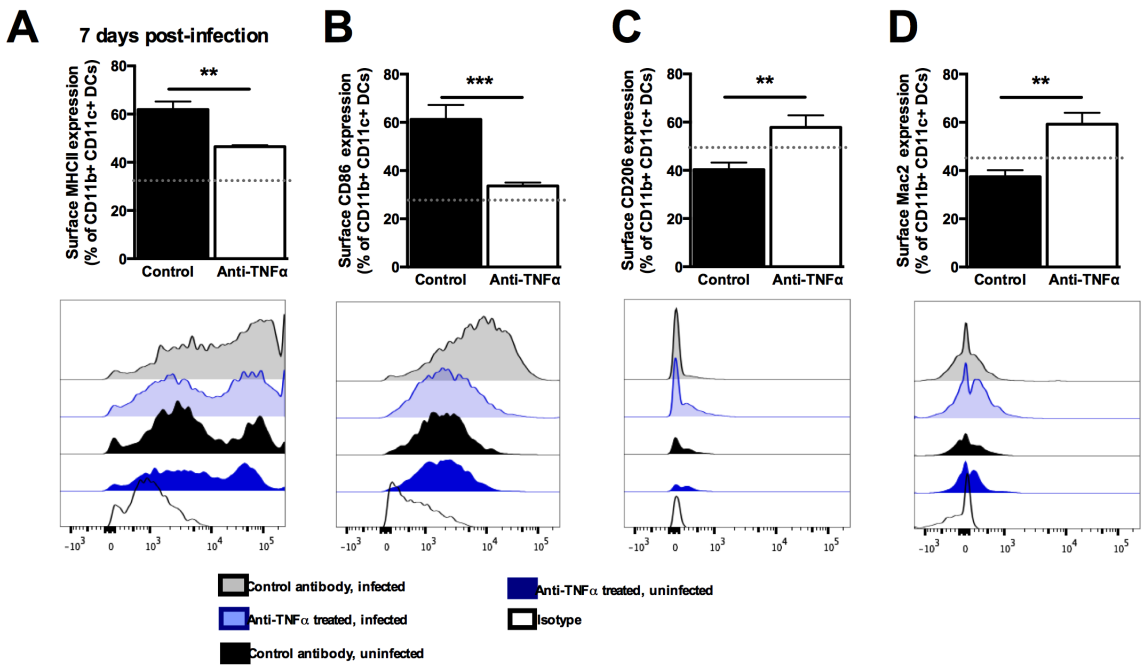

Figure 3-7 TNFα is required for increased surface expression of MHCII and costimulatory molecules and suppression of DC2 marker surface expression.

Extracellular flow cytometry performed on enzymatically-digested lung at 7 dpi. DCs were gated on $CD45^{+}/CD19^{-}/CD3^{-}/Ly6G^{-}/CD11b^{+}/CD11c^{+}$. DCs were then assessed for surface expression of MHCII (A), CD86 (B), CD206 (C), and Mac2/Gal3 (D). Representative histogram overlays are presented with bar graphs representing average percent positive. N = 8 from two separate, matched experiments. Statistical analysis was performed using student's t-test. ** $p < 0.01$; ***$p < 0.001$.

DC (BMDC) obtained from uninfected CBA/J mice were sequentially stimulated with DC1 (IFNγ) or DC2 (IL-4) polarizing cytokines in the presence or absence of TNFα. Specifically, BMDC were stimulated with IFNγ for 24 hours in the presence or absence of TNFα (training period), washed, and cultured with IL-4 for 24 hours (challenge period), and DC1 and DC2 marker gene expression was assessed by qRT-PCR and flow cytometry (for schematic, see Figure 6-1). All data was compared to media only-treated BMDCs, and each experiment included TNFα only-treated controls, which did not differ significantly from media-only treatment (data not shown). First, we assessed the expression of DC1 activation hallmark iNOS and DC2 activation hallmark Fizz1 by mRNA expression. Cells treated and challenged with IFNγ (γ-γ) alone had high expression of iNOS and low expression of Fizz1, consistent with DC1 activation (**Figure 3-8**A and B, black bars). Cells treated with IFNγ alone and challenged with IL-4 (γ-4) had low expression of iNOS and high expression of Fizz1, consistent with DC2 activation (**Figure 3-8**A and B, clear bars). However, cells trained with IFNγ and TNFα together had sustained high expression of iNOS and low expression of Fizz1 regardless of whether they were challenged with IFNγ or IL-4 (γα-γ and γα-4, respectively) (**Figure 3-8**A and B, dark and light grey bars, respectively). This decrease in DC1 polarization plasticity due to TNFα exposure during the training period will henceforth be referred to as TNFα training, similar to the innate immune training previously described (218, 219).

We next tested whether TNFα could train a DC2 phenotype brought about by IL-4 treatment or if the reduction in plasticity was unique to DC1/IFNγ-polarized cells. DCs were treated with IL-4 in the presence or absence of TNFα for 24

hours, washed, and challenged with IL-4 or IFNγ for 24 hours. DCs remained plastic to their environment regardless of whether TNFα was present (**Figure 3-8**C and D), showing that TNFα training was specific to DC1/IFNγ polarization.

In order to characterize the extent of TNFα training in DCs, we performed a screen for DC1 genes that encompassed many classical and alternative activation functional marker genes (Table 3-1). We observed a similar pattern of DC1 gene upregulation and DC2 gene downregulation in TNFα trained DCs in many classes of DC polarization and maturation genes, including antigen presentation and costimulatory molecules (MHCII, CD80, CD86), cytokines (IL-5, IL-12b, IL-13), and phagocyte/antigen processing genes (iNOS, Fizz1, Mac2). Interestingly, not all genes associated with DC1 polarization responded to TNFα training– specifically, the DC1 genes CD40 and IFNγ– whereas the DC2 gene Arginase was also resistant to TNFα-mediated training.

We next verified the TNFα training of MHCII and CD206 at the protein level using flow cytometry. γ-4 DCs had low MHCII surface expression, by both percent positive staining and mean fluorescence intensity, while γ-γ, γα-γ, and γα-4 DCs had both a higher percent positive cells and greater mean fluorescence intensity staining (Figure 3-9B). Conversely, γ-4 DCs had high CD206 surface expression and high mean fluorescence intensity, while γ-γ, γα-γ, and γα-4 DCs had low expression (Figure 3-9D). This TNFα training of MHCII and CD206 *in vitro* correlated to the sustained increase of MHCII and decrease of CD206 surface expression from gated DCs *in vivo*. CFSE proliferation assays confirmed that all treatment groups underwent similar, limited proliferation during the

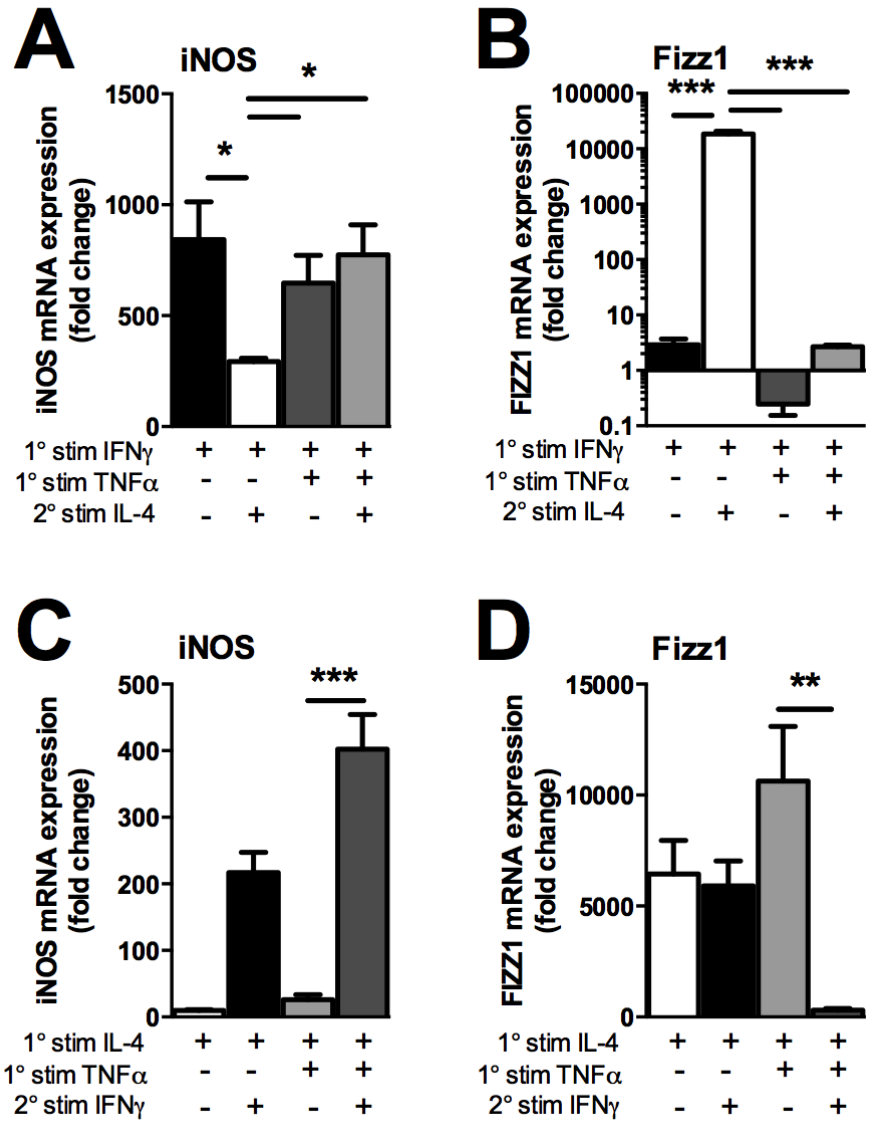

Figure 3-8 DC1 and DC2 marker genes exhibit plasticity *in vitro,* which can be reduced by the addition of TNF α .

Bone marrow-derived DCs from CBA/J mice were matured in GM-CSF over 7 days. Cells were plated and exposed to IFNγ in the presence or absence of TNFα for 24 hours (training phase). Cells were then washed and treated with IL-4 (challenge phase), or with IFNγ as a control. All qRT-PCR data is presented as relative to media-only-treated cells. (A and B) DC1 BMDCs polarized by IFNγ in the presence or absence of TNFα during the training phase were challenged with IL-4 to determine plasticity of DC1 and DC2 marker gene expression. iNOS (A) and Fizz1 (B) expression was assessed at the mRNA level by RT-qPCR. (C and D) DC2 BMDCs polarized by IL-4 in the presence or absence of TNFα during the training phase were challenged with IFNγ to determine whether training is specific for DC1 or also applicable to DC2. iNOS (G) and Fizz1 (H) levels were

analyzed by RT-qPCR. Statistical analysis was performed using 1-way ANOVA.* $p < 0.05$; ** $p < 0.01$; ***$p < 0.001$.

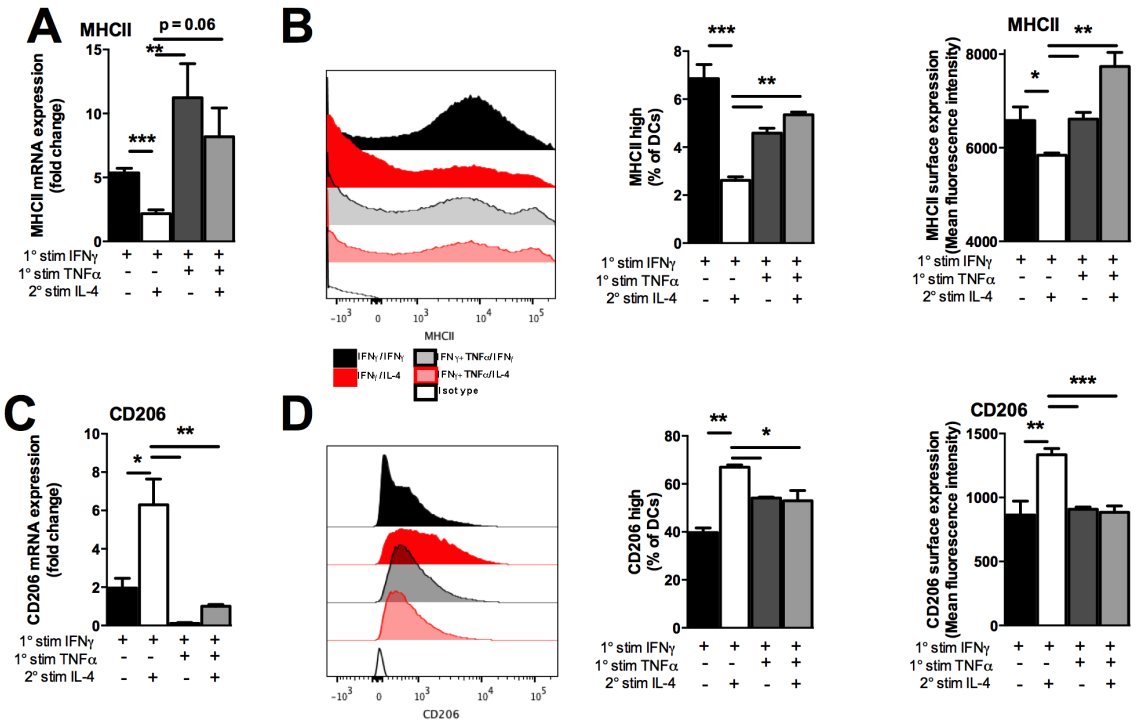

Figure 3-9 TNFα -mediated training observed at the mRNA level can also be seen in surface expression of DC1 and DC2 markers at the protein level.

(A and B) DC1 BMDCs polarized by IFNγ in the presence or absence of TNFα during the training phase were challenged with IL-4 to determine plasticity of DC1 and DC2 marker gene expression. MHCII (A) and CD206 (B) expression was assessed at the mRNA level by RT-qPCR.
(C and D) DC1 BMDCs polarized by IFNγ in the presence or absence of TNFα during the training phase were challenged with IL-4 to verify plasticity of surface marker expression at the protein level. MHCII (C) and CD206 (D) expression was assessed on the cell surface by flow cytometry. Representative histogram overlays are presented with bar graphs representing average percent positive. Statistical analysis was performed using 1-way ANOVA.* $p < 0.05$; ** $p < 0.01$; ***$p < 0.001$, or otherwise indicated

Gene class	DC1 genes
Gene	Pattern
IFNg	None
iNOS	Up in DC1
IL-2	Up in DC2
IL-6	Up in DC1
IL-12a	Up with IL-4 challenge
IL-12b	Up in DC1
IL-17	Up in DC1
IL-23	Unclear
TNFα	Unclear

Gene class	DC2 genes
Gene	Pattern
Arg1	Up with IL-4 challenge
CD206	Up in DC2
Fizz1	Up in DC2
Gal3	Up in DC2
IL-4	Up in non-trained DC1
IL-5	Up in DC2
IL-10	Up in non-trained DC
IL-13	Up in DC2
TGFb	Up in DC2
YM-2	Up with IL-4 challenge

Gene class	Methyltransferases and demethylases
Gene	Pattern
CBP	Up with IL-4 challenge
Dnmt3a	Up in TNFα-trained DCs
Dot1L	Up in DC2
EZH2	Up in DC2
G9a	Up in DC2
Jmjd3	Unclear
KDM3b	No differences
KDM5d	No differences
MLL1	Up in TNFα-trained DCs
Suv39h1	Up in DC2

Gene class	Maturation markers
Gene	Pattern
CCR7	Unclear
CD40	Unclear
CD80	Up in DC1
CD86	Up in DC1
MHCII	Up in DC1

Table 3-1 Genes screened for TNFα-mediated training

Tables of genes organized according to class of gene: DC1, DC2, maturation, or epigenetic modification enzymes. Patterns denoted are as follows:
None: no significant differences between treatments.
Up in DC1: γ-γ, $\gamma\alpha$-γ, $\gamma\alpha$-4 cells all have increased expression
Up in DC2: γ-4 cells have increased expression
Up with IL-4 challenge: up in γ-4 or $\gamma\alpha$-4 treatment, these genes appear to be not TNFα-trainable

Up in non-trained DC: γ-γ and γ-4 have increased expression
Up in non-trained DC1: γ-γ alone has increased expression.
Unclear: significant differences exist between some treatments, but the relationship between stimulus and gene regulation is unclear (and is not any other specified pattern).

training and challenge phases (Figure 3-10), which reinforces the idea that these changes are not being skewed by differential proliferation between treatment groups.

Finally, we tested whether secreted cytokines, in addition to intracellular and surface markers, responded to TNFα-mediated training. IL-12b was induced in γ-γ and $\gamma\alpha$-trained cells, but not in γ-4 DC2s (Figure 3-11A), whereas IL-13 was induced only in γ-4 cells and not in γ-γ or $\gamma\alpha$-trained DC1s (Figure 3-11B). Thus, TNFα was able to train DC1s to maintain high expression of DC1 functional surface proteins, cytokines, and polarization markers and low expression of DC2 functional surface proteins, cytokines, and polarization markers, even when DCs were challenged with pro-DC2 cytokines.

TNFα is required for induction of DC1 programming in the presence of cryptococcal antigen

Cryptococcal antigens are known modulators of DC activation (148, 149, 151, 157). Therefore, we next determined whether the addition of heat-killed *C.neo* (HKC) to the DC cultures during the training period would alter DC1 and DC2 marker expression. Surprisingly, γ-γ DCs were unable to upregulate IL-12b in the presence of HKC and exhibited IL-12b transcript levels similar to γ-4 DC2s; in contrast, $\gamma\alpha$-γ and $\gamma\alpha$-4 TNFα-trained DC1s upregulated DC1 cytokine expressions (Figure 3-11C), suggesting they were able to overcome the immunomodulatory effects of the HKC. We observed a similar pattern with iNOS expression upon exposure to HKC where γ-γ DCs were unable to upregulate iNOS transcript (data not shown). Both γ-γ and γ-4 DCs increased

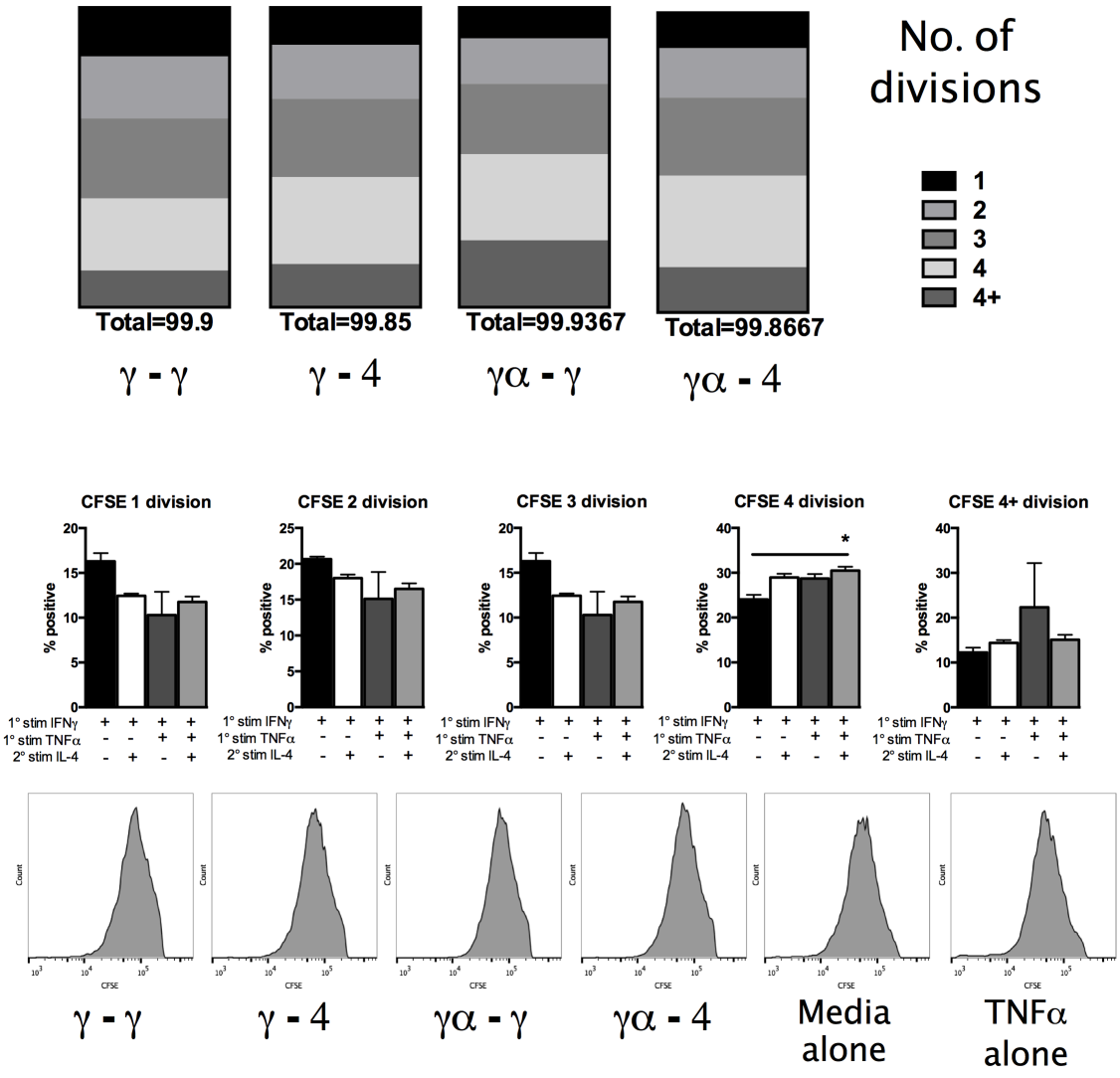

Figure 3-10 BMDCs receiving different training and challenge phase stimulations do not exhibit differences in proliferation.

BMDCs were loaded with CFSE to track proliferation in order to ensure that differences in mRNA expression analyzed in BMDC experiments based on

Figure 3-8 could not be attributed to differences in proliferation between the treatment groups. There was a slight but significant difference in proliferation between γ-γ cells and γα-4 treated cells that had moderate CFSE dilution (approx. 4 divisions), but no other significant differences in proliferation. Statistical analysis performed using 1-way ANOVA. * $p < 0.05$.

expression of IL-13 mRNA when stimulated with HKC, but TNFα training prevented DC IL-13 upregulation (Figure 3-11D). To validate this *in vivo*, we analyzed serum from infected mice and found that infected control mice had consistently elevated IL-12p70 and low IL-13 levels consistent with DC1/Th1 skewing, while serum from the TNFα-depleted infected mice had suppressed IL-12p70 and elevated IL-13 levels (Figure 3-11E and F) throughout infection, consistent with DC2/Th2 systemic polarization. Thus, not only were TNFα-trained DCs resistant to changes in polarization mediated by cryptococcal antigen, TNFα was uniquely necessary to overcome cryptococcal antigen-mediated suppression of DC1 activation.

Adoptive transfer of TNFα-trained DC1s rescues Th1 polarization in CD4 T cells from TNFα-depleted mice

We next tested whether TNF α -trained DCs were sufficient to skew Th polarization in TNF α -depleted, *C.neo*-infected mice. As detailed in Figure 3-12A, we infected and TNF α -depleted CBA/J mice on day 0. At 1 dpi and 8 dpi, mice received i.v. transfer of 1 million TNF α -trained DC1s (γ α) or untrained DC1s (γ only), and mice were sacrificed at 14 dpi to assess the polarization of CD4 T cells. The CD4 T cells of TNF α -depleted mice that received γ α DCs had a significant increase in frequency of cells staining positively for IFN γ , as well as increased intensity of IFN γ staining (Figure 3-12B and C). Untrained DC1s were insufficient to modulate Th polarization.

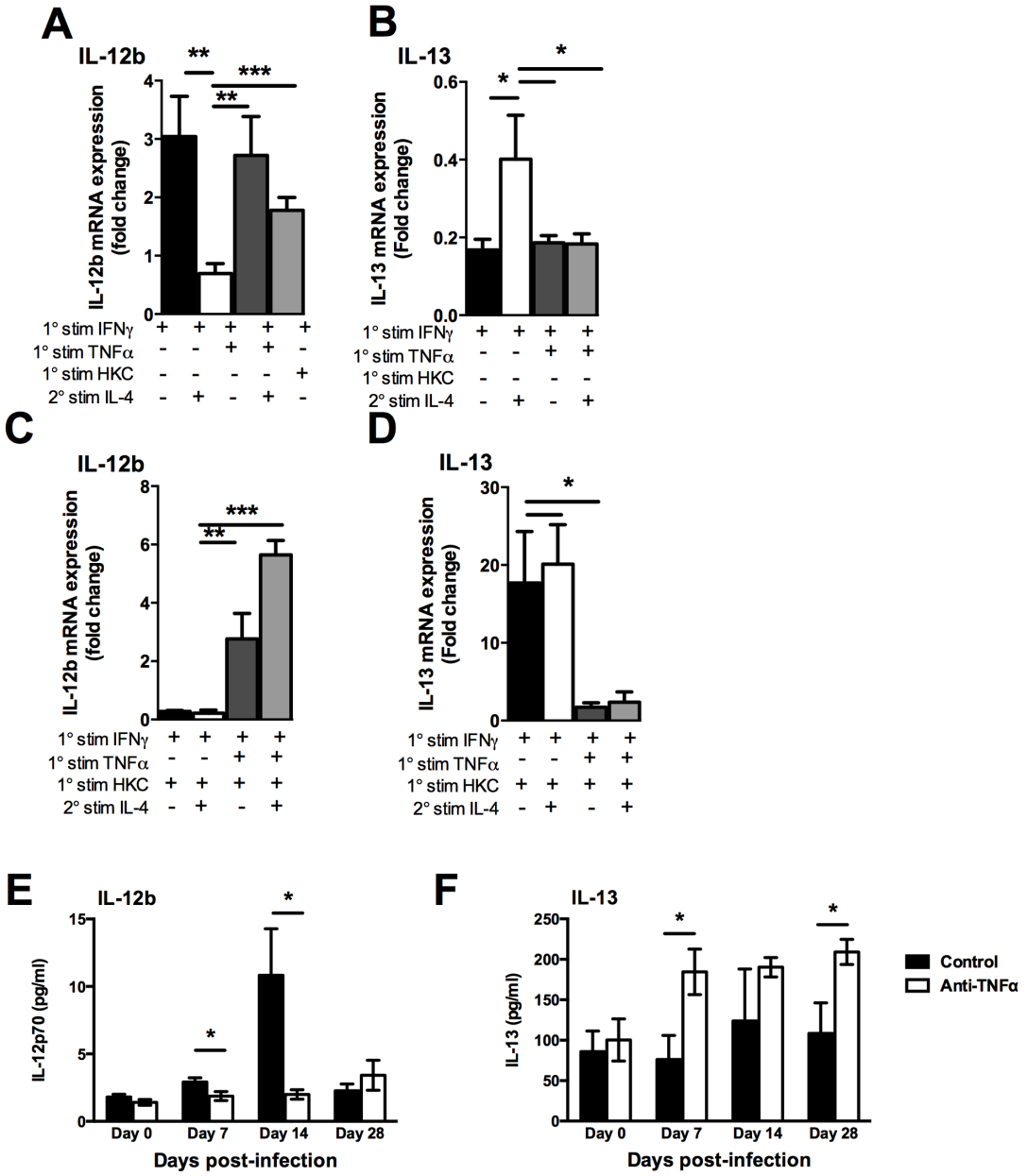

Figure 3-11 TNF α -mediated training applies to secreted cytokines in the presence of antigen *in vitro* and *in vivo*.

(A-D) BMDCs treated as in

Figure 3-8 but including heat-killed *C.neo* (HKC) during the training phase were assessed for IL-12b (A, B) and IL-13 (C, D) cytokine production by RT-qPCR to determine TNFα training of DC1 and DC2 cytokines and the effect of HKC on this training. Note the modulation of untrained, IFNγ-treated DCs (first column, C and D) by HKC preventing DC1 gene induction and inducing DC2 gene expression. (E and F) Serum levels of IL-12p70 (E) and IL-13 (F) from infected mice at 0, 7, 14, and 28 dpi were assessed by cytometric bead array. A, C: N = 18

from six separate, matched experiments; B, D: N = 9 from three separate, matched experiments; E, F: N = 4-12 from three separate, matched experiments. Statistical significance was determined by unpaired two-way ANOVA with multiple comparisons test. * $p < 0.05$; ** $p < 0.01$; ***$p < 0.001$, or otherwise indicated.

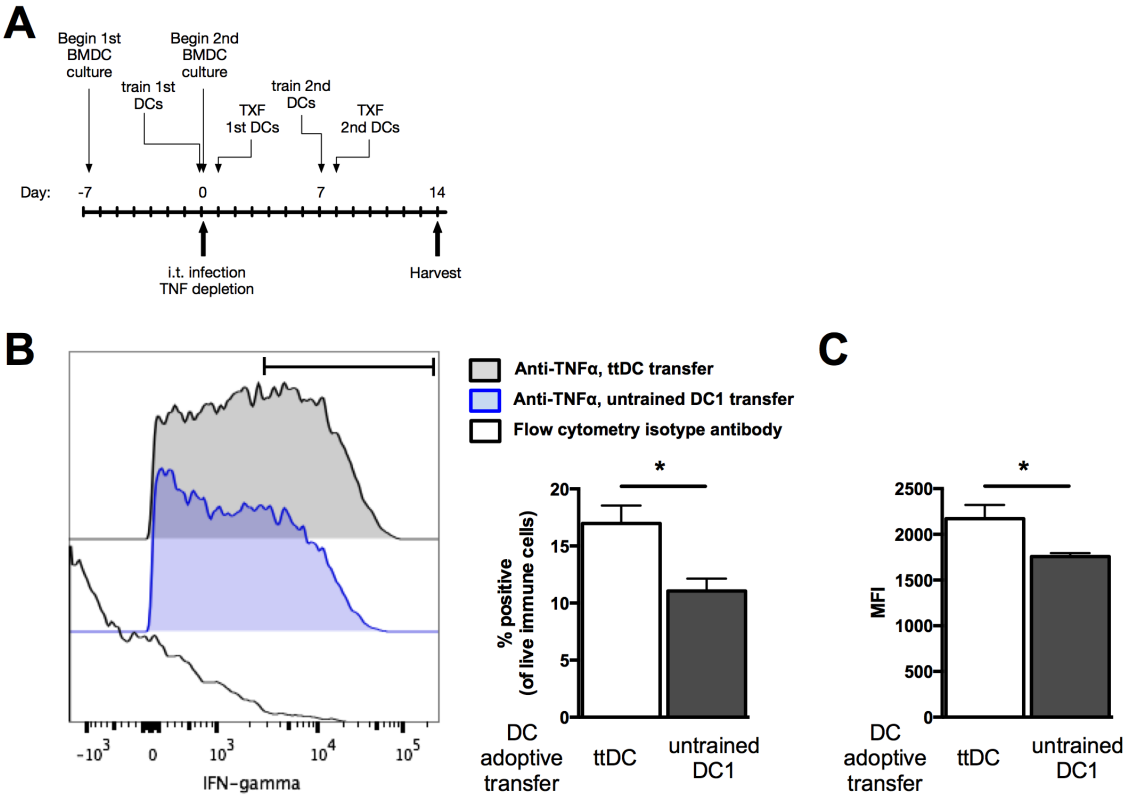

Figure 3-12 Transfer of TNF α -trained DCs rescues Th1 polarization in TNF α -depleted, *C.neo*-infected mice.

BMDCs were generated as in Figure 3-7, TNF α –trained or treated with IFN γ alone, and 1 million cells were transferred into infected, TNF α -depleted mice according to the schematic in (A). A greater frequency of CD4 T cells harvested at 14 dpi from mice receiving TNF α -trained DCs made IFN γ than from mice that received untrained DC1 (B). CD4 T cells from mice receiving TNF α -trained DCs also had a higher intensity of staining than CD4 T cells from mice that received untrained DC1 (C). N = 5. Statistical significance was determined using student's t-test. * $p < 0.05$.

TNFR1 and TNFR2 contribute non-redundantly to TNF α-mediated training in DCs

Lastly, we wanted to determine which receptor for TNF α was responsible for the observed TNF α-mediated training, TNFR1 or TNFR2. Blocking antibodies for TNFR1, TNFR2, or TNFR1 and 2 together were added to wells of the BMDC cytokine cycling experiments during the training phase, and RNA was harvested to assess loss of training. We found that iNOS training (upregulation) was partially blocked when TNFR1 was inhibited (Figure 3-13B), partially blocked when TNFR2 was inhibited (Figure 3-13C), but completely blocked upon dual receptor blockade (Figure 3-13D). Similarly, Fizz1 training (downregulation) was partially blocked when TNFR1 was inhibited (Figure 3-14B), partially blocked when TNFR2 was inhibited (Figure 3-14C), but completely blocked upon dual receptor blockade (Figure 3-14D). Thus, complete TNF α training requires signaling from both TNFR 1 and TNFR2.

Discussion

The present study examines the requirement for TNF α during the early stages of *C.neo* infection. We fully immunophenotyped pulmonary CD4 T cells (Figure 3-2, Figure 3-3, Figure 3-4), through 28 dpi, and show that TNF α mediates lasting protective immune responses. We determined that DCs activated in the presence of TNFα adopted a lasting DC1 phenotype and primed protective Th1/Th17 immune responses (Figure 3-5, Figure 3-6, Figure 3-7) sufficient to change the polarization of T cells from *C.neo*-infected, TNF α-depleted mice from

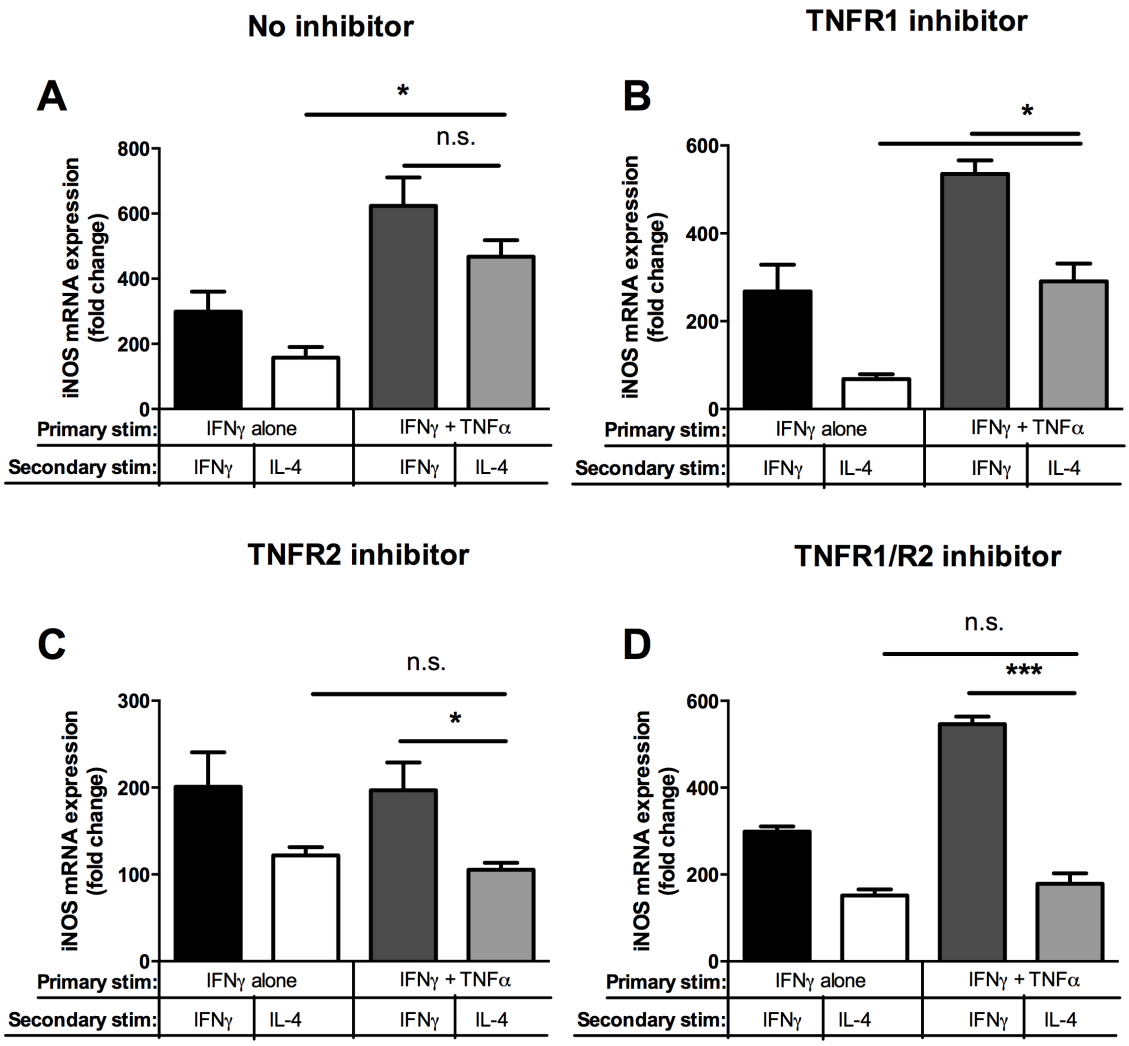

Figure 3-13 TNF α -mediated DC1 gene training is reliant on both TNFR1 and TNFR2 signaling.

BMDCs were treated with IFNγ and/or TNFαduring the training phase and IL-4 or IFNγ during the challenge phase as in

Figure 3-8. During the training phase, cells received either: no blocking antibodies (A), TNFR1 blocking antibodies (B), TNFR2 blocking antibodies (C), or TNFR1 and TNFR2 blocking antibodies (D). mRNA expression of iNOS was assessed for each group. Note the partial loss of training with each individual TNFR inhibitor, and the complete loss of training with blockade of both TNFR. Statistical significance was determined by unpaired two-way ANOVA with multiple comparisons test. * $p < 0.05$; ***$p < 0.001$.

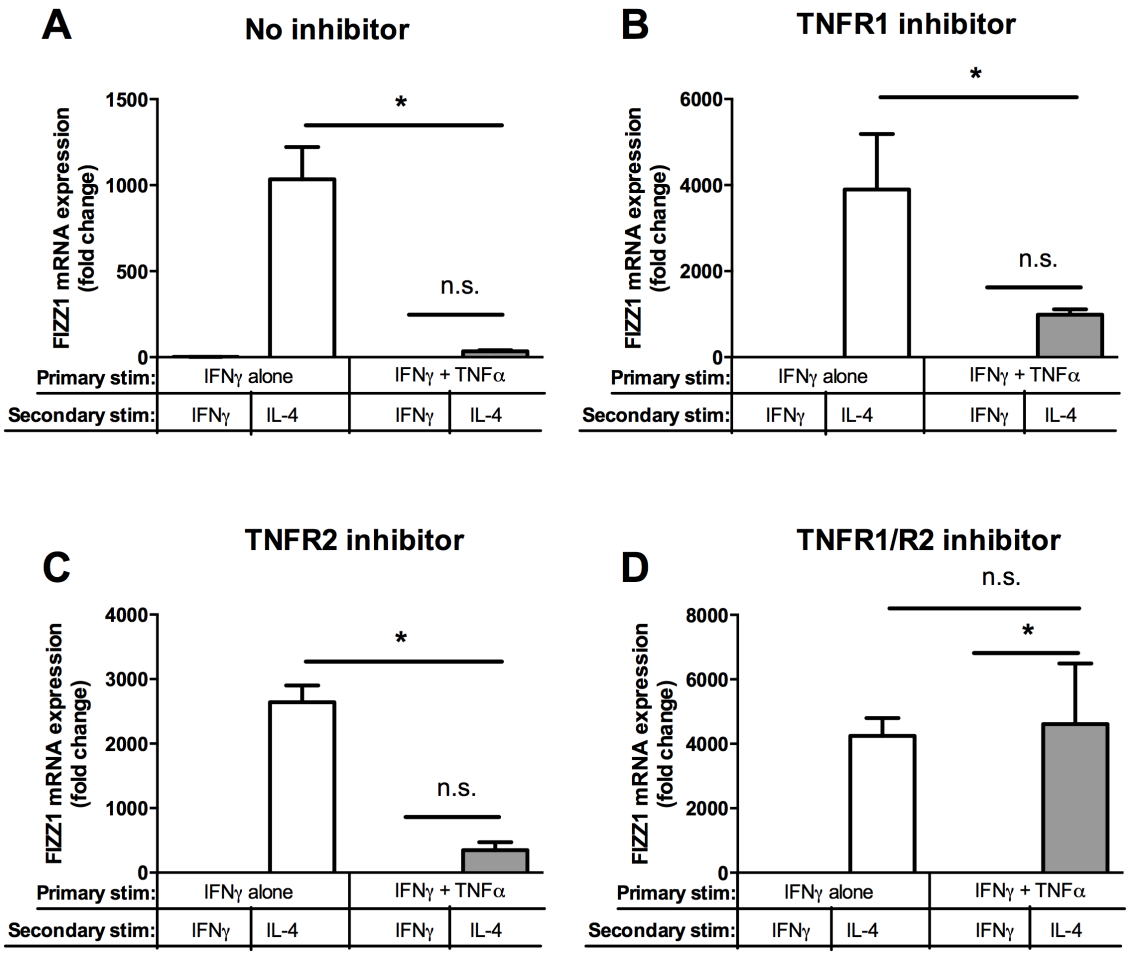

Figure 3-14 TNF α -mediated DC2 gene training is mediated by both TNFR1 and TNFR2 signaling.

BMDCs were treated with IFNγ and/or TNFαduring the training phase and IL-4 or IFNγ during the challenge phase as in

Figure 3-8. During the training phase, cells received either: no blocking antibodies (A), TNFR1 blocking antibodies (B), TNFR2 blocking antibodies (C), or TNFR1 and TNFR2 blocking antibodies (D). mRNA expression of Fizz1 was assessed for each group. Note the partial loss of training with each inhibitor individually, and complete loss of training with both TNFR blocking antibodies. Statistical significance was determined by unpaired two-way ANOVA with multiple comparisons test. * $p < 0.05$; ***$p < 0.001$.

Th2 to Th1 (Figure 3-12). Finally, we linked TNF α -mediated DC training to the nonredundant signaling of both TNFR1 and TNFR2 (Figure 3-13, Figure 3-14). The data presented in this manuscript represents a significant advance in our understanding of the necessity for TNFα during fungal infection.

We find here that early TNFα signaling is responsible for the generation of a stable DC1 population that sustains its robust DC1 phenotype throughout several weeks of infection, which is the time required for efficient clearance of *C.neo*. The sustained DC1 presence leads to generation of lasting protective Th1 anticryptococcal immunity. Consistently robust Th1/Th17 immune responses are necessary for control and clearance of *C.neo* from the lungs (3, 64, 69, 72, 169). Previous work using this model of transient TNFα depletion has shown that TNFα is critical for early induction of pro-Th1 cytokines at the global lung level (85). Those studies also suggested that immature DCs migration to the draining lymph nodes may account for the subsequent development of defective, non-protective immune responses (84). However, as we show here, the DCs in the *C.neo*-infected lung in the absence of TNFα display many characteristics of mature DCs, with robust co-expression of markers of DC2 activation (of which, some are shared with markers of immaturity, such as CD206) (Figure 3-5C, Figure 3-6, Figure 3-7). Our adoptive transfer studies showed conclusively that DCs activated with TNFα and IFNγ combined (trained DCs) are uniquely able to enhance Th1 polarization in *C.neo*-infected TNFα-depleted mice, in contrast with unstable DC1s (activated with IFNγ alone), which were unable to improve the Th1 response (Figure 3-12). Thus, we conclude that TNFα signaling is a necessary

component for the robust and stable DC1 phenotype, and perpetuates the robust and stable Th1 response necessary for clearance.

Our *in vitro* modeling clearly shows fundamental differences in how DCs respond to changing environments (i.e. pro-DC1 to pro-DC2), depending on how they were initially activated. While γ-only-activated DCs (γ- γ) had an obvious DC1 phenotype, this phenotype switched to DC2 upon changing the cytokine environment to pro-DC2 (γ -4). However, DCs activated with IFNγ and TNFα (γα- γ or γα -4) had the same obvious DC1 phenotype as γ-only DCs, but they maintained their DC1 phenotype upon changing the cytokine environment to pro-DC2. γα DCs reacted differently than γ-only DCs to the same secondary stimulus.

Our *in vitro* experiments show that TNF α -mediated training of DCs is not a phenomenon restricted to *C.neo* infection; indeed, initial testing of the model took place in the absence of an antigen (**Figure 3-8**, Figure 3-9). This is unique in the field of innate immune training, where reports of training in monocytes occur in response to sepsis and serum LPS (188, 192, 220, 221), and in response to fungal β -glucans and the BCG vaccine (218, 219, 222, 223). For our model, in the absence of *C.neo* antigen, DC1 polarization can be induced by treatment with IFNγ alone, but this is not a long-lasting DC1 polarization, and can quickly change to DC2 in response to changing cytokine environment (**Figure 3-8**, Figure 3-9). However, in the presence of *C.neo* antigen– known to be a suppressor of DC classical activation (148, 149, 151, 157)– our experiments show that IFNγ alone cannot induce DC1 polarization (Figure 3-11), and in the presence of *C.neo*

antigen, TNF α is absolutely necessary to both induce DC1 and suppress DC2 cytokine expression.

Interestingly, our data reveals that not all DC1 genes are subject to TNFα-mediated training, nor are all DC2 genes stably downregulated by TNFα training when followed by IL-4 challenge in vitro (Table 3-1). This division of genes into "TNFα-trainable" and "TNFα non-trainable" expands on work done by Foster *et al.* in 2007 (190) in a model of endotoxin tolerance, wherein specific genes (i.e. RANTES) could always be expressed regardless of whether the macrophage was endotoxin-tolerant, while other genes (i.e. IL-6) were consistently suppressed in endotoxin-tolerant macrophages but not in non-endotoxin-tolerant macrophages. A similar phenomenon may be occurring in TNFα-trainable genes versus non-TNFα-trainable genes.

The TNF α receptors necessary for signaling during cryptococcal infection, particularly in DCs, have not been elucidated yet. We found that blocking each TNF α receptor individually decreased the magnitude of TNF α -mediated training, but did not completely ablate training, while blockade of both receptors did ablate training (Figure 3-13, Figure 3-14). Work by Dong *et al.* implicated TNFR p75-80 (TNFR2) on the neutrophil cell surface as a target of immune modulation by cryptococcal polysaccharide capsule (224). Further, soluble TNFR2 in the cerebral spinal fluid of cryptococcal meningitis patients was correlated with survival (225). However, neither of these studies 1) investigates the role of TNFα signaling through the receptors, instead using them as markers; 2) directly reference DCs; and 3) specifically address and/or exclude the contributions of TNFR1 (due in part to complications with antibodies against

TNFR1 at the time of these studies). Thus, our findings that each receptor contributes non-redundantly to DC training *in vitro* represent a significant step forward.

Based on our findings from this paper and other recent work from our laboratory, we have assembled a model mechanism for the requirement of TNFα early during *C.neo* infection. Early signaling through TNFα receptors in DCs is necessary to classically activate DCs upon initial exposure to *C.neo*, and to maintain that polarization throughout many weeks of infection (Figure 3-5, Figure 3-6, Figure 3-7A, B). These DC1 cells matured in the presence of TNFα are resistant to changing their polarization caused by changes in cytokine environment (**Figure 3-8**, Figure 3-9) and/or by immune modulation by *C.neo* antigen (Figure 3-11). For human patients receiving TNF α monoclonal antibody therapy, this defect in DC1 activation may be responsible for their heightened susceptibility to *C.neo* and other infections, such as *Histoplasma capsulatum* or *Mycobacterium tuberculosis*. Based on our adoptive transfer studies (Figure 3-12), a potential therapy whereby DCs from the same patient are harvested and re-polarized may prove successful in controlling and eventually clearing infection.

Chapter 4 Epigenetic modification of DCs and DC precursors within the bone marrow by TNFα during cryptococcal infection[4]

Abstract

TNFα is required for protective Th1 immunity to *Cryptococcus neoformans* (*C.neo*) and these effects are linked to the stable, early classical activation of dendritic cells (DC1), preventing alternative (DC2) activation. We hypothesized that TNFα trains DC1s by inducing activating epigenetic modifications of key DC1 genes. We first assessed levels of the activating histone modification histone 3 lysine 4 trimethylation (H3K4me3) signature in DCs *in vitro* and *in vivo*. TNF α -trained BMDCs had a high H3K4me3 signature; DC1 DCs from 7 dpi *C.neo*-infected mouse lung also had high H3K4me3, while DC2 DCs from 7 dpi TNF α -depleted *C.neo*-infected mouse lungs did not. We performed chromatin immunoprecipitation from $CD11c^+$ lung cells and found that DC1 genes iNOS

[4] Excerpts of this chapter taken from:

Eastman, A.J., J. Xu, N. Potchen, A. denDekker, L. M. Neal, G. Zhou, A. Malachowski, S. Kunkel, J. J. Osterholzer, and M. A. Olszewski. TNF α is necessary for long lasting protective immunity to fungal infection through epigenetic stabilization of classically activated dendritic cells and bone marrow dendritic cell precursors. In submission at Science Immunology.

and IL-12b were associated with the H3K4me3 modification in DC1s from *C.neo*-infected mice at a greater rate than from TNFα-depleted *C.neo*-infected mice. The H3K4me3 signature appears to be dependent on the H3K4 methyltransferase MLL1 in TNFα-trained DCs, as opposed to being mediated by H3K4 demethylase KDM5d in DC2 cells. Because the DC1 polarization was so long lasting *in vivo*, we assessed myeloid precursor cells and pre-DCs within the bone marrow compartment for evidence that they were being recruited already predisposed to DC1 or DC2 activation. Pre-DCs from *C.neo*-infected mice sorted by flow cytometry had increased H3K4me3 signature consistent with those of pulmonary DC1s, while pre-DCs from TNFα-depleted *C.neo*-infected mice did not. Finally, BMDCs matured *ex vivo* from infected mouse bone marrow were assessed for TNFα-mediated training and plasticity; BMDCs from *C.neo*-infected mice already exhibited TNFα-mediated training, while BMDCs from TNFα-depleted *C.neo*-infected mice were unable to responds to TNFα. We conclude that histone modifications in DC are significantly altered by TNFα, and that this correlates with increased DC1 stability during protective responses to *C.neo* infection, and further extends to pre-polarization of DC precursors in the infected mouse bone marrow compartment.

Introduction

In the previous chapter, we showed that afferent-phase TNFα was necessary for long-lasting efferent Th1/Th17 immune responses. DCs, responsible for priming and restimulating T cells during *C.neo* infection, had stable and robust DC1

programming during both the efferent and afferent phases of the immune response to *C.neo* infection in the presence of TNFα, and thus primed and perpetuated protective Th1 T cell-mediated immunity throughout the infection. We modeled this *in vitro*, and show a unique phenotype of DC reliant on the combined signaling of TNFα and IFNγ; these DCs maintained DC1 polarization even upon challenge with pro-DC2 environments. We determined *in vitro* that the TNFα-mediated training was due to both TNFR1 and TNFR2. This addressed the cellular mechanism behind the necessity for TNFα during *C.neo* infection, but did not yet address the molecular mechanism. The following experiments in Chapter 4 determine the mechanism behind TNFα-mediated training of DCs.

It is largely unknown how innate immune cells remember to respond to particular pathogens throughout infection– particularly chronic infections– although epigenetic modifications are increasingly appreciated as a potential mechanism. TNFα signaling itself has been shown to stimulate chromatin modification in endothelial cells (186), but its effects on immune cell chromatin remodeling during infection remain unstudied. Trained immunity has been elegantly characterized in effector macrophages in a model of restimulation following acute fungal infection (218, 219, 222), as a lasting consequence of sepsis in circulating monocytes (188, 192, 220, 226), and proposed as the mechanism behind broad antimicrobial effects of infant BCG vaccination (223, 227, 228). However, much of these studies focus on the effector function of myeloid cells, and not on priming of adaptive immune responses.

In this chapter, we determined the molecular mechanism behind TNF α-mediated training of DCs, and propose a mechanism for perpetuating the stable DC1 population *in vivo*. Because the TNF α depletion only lasts 7-14 days, and TNF α levels recover in *C.neo*-infected mice, but the non-protective immune response to *C.neo* persists many weeks after TNF α recovery, we hypothesize that TNF α is responsible for epigenetic modifications that promote and/or reinforce DC1 programming. Thus, these TNFα-trained DC1s are able to prime Th1 responses in TNFα-depleted *C.neo*-infected mice. To address this, we first assessed differences in selected epigenetic modifications at the global level in TNF α-trained DCs, untrained DC1s, and DC2s *in vitro* and *in vivo*. We then used chromatin immunoprecipitation to determine whether DC1 or DC2 genes are associated with activating epigenetic modifications. We tested which epigenetic modification enzyme(s) are responsible for our TNF α-trained DC phenotype. Finally, we performed *ex vivo* experiments on the bone marrow from *C.neo*-infected mice to probe whether recruited monocyte-derived DCs differ in the presence or absence of TNF α.

Results

TNFα and IFNγ signaling results in epigenetic activation of DC1 genes in an MLL1-dependent manner

The sustained changes to DC polarization and plasticity observed *in vivo* and *in vitro* from Chapter 3 suggested to us an epigenetic mechanism. We first broadly characterized the H3K4me3 profile of DC1, DC2, and TNFα-trained DCs *in vitro*

by intranuclear flow cytometry. Non-TNFα-trained DC1 and DC2 cells had a similar, low H3K4me3 signature and a lower frequency of cells staining intensely for H3K4me3 (Figure 4-1A, black and white bars). Both $\gamma\alpha$-γ and $\gamma\alpha$-4 TNFα-trained DCs had an increase in both the frequency and intensity of staining for H3K4me3, further suggesting that TNFα-trained DCs are distinct from both DC2 and untrained DC1 cells (Figure 4-1A, grey bars). We confirmed these findings *in vivo* from DCs isolated from the lungs of infected mice at 7 dpi. Sorted DCs from infected control mice, which we have shown to be DC1, had higher levels of H3K4me3 compared to DCs from infected TNFα-depleted mice (DC2-skewed) or uninfected mice (Figure 4-1B). These data supported our hypothesis that epigenetic mechanisms, specifically changes in the activating histone modification H3K4me3, are involved in TNFα-mediated stabilization of DCs.

We next performed chromatin immunoprecipitation on $CD11c^+$ cells magnetically separated from the lungs of mice at day 14 post-infection to determine whether changes in the global H3K4me3 signature of the DCs corresponded to the activation or repression of relevant DC1 or DC2 genes *in vivo*. This is a time point where there is a small but significant difference in antigen levels between the two treatment groups, but where TNFα levels have recovered in TNFα-depleted mice. Using antibodies specific for H3K4me3, we pulled down antibody-histone-DNA complexes, purified the DNA, and performed qPCR with primers specific for the promoter regions of key DC1 genes. We observed that infection with *C.neo* resulted in strong enrichment of H3K4me3 at the iNOS and IL-12b promoter regions of control mice (Figure 4-2 A and B), indicating epigenetic activation of these genes, which is consistent with

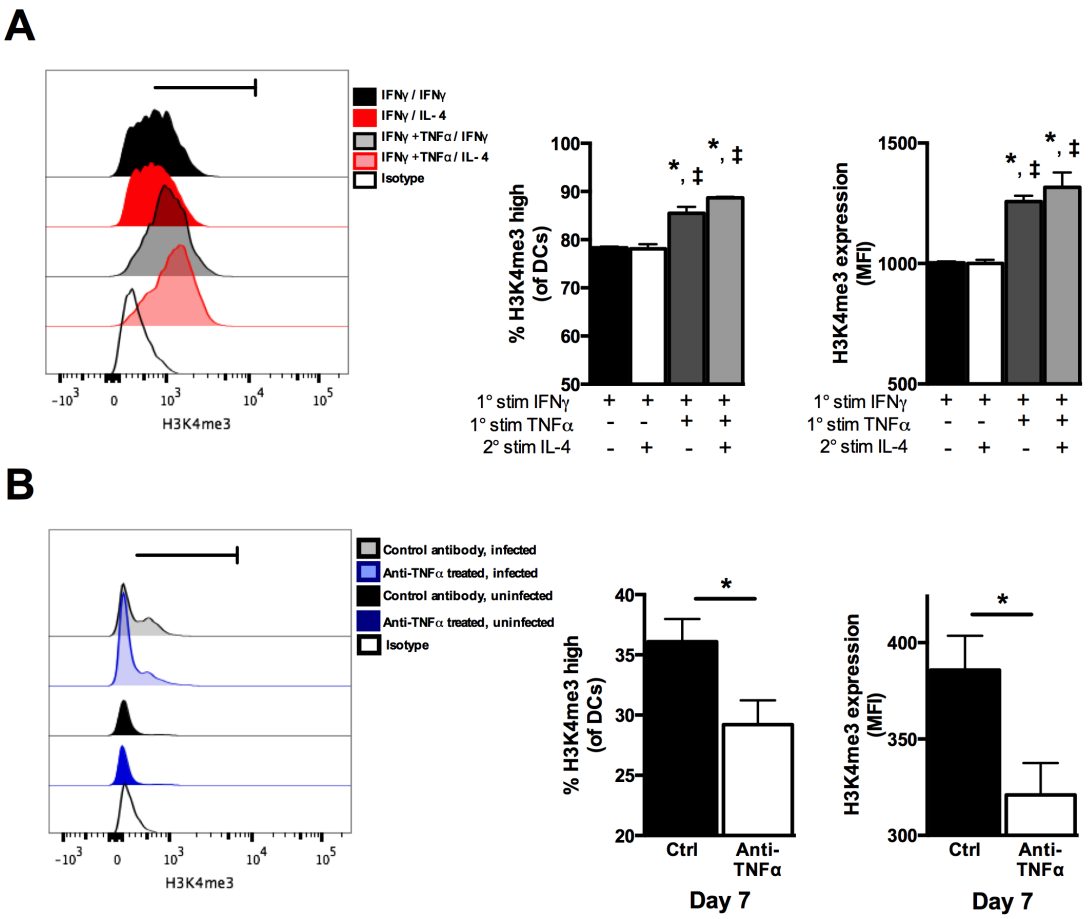

Figure 4-1 High H3K4me3 signature associated with TNF α -trained DC1s *in vitro* and *in vivo*.

BMDCs were treated as in

Figure 3-8 and subjected to flow cytometric analysis (A) or cell populations were flow cytometry-gated DCs from 7 dpi enzymatically digested mouse lungs (B). Cells were stained for intranuclear expression of H3K4me3 and analyzed by flow cytometry. Data is presented as representative histogram, percent positive/high, and mean fluorescence intensity. N = 6-8 from two separate, matched experiments.

their increased mRNA expression. In contrast, CD11c$^+$ cells from TNFα-depleted mice showed significant suppression of H3K4me3 signature at these promoter regions (Figure 4-2A and B) consistent with their decreased mRNA expression. There were no differences in enrichment of H3K4me3 for the β-actin promoter, our positive control (Figure 4-2C). Interestingly, in the infected, TNFα-depleted mice, we observed a trend towards enrichment of H3K4me3 at the promoter region of Fizz1 (Figure 4-2D), which was not seen in the infected control mice.

To mechanistically link the effects of TNFα signaling with an increased H3K4me3 signature, we next assessed the induction of H3K4 histone demethylase KDM5d and H3K4 histone methyltransferse MLL1, as these two kinases are largely responsible for proximal gene repression/de-repression at H3K4 (229, 230). KDM5d mRNA expression was not induced by TNFα or uniquely induced in DC1 or DC2 cells (Figure 4-3A). However, MLL1 mRNA expression was highly induced in TNFα-trained DC1s, both in the presence and absence of cryptococcal antigen (Figure 4-3B). Interestingly, the addition of TNFα alone to BMDCs was insufficient to increase MLL1 mRNA levels (Figure 4-3C). Furthermore, TNFα-depletion resulted in significant suppression of MLL1 mRNA levels in CD11c$^+$ cells isolated from the lungs of infected mice at both early (7 dpi) and late (28 dpi) timepoints (Figure 4-3D).

MLL1 is essential for adding the mono- and di-methylation onto H3K4me3, while MLLs 3 and 4 add the final trimethylation (179). Using the MLL1 inhibitor MM102 (231) during the initial 24-hour training phase, followed by the 24-hour challenge phase without the inhibitor, we found that inhibition of MLL1 did not prevent induction of DC1 genes iNOS and IL-12b in $\gamma\alpha$-γ DCs (Figure 4-4A and

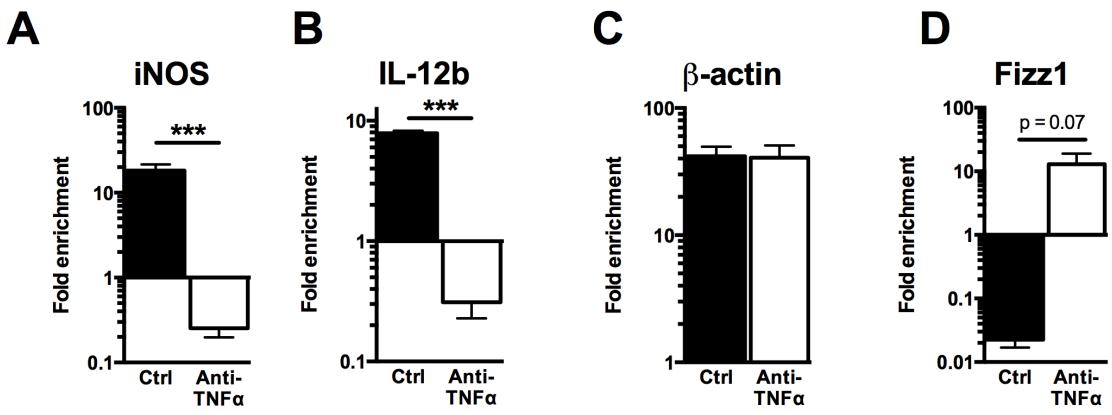

Figure 4-2 DC1 gene promoter regions of DCs matured in the presence of TNFα and cryptococcal antigen *in vivo* are associated with H3K4me3.

Mice were infected and/or TNFα-depleted as in Figure 3-1. $CD11c^{+}$ cells were magnetically sorted from enzymatically digested mouse lung at 14 dpi, then fixed and frozen at -80 (data is pooled from 12 samples each treatment from three separate, matched experiments). Chromatin immunoprecipitation was performed using anti-H3K4me3 or control antibodies. RT-qPCR was performed on purified immunoprecipitated DNA using primers specific for iNOS (A), IL-12b (B), β-actin (C) and Fizz1 (D) promoter regions.
Statistical significance was determined by student's t-test. ***$p < 0.001$ or otherwise indicated.

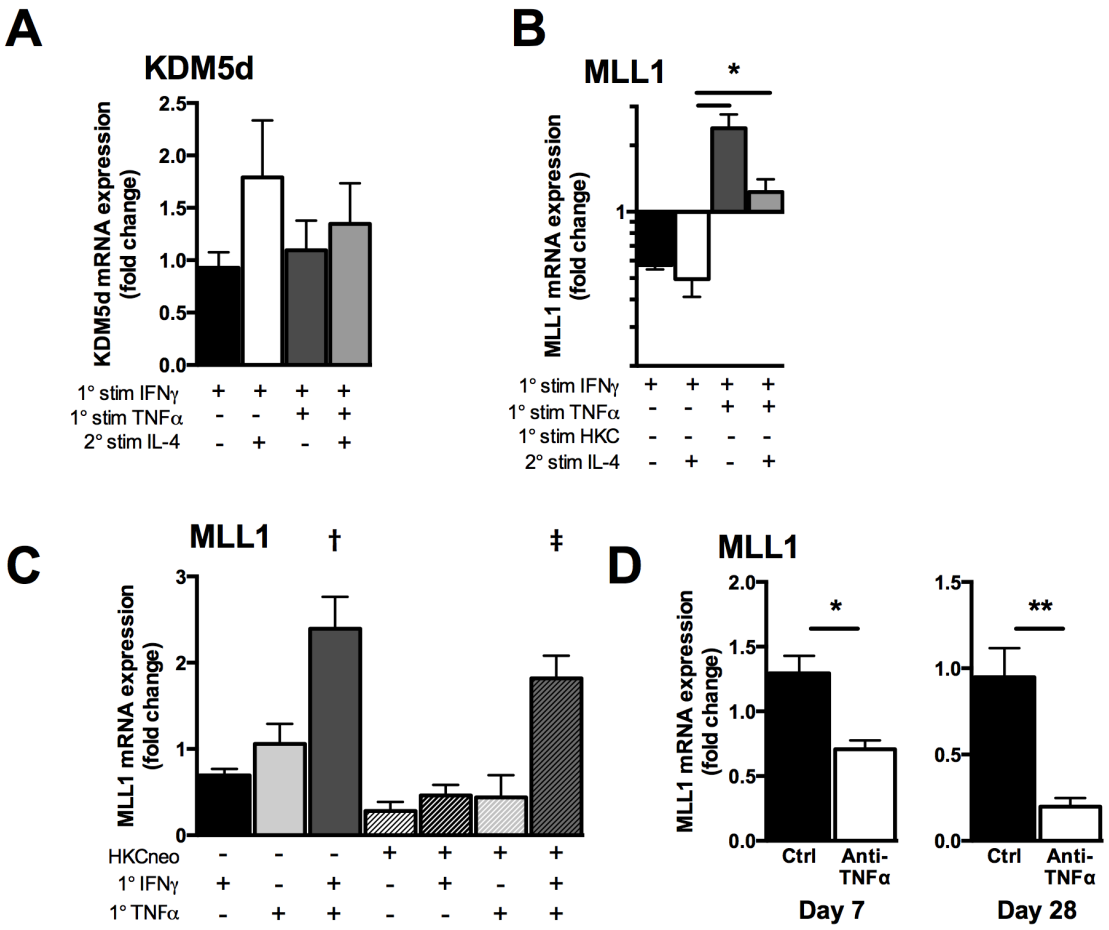

Figure 4-3 MLL1 mRNA expression is induced by TNFα and IFNγ combined, but not separately *in vitro* and is induced only in DC1s from infected control animals *in vivo*.

(A and B) BMDCs were treated as in

Figure 3-8. mRNA levels of KDM5d (A) and MLL1 (B) were assessed for induction in TNFα-trained DCs by qRT-PCR. N = 18 from six separate, matched experiments.

(C) MLL1 induction was subsequently tested in the indicated conditions with and without HKC to determine specificity of induction. † represents statistically significant difference between $\gamma\alpha$ and γ alone, while ‡ represents statistically significant difference between $\gamma\alpha$HKC and γHKC alone. N = 9-18 from separate, matched experiments.
D) Mice were infected and a subset was TNFα depleted as in Fig. 1. Magnetically separated CD11c $^{+}$ cells from enzymatically digested mouse lung at 7 dpi (early) and 28 dpi (late) were assessed for MLL1 expression by RT-qPCR. N = 6-8 from two separate, matched experiments.

B). However, when TNFα-trained DCs were challenged with IL-4 after MLL1 inhibition during the training phase, the training was ablated and $\gamma\alpha$-4 DCs were plastic to their cytokine environment similar to untrained DCs (Figure 4-4A and B). This finding shows that inhibition of MLL1 prevents the TNFα-mediated training of DC1 genes.

TNFα is required for DC1 pre-programming in the bone marrow of C.neoformans*-infected mice*

Because the duration of the TNFα-trained pulmonary DC phenotype *in vivo* during *C.neo* infection last far longer than the expected lifespan of inflammatory DCs in the lungs, we hypothesized that myeloid precursor populations in the bone marrow of *C.neo*-infected mice may require TNFα to pre-program DC-precursors into DC1s. Initial characterization of the bone marrow compartment revealed no significant differences in overall cell numbers until 28 dpi, when the TNFα-depleted mice had a reduced total bone marrow population relative to isotype-treated mice (Figure 4-5A). Furthermore, general myeloid precursor cells (MPCs: lin$^-$/SCA1$^-$/Flt3$^+$/CD115$^+$) and specific pre-DCs (pre-DCs: lin$^-$/SCA1$^-$/Flt3$^+$/CD115$^+$/c-kit$^-$) showed no effect of TNFα depletion on frequencies of DC precursors relative to total bone marrow cells (Figure 4-5B, C; see Figure 6-4 for gating). Subsequent assessment of global H3K4me3 signature within MPCs by intranuclear flow cytometry demonstrated that greater numbers of MPCs in isotype-treated infected mice displayed high H3K4me3 signature compared to MPCs in TNFα-depleted mice, at 14 dpi (Figure 4-5D). Furthermore, intranuclear flow cytometry revealed strongly increased mean fluorescence intensity of H3K4me3 in MCP cells from control mice compared to TNFα-depleted mice by

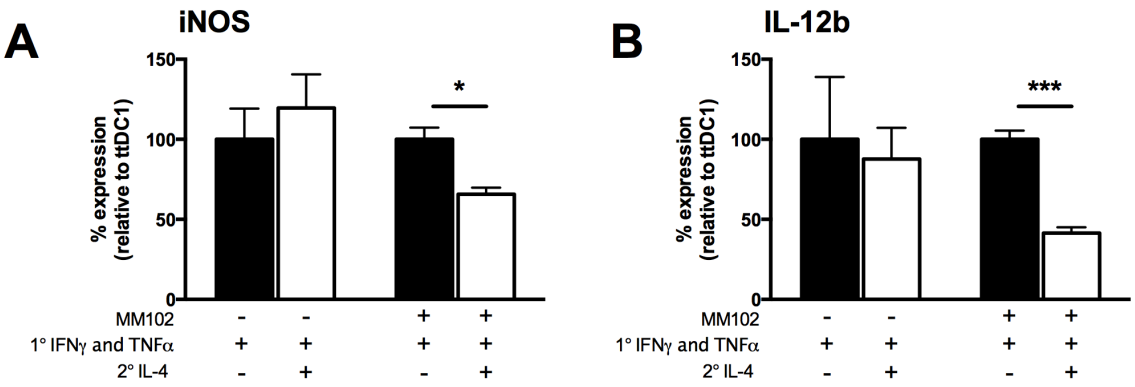

Figure 4-4 Training of DC1 genes by TNF α and IFN γ is abrogated by inhibition of histone methytransferase MLL1 during the training phase.

MLL1 inhibitor MM102 was added during the training phase of *in vitro* experiments as in

Figure 3-8. mRNA was isolated after the challenge phase and assessed for DC1 markers iNOS (A) and IL-12b (B) by RT-qPCR. N = 6 from two separate, matched experiments.
Statistical significance was determined by two-way ANOVA with multiple comparisons test or student's t-test where appropriate. * $p < 0.05$; ** $p < 0.01$; ***$p < 0.001$.

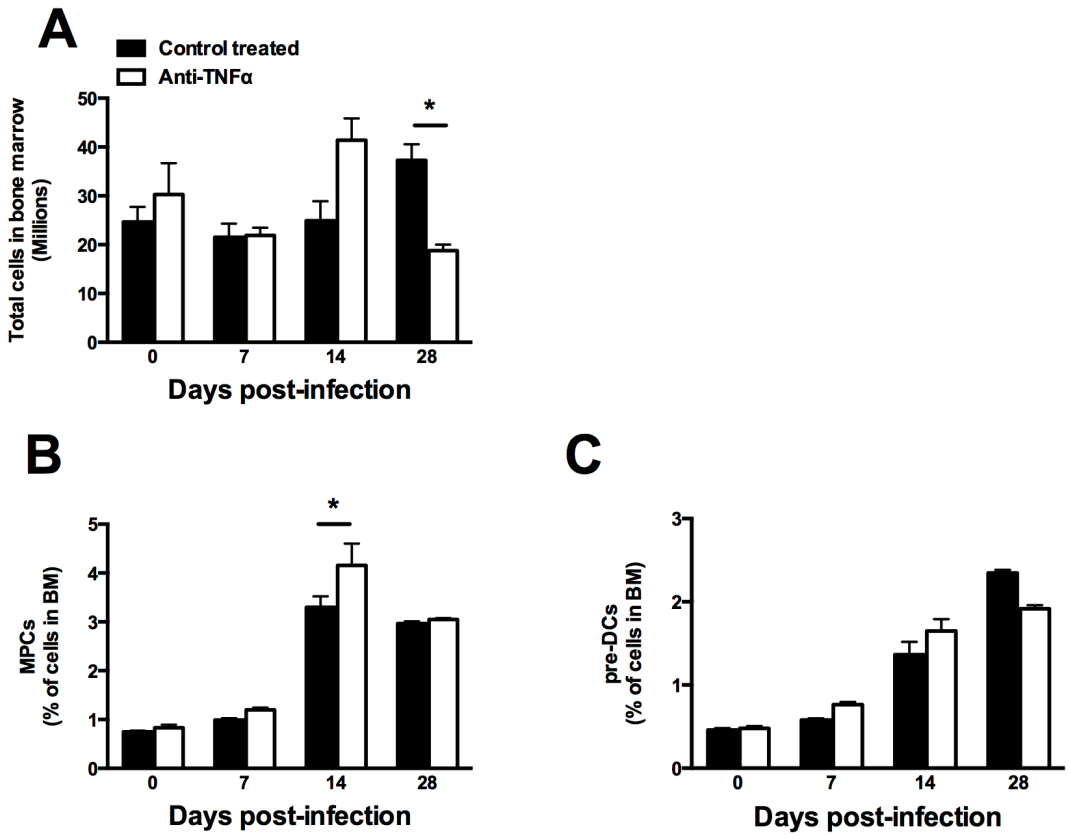

Figure 4-5 The bone marrow compartment, including MPCs and pre-DCs, is roughly similar between *C.neo*-infected mice, regardless of TNF α depletion.

(A) Mice were infected and/or TNFα depleted as in Figure 1. One femur from each mouse was dissected, the marrow flushed, and total cell numbers enumerated by light microscopy.
(B and C) Counted marrow cells were stained for flow cytometric analysis. Myeloid precursor cells (MPCs) were gated as: live/lin^-/$SCA1^-$/$Flt3^+$/$CD115^{high}$ (B). Dendritic cell precursors (pre-DCs) were gated as live/lin^-/$SCA1^-$/$Flt3^+$/$CD115^{high}$/c-kit^{low} (C).
Statistical significance was determined by two-way ANOVA with multiple comparisons test or student's t-test where appropriate. * $p < 0.05$; ** $p < 0.01$.

at both 7 and 14 dpi (Figure 4-5D). To confirm and visualize these findings, we magnetically isolated CD11b^{+} bone marrow cells and used antibody staining and fluorescence microscopy to further demonstrate that pre-DCs from TNFα-depleted mice displayed reduced H3K4 trimethylation staining compared to that of control mice (Figure 4-6). Taken together, these findings support the idea that TNFα signaling may pre-program bone marrow pre-DCs during infection.

Finally, to determine whether these pre-DCs could be arriving to the lung predisposed to DC1 or DC2 polarization, we collected bone marrow from 4 cohorts of mice: 1) uninfected isotype-treated mice; 2) uninfected anti-TNFα-treated mice; 3) isotype-treated mice at 7 dpi; and 4) anti-TNFα-treated mice at 7 dpi. Bone marrow obtained from each cohort of mice was cultured for 7 days in the presence of GM-CSF to generate BMDCs. Thereafter, these BMDC from 4 groups were used in our TNFα-training and challenge experiments. BMDCs obtained from uninfected mice treated with either isotype-control or anti-TNFa antibody were receptive to TNFα-mediated training; γ-γ cells adopted a DC1 polarization, γ-4 cells became DC2 polarized, and the TNFα-trained DCs resisted DC2 polarization by IL-4 challenge (Figure 4-7A). In contrast, the DCs from infected mice treated with either isotype-control or anti-TNFα antibody did not respond to TNFα training or to IFNγ or IL-4 challenges. Rather, BMDCs matured from infected, isotype-treated mice maintained high expression of DC1 marker iNOS regardless of treatment (Figure 4-7B, right half), indicating that DCs from the bone marrow of *C.neo*-infected mice with intact TNFα signaling were already programmed for DC1 polarization. In contrast, BMDCs matured from *C.neo*-infected mice depleted of TNFα displayed uniform downregulation of iNOS

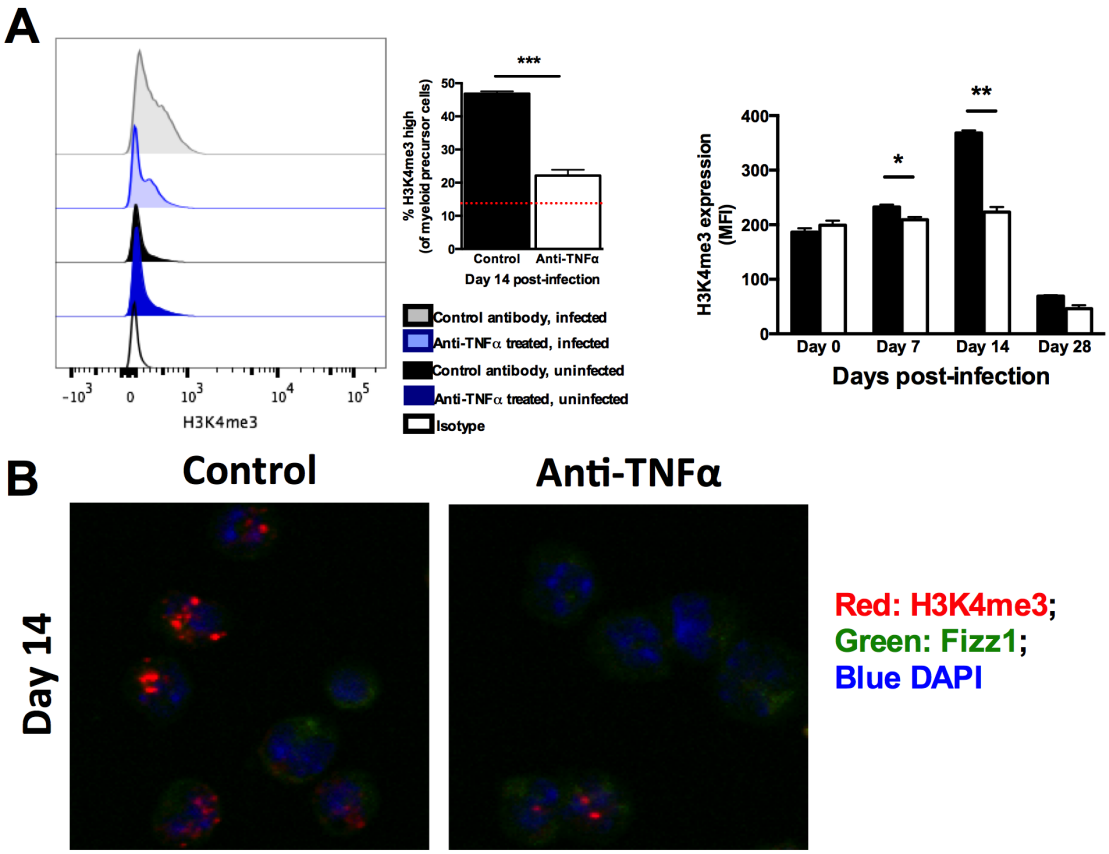

Figure 4-6 Myeloid precursor cells of the bone marrow in infected control mice bear high H3K4me3 signature consistent with DC1 phenotype observed in lungs.

(A) Flow cytometric analysis of H3K4me3 signature in MPCs isolated from 14 dpi bone marrow. Data is shown as representative histogram, percent $H3K4me3^{high}$ and mean fluorescence intensity staining. Dotted red bar indicates % high in uninfected mouse MPCs.

(B) From 14 dpi mice, final stage pre-DCs ($CD11b^{+}$) were sorted by magnetic bead separation. 1 x 10^5 cells were cytospun onto slides, fixed, and stained for H3K4me3 (red) and Fizz1 (green), followed by the appropriate fluorescently-conjugated secondary antibodies, and DAPI (blue). Slides were imaged by confocal microscopy.

Statistical significance was determined by two-way ANOVA with multiple comparisons test or student's t-test where appropriate. * $p < 0.05$; ** $p < 0.01$.

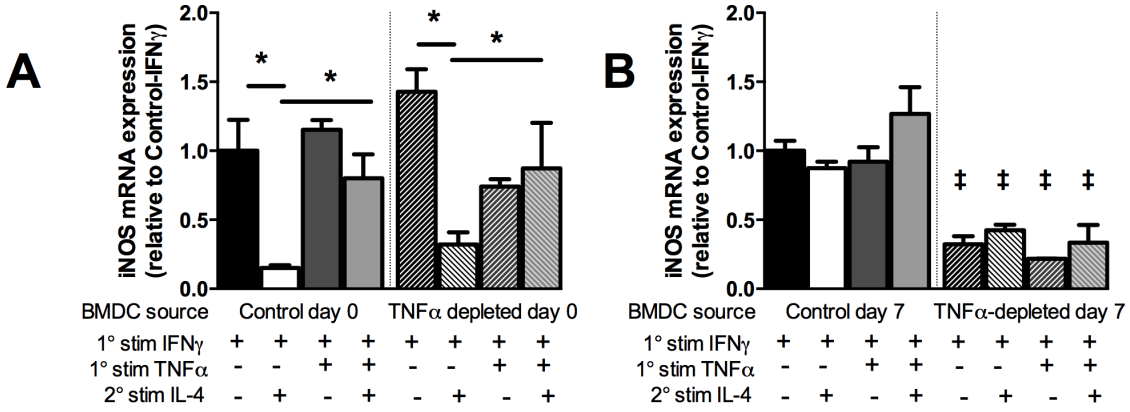

Figure 4-7 Myeloid precursor cells in the bone marrow of infected mice are predisposed to DC1 polarization in the presence of TNFα.

Bone marrow was taken from mice at 7 dpi following infection and/or TNFα depletion. Four femurs from each condition were pooled. Bone marrow was then matured over 7 days in the presence of GM-CSF. The loosely adherent fraction was harvested and plated, and subjected to cytokine training and challenge phases as in Figure 2. mRNA was isolated and RT-qPCR performed for iNOS on the marrow matured from each condition. *ex vivo* BMDCs from uninfected mice responded to TNFα training regardless of TNFα depletion (A). *ex vivo* BMDCs from infected control mice all had high DC1 gene induction regardless of further training or challenge (B, left half), while *ex vivo* BMDCs from infected TNFα depleted mice had no induction of DC1 genes regardless of further training or challenge (C, right half). Data is presented as normalized to each graph's "control day 7 γ-γ" treatment. ‡ represents statistically significant differences between the indicated values in the TNFα depleted samples relative to "control day 7 γ-γ" values. Statistical significance was determined by two-way ANOVA with multiple comparisons test or student's t-test where appropriate. * $p < 0.05$; ** $p < 0.01$.

regardless of training or challenge (Figure 4-7B, left half), suggesting that the DCs from TNFα-depleted were not predisposed to a DC1 polarization, and remained unresponsive to a subsequent DC1 polarizing stimulation.

Discussion

In this chapter, we have determined that the cellular basis for long lasting protective immunity is tied to association of DC1 gene promoters with the activating histone modification H3K4me3 (Figure 4-1 and Figure 4-2,), which occurs in an MLL1-dependent manner (Figure 4-3 and Figure 4-4); and traced these modifications back to the myeloid progenitor cells in the bone marrow (Figure 4-5, Figure 4-6, and Figure 4-7). Further, we have found that TNFα-mediated epigenetic training of DCs occurs both with and without antigen, which extends the application of TNFα-mediated innate immune training beyond anticryptococcal immune responses and into the realm of basic DC biology and function. Epigenetic modifications to innate immune cells and their precursors described herein serve as an attractive general mechanism behind the requirement for early TNFα in generation of protective immunity. In addition to increased risk of *C.neo* infection, similar mechanisms are likely contributors to increased susceptibility to *Histoplasma capsulatum* and *Mycobacterium tuberculosis* in patients on TNF α monoclonal antibody therapy, which is broadly documented in the literature (30, 232, 233). To our knowledge, this is the first time that TNFα has been linked to epigenetic modification of DC1 immune genes during a primary immune response to a pathogen (*C.neo*).

We show here that the molecular basis for perpetuating this DC1 programming during TNFα-training is via epigenetic modifications to the H3K4 residue. The global H3K4me3 signature is elevated in IFNγ/TNFα-trained DCs, while this was absent from IFNγ-only-treated DCs (Figure 4-1), despite the fact that both types of DCs were phenotypically DC1. Furthermore, TNFα is necessary for DC1s to "remember" to maintain DC1 polarization despite subsequently changing environments, through the specific enrichment of activating histone modification H3K4me3 at DC1 gene promoter regions (iNOS, IL-12b; Figure 4-2). We also show that TNFα signaling leads to changes in H3K4me3 through the histone methyltransferase MLL1. MLL1 becomes uniquely upregulated in $\gamma\alpha$ DCs (and not in γ-alone or α-alone DCs; Figure 4-3A-C) in the presence and absence of *C.neo* antigen. Consistently, MLL1 inhibition during training prevents $\gamma\alpha$ DCs from maintaining high DC1 gene expression when challenged by pro-DC2 cytokine environments (Figure 4-3D). Collectively, these data suggest that TNFα and IFNγ receptor signaling synergizes to increase MLL1 expression and target its activity to DC1 gene promoters. TNFα and IFNγ signaling are known to synergistically activate certain genes, and this has been linked to NFκB and STAT activation (234-236), but to our knowledge, this has not been demonstrated for genes of epigenetic machinery. Thus, DCs are able to remember and maintain robust DC1 activation throughout weeks of infection regardless of changing cytokine environments found in different microenvironments (i.e. regions of the lung, different organ systems) through MLL1-mediated H3K4 methylations, mechanistically linking TNFα signaling to the stable, robust DC1 phenotype, resulting in generation of protective Th1 immunity.

Finally, we find that perpetuation of this stable DC1 phenotype is linked to TNFα-mediated epigenetic modification to the DC precursor population in the bone marrow during *C.neo* infection. In our model, we observe CD103$^-$/CD11b$^+$ DCs in the lungs exhibiting distinct characteristics of DC1 or DC2-ness based on the inflammatory milieu of the host, and that DC1s from the lungs of infected mice that had TNFα displayed a global increase in H3K4me3 relative to DCs from infected, TNFα-depleted mice. We see this mirrored in the bone marrow DC precursor populations: a) bone marrow DC precursors from infected mice that have TNFα have a higher global H3K4me3 signature than precursors from infected, TNFα-depleted mice (Figure 4-6); b) we show that the bone marrow DC precursor population matures *ex vivo* into DC1 if it was harvested from an infected, TNFα-containing host (Figure 4-7B, left half); and c) the bone marrow DC precursor population matures into DC2 if it was harvested from an infected, TNFα-depleted host (Figure 4-7B, right half). Thus, DCs recruited from the bone marrow during infection appear to arrive epigenetically pre-programmed to be DC1 in the presence of TNFα. There is a precedent for pre-polarization of myeloid cells from the bone marrow, as evidenced by Schlitzer *et al.* in 2015 (237). In their model, which utilizes a different strain of mice and a very different pathogen, conventional DC1 cells expressing either CD8 or CD103 become DC1 in the bone marrow, while conventional DC2 cells expressing either CD4 or CD11b become DC2 polarized while in the bone marrow. This phenomenon may be occurring in the bone marrow during *C.neo* infection, and be mediated by TNFα and other components of the systemic inflammatory milieu.

In the absence of TNFα during *C.neo* infection *in vivo*, it remains unclear whether DCs and their precursors are subjected to epigenetic modifications and, if so, which genes are affected positively or negatively. Despite the recovery of TNFα within 14 dpi, DCs from TNFα-depleted infected mice maintain their DC2 polarization (Figure 3-5, Figure 3-6, and Figure 3-7), suggesting that an alternative set of epigenetic modifications promotes the sustained DC2 gene expression in TNF α -depleted *C.neo*-infected mice. We observe a change in H3K4me3 signature *in vivo* between DC2s and immature DCs (Figure 4-1 B), and we show a strong trend over baseline towards H3K4me3 association with DC2 gene Fizz1 in DC2s *in vivo* (Figure 4-2D). Finally, DCs developed from the bone marrow of infected TNFα-depleted mice resists changes to their non-DC1 polarization by maintaining low expression of iNOS, regardless of TNC α or IFN γ treatment (Figure 4-7B, right half). However, if DC2s from infected TNFα-depleted mice are indeed trained DC2s, it is unclear what may be stimulating the training. Our *in vitro* model system shows that IL-4, regardless of the presence or absence of TNFα, is insufficient to train DC2s (**Figure 3-8**C and D).

We have given much thought to the signaling pathways leading from one or both TNFα receptors to chromatin rearrangement machinery, in particular to MLL1. We assessed TNFR1 and TNFR2 expression on the surface of bone marrow DC precursor cells, and found slight but significant increases in surface expression of both TNFR1 and TNFR2 in infected control mice. In the previous chapter (Figure 3-13 and Figure 3-14), *in vitro* studies in BMDCs utilizing TNFR1, TNFR2, or combined TNFR1 and 2 blocking antibodies during the TNFα training period prevented TNFα-mediated training. TNFR1 and 2 blockade each

individually partially blocked training, while the combination of TNFR1 and 2 blockade completely blocked training, suggesting that MLL1 is maximally induced when both TNFR pathways are stimulated. Using these findings and assessing TNFR expression in the bone marrow pre-DCs, we found indeed that the majority of TNFR-expressing cells were doubly positive for TNFR1 and TNFR2 expression. Mechanisms further upstream may include differential stimulation of MLL1 co-factors WDR5, RBBP5, and ASH2L by TNFR1 and TNFR2 signaling (238). NFκB, downstream of TNFR signaling, has been shown previously to activate MLL1 (186), which is a likely mechanism because both TNFR1 and TNFR2 utilize the NFκB pathway (reviewed in (239)).

Based on our findings from this chapter and other recent work from our laboratory, we have assembled a model mechanism for the requirement of TNFα early during *C.neo* infection, which is detailed in Figure 5-1. Early signaling through TNFα receptors in DCs is necessary to classically activate DCs and to maintain that polarization throughout many weeks of infection, resulting in a long-term, stable Th1/Th17 polarized immune response. These DC1 cells matured in the presence of TNFα are resistant to changing their polarization– potentially caused by changes in cytokine environment and by immune modulation by *C.neo*– through MLL1-mediated H3K4me3 epigenetic modifications to the histone proteins proximal to DC1 gene promoters; in the absence of TNFα, *C.neo* antigen can polarize DCs to DC2 despite pro-DC1 cytokine environments. DC1s activated in the presence of TNFα during infection traffic to the lung-associated lymph nodes, where they prime Th1 responses (Xu, Eastman *et al.* 2016, mBio, in press) and restimulate effector T cells recruited to

the lungs to perpetuate Th1 responses (9). Simultaneously, the inflammatory milieu in the lungs, combined with elevated circulating levels of TNFα, stimulates the bone marrow to produce and send DCs pre-polarized as DC1, already bearing the high H3K4me3 signature of lung DC1s. This necessity for long-term epigenetically-stabilized DC1 polarization in anti-cryptococcal host defense (and likely other pathogens that thrive in TNFα-depleted patient populations) suggests that immunotherapies which epigenetically re-program DCs or transfer in DC1s may provide long-term benefit patients suffering from persistent *C.neo* infection and prevent lethal extra-pulmonary dissemination of *C.neo*.

Chapter 5 Discussion

Summary

This dissertation has investigated afferent and efferent immune responses to the opportunistic pulmonary fungal pathogen *Cryptococcus neoformans*. Here we discuss mechanisms by which the afferent immune response affects the developing efferent response, and instances in which it does not. We then investigate the many ways in which TNF α and IFN γ are known to synergize, and how that applies to our findings from chapters 3 and 4. Finally, we place all of the findings from this dissertation into the broader context of antigen presentation and adaptive immune priming and expound upon the implications of this work.

Main results: Ssa1 modulates afferent, but not efferent, macrophage activation

In chapter 2, we used a mutant strain of the highly pathogenic strain of *C.neo*, H99 (serotype A) with a targeted deletion of the heat shock protein 70 homologue and cryptococcal virulence factor Ssa1, *Δssa1*, in order to determine the mechanism behind Ssa1-mediated immune modulation. We first found, to our surprise, that Ssa1– which was necessary for the production of another cryptococcal virulence factor, laccase, in a strain of serotype D *C.neo*– was dispensable for the production of laccase in H99. This made assessment of Ssa1 as a standalone virulence factor, independent of its effects on laccase, more

straightforward. We found that deletion of *ssa1* resulted in decreased pulmonary fungal burden during the early/afferent, but not the later/efferent, immune response. This ultimately resulted in a slight but significant increase of median survival time in the *Δssa1* infected mice. The differences in fungal control observed throughout the studies were linked to macrophage M1/M2 polarization status. Macrophages stimulated with *Δssa1 in vitro* upregulated M1 and downregulated M2 markers relative to H99-stimulated macrophages. However, while *ssa1* deletion resulted in increased M1 and decreased M2 phenotype during the afferent response *in vivo*, *ssa1* deletion had no effect on macrophages *in vivo* during the efferent response phase, consistent with the improved early but not late pulmonary growth control of *Δssa1*. We concluded that Ssa1 was an virulence factor acting to promote early M2 polarization in isolation *in vitro* and *in vivo*, but that it ultimately had no effect on the development of the efferent immune response. Further, while Ssa1 itself can modulate macrophages early during infection, the effect of Ssa1 on macrophages was eventually overpowered by the immunophenotype of the efferent response, which is largely dependent upon DCs. Ssa1 did not promote DC2 polarization, in the way that it was able to promote M2 polarization, and thus had limited effects on the developing adaptive, efferent response.

Main results: Afferent TNFα is necessary for epigenetic modifications to stabilize long-term DC1 programming in pulmonary DCs and bone marrow DC precursors, resulting in efferent Th1/Th17-polarized protective immunity during *C.neoformans* infection

In chapters 3 and 4, we found that TNFα was necessary for long-term, stable, and robust Th1/Th17 immune polarization; in the absence of TNFα, a non-protective Th2 response lasted through 4 weeks of infection, significantly outlasting the transient TNFα depletion (TNFα levels recovered within 14 dpi). We traced this defect in Th polarization to DCs: in the presence of TNFα during *C.neo* infection, there was a sustained and robust DC1 activation throughout the infection, which resulted in stable Th1 immunity and progressive clearance. In contrast, in the absence of TNFα during *C.neo* infection, there was a lasting DC2 polarization that resulted in dysregulated immune responses with a strong Th2 component and fluctuation of cytokine levels and lack of fungal clearance. Modeling this *in vitro*, we found that TNFα and IFNγ stimulation together result in DC1s that can resist changes in their polarization due to changing cytokine environments and the highly immunomodulatory *C.neo* antigen, called TNFα-trained DCs. The mechanism behind this TNFα training is epigenetic: TNFα-trained DCs have the activating histone modification H3K4me3 associated with promoter regions of key DC1 genes iNOS and IL-12b *in vivo*, while this is not seen in the DC2s from TNFα-depleted infected mice. *In vitro* inhibition of MLL1, responsible for beginning the activating methylations on

H3K4, resulted in ablation of TNFα-mediated training of DCs. Further, we traced this defect in epigenetic stabilization of DC1 gene promoters to the bone marrow DC precursors *in vivo*; in the presence of TNFα during *C.neo* infection, bone marrow DC precursors undergo an increase in global H3K4me3 distinct from uninfected mice and TNFα-depleted, *C.neo*-infected mice. Bone marrow from *C.neo*-infected mice that had TNFα differentiated *ex vivo* into TNFα-trained DC1, unresponsive to pro-DC2 cytokine challenge regardless of the presence or absence of TNFα treatment. However, DCs matured *ex vivo* from the marrow of TNFα-depleted, *C.neo*-infected mice maintained uniformly low DC1 gene expression, regardless of the pro-DC1 cytokine challenge and/or the presence or absence of TNFα treatment. Our data led us to the conclusion that the stable DC1 (and the concomitant Th1/Th17) phenotype we observed *in vivo* during *C.neo* infection in the presence of TNFα was due to MLL1-mediated epigenetic modifications to H3K4 at DC1 gene promoters; in the absence of TNFα, MLL1 is not stimulated and these activating modifications to the histones, which open DC1 gene promoter regions, were not made. Further, TNFα signaling during *C.neo* infection resulted in changes to the DC precursors (Ly6C^{high}/CD11b^{+} monocyte) in the bone marrow, which allowed for perpetual recruitment of TNFα-trained DCs and maintaining robust Th1/Th17 immune responses throughout infection. In the absence of TNFα during *C.neo* infection, DCs recruited from the bone marrow did not upregulate DC1 genes, thus

perpetuating recruitment of non-DC1s and maintaining the nonprotective Th2-biased immune response that results in persistent *C.neo* infection.

Significance: the timing of immune modulation during cryptococcosis

The immune response to *C.neo* is divided up into two general, but overlapping phases: the afferent phase, comprised largely of innate cells containing the infection or exiting the site of infection to prime adaptive immune responses (2, 10, 37, 41, 48, 151, 176, 240, 241); and the efferent phase, comprised of adaptive immune cells directing and facilitating microbial clearance (10, 69, 70, 72, 74, 175, 242). The afferent phase in mice begins soon after infection and lasts until between 7 and 14 days post-infection (dpi), while the efferent phase begins slightly prior to 14 dpi when we observe several fold more pulmonary lymphocytes relative to 7 dpi. The research from this dissertation highlights important distinctions between the afferent and efferent immune responses and their ultimate effects on infection outcomes. In Chapter 2, the absence of the cryptococcal virulence factor Ssa1 increased the ability of the innate immune system to contain and kill the fungus at very early time points (Figure 2-1). However, despite this early difference in pulmonary fungal burden, the absence of Ssa1 did not ultimately affect host survival or clearance of the microbe during the later time points in a profound way. The absence of Ssa1 was sufficient to inhibit fungal growth early during the afferent phase, but ultimately insufficient to alter the resulting efferent immune response. In contrast, data from Chapters 3 and 4 show that host TNFα was depleted with a single intraperitoneal injection of anti-TNF α antibody only during the afferent phase of the immune response; however, despite an absence of TNFα during 0-7 dpi and TNF α recovery during

7-14 dpi, there was no difference in pulmonary fungal burden between control mice and TNFα-depleted mice until 14-28 dpi, which is well into the efferent response (Figure 3-1). The transient depletion of TNFα from the afferent inflammatory milieu was able to affect the efferent immune response for many weeks after TNFα levels had recovered. It is remarkable that transient TNFα depletion during the afferent immune response is sufficient to permanently skew the efferent immune response, while permanent deletion of Ssa1 only transiently skews the immune response.

The differential ability of factors to affect long-term immune polarization in the mouse model may come down to whether or not these factors modulate the initial DC-mediated priming of T cells in the lymph nodes and restimulation of T cells in the lungs. Chapter 2 focused on the interplay of Ssa1 with macrophages specifically, but not DCs; we exhaustively analyzed the effect of Ssa1 on DCs but found that deletion of Ssa1 had little to no effect on DCs (Figure 2-10). The absence of the effect on DCs was surprising, considering the significant changes in early DC1/DC2 cytokine ratios (Figure 2-8); however, it could be explained by the lack of effect of Ssa1 deletion on the very low levels of TNFα during the afferent response in this model (Figure 2-11). Our subsequent data on the role of TNFα signaling, motivated in part by the findings from this chapter, indeed demonstrate that TNFα is required for DCs to overcome the suppressive effect of cryptococcal antigen and gain the ability to become DC1-polarized (Figure 3-11). These findings contain critical implications for the immunoprotection against *C.neo*, and are discussed in greater detail below. The overall implication of our results from Chapter 2 are that factors sufficient to modulate DCs will

ultimately change the efferent response to *C.neo*, and ultimately have a more profound effect on fungal clearance during the efferent phase of the immune response than factors that do not.

TNF α and IFN γ synergy: crosstalk and signaling pathway integration

Throughout chapters 3 and 4, our *in vitro* modeling of TNF α-trained DCs utilizes TNF α and IFN γ in combination. We attribute TNF α-mediated training to epigenetic mechanisms, but the synergy of TNFRs and IFNGR signaling is a known phenomenon that must be acknowledged. TNF α and IFN γ are quite capable of inducing many inflammatory genes on their own; however, numerous genes are induced to a greater extent by the combination of TNF α and IFN γ, and the effect size is often more than an additive effect. For instance, MHC class I is regulated synergistically by TNF α and IFN γ in non-immune cells (243, 244), and in macrophages, complement factor B expression is induced by IFN γ 1.8x, by TNF α 1.3x, but by the combination of IFN γ and TNF α by 4.75x (245). Depending on the cell and model, synergy is linked to the activation and binding of STAT1, IRF-1, and NFκB simultaneously at each transcription factor's binding sites (235, 245, 246), or a TNF α-mediated increase of IFN γ receptor surface expression, thus increasing the cell's capacity for IFN γ signaling (236). In our *in vitro* model, DC1 gene upregulation by the combination of TNF α and IFN γ is roughly similar in magnitude to the upregulation due to IFN γ alone (Figure 3-7,**Figure 3-8**,Figure 3-10), with the notable exception of DCs treated with HKC (Figure 3-10C and D), which were unable to upregulate DC1 genes without

combined TNF α and IFN γ. Thus, we attribute our stable TNF α-trained DC1 phenotype to the chromatin modifications induced by TNF α and via MLL1, and we minimally attribute these effects to the synergistic enhancement of gene expression via transcription factor activation alone.

In chapter 4, we show that neither MLL1 nor KDM5d are induced by TNF α or IFN γ stimulation alone, and only MLL1 is induced by the combination of TNF α and IFN γ stimulation (Figure 4-3A and B). Very little has been published linking TNF α and IFN γ receptor signaling synergy to chromatin modification machinery. CXCL10 activation, and possibly similarly regulated chemokines, in human airway smooth muscle cells is synergistically activated by TNF α and IFN γ through the action of Creb-binding protein (CBP), which possesses histone acetyltransferase activity (234). When we assessed levels of CBP both *in vivo* and *in vitro*, we found no differences at the transcriptional level between DC1, DC2, and TNF α-trained DCs (data not shown). Synergy from the IFN γ receptor and TLRs has been implicated in stabilization and perpetuation of many inflammatory genes, such as TNF α, IL-6, IL-12b (247). However, in our *in vitro* model in the presence of HKC, IFN γ-alone stimulated DCs are unable to upregulate DC1 genes (including IL-12b Figure 3-10C); IL-12b induction in the presence of HKC is only induced when IFN γ and TNF α are both added.

Greater question of DC biology

The work from chapters 3 and 4 of this dissertation links the common pro-inflammatory cytokine TNF α to a unique state of DC activation where, even in the absence of antigen, DCs are able to maintain a polarization in the face of changing cytokine environments. As we show *in vitro* in Chapter 3, activated DC1s can either maintain plasticity of their polarization, adapting with their changing cytokine environments, or they can maintain robust expression of DC1 genes despite changing cytokine environments. In Figure 4-6 and Figure 4-7, we link infection and systemic TNF α to modulation of the polarization of the bone marrow DC precursor population. As recently as 2003, the idea that DC subsets developing within the bone marrow could be modulated by the inflammatory milieu of the body was controversial (166). There are few studies characterizing the modulation of developing bone marrow DC populations; however, in addition to recent work by Schlitzer *et al.* characterizing specific subsets of DC1 and DC2 cells developing within the bone marrow (237), the sepsis field has also characterized this phenomenon, relating it specifically to the generation of broadly immunosuppressive DCs (226). In certain pathologies (i.e. sepsis), this results in long-term immune suppression, which can be ultimately detrimental for the host; however, in an infection model that lasts weeks, such as *C.neo*, maintenance of DC phenotype is necessary for the perpetuation of protective immunity, and ultimately benefits the host.

This topic of epigenetic modification to immune cell precursors has been the subject of a number of recent reviews addressing the potential for immunotherapies to preferentially differentiate specifically polarized DC subsets

in patients with sepsis-induced immune dysfunction (248) and how the microbiome influences myeloid subset development and polarization (249, 250). Thus, there is also potential for immunotherapies to change DC subset differentiation and polarization within the bone marrow, either for treatment purposes during chronic fungal infections (i.e. *C.neo*) with underlying immune polarization defects or prophylactically at the onset of other immune therapies (i.e. TNF α monoclonal antibody therapy). We have shown that transfer of epigenetically stable TNF α -trained DC1s is sufficient to overcome the recruitment of pre-DC2s from the bone marrow of TNF α -depleted *C.neo*-infected mice and prime Th1 immune responses (Figure 3-12). Harvest, training, and reintroduction of *ex vivo*-TNF α -trained syngeneic DCs to a patient with chronic *C.neo* infection, possibly coupled with future epigenetic modification therapies to erase or write particular modifications in DC precursor cells in the bone marrow, may eliminate the need for extensive pharmaceutical intervention, instead relying on transfer and continued recruitment of trained DCs to re-polarize the pulmonary immune environment.

Unanswered questions and future directions: the role of repressive modifications in TNF α -trained DCs

In Chapter 4, we have shown that TNF α signaling results in MLL1-mediated H3K4 methylation at the DC1 gene promoters iNOS and IL-12b. We also show that there is decreased H3K4me3 at the Fizz1 gene promoter in TNF α -trained DCs. This decrease in H3K4me3 correlates to the decrease in Fizz1 mRNA

expression in TNF α-trained DCs; however, we have not assessed whether Fizz1 and other DC2 genes are epigenetically repressed in TNF α-trained DCs, nor do we have clues at to the modification machinery involved (for instance, by DNA methylation or repressive histone modifications like H3K27me3). There is a high likelihood of repressive modifications to DC2 genes in TNF α-trained DC1s, because they achieved a stable state of down-regulated of certain DC2 genes even upon challenge with the pro-DC2 cytokine IL-4. We found that this is not a general desensitization (or lack of IL-4 receptor expression) because some genes such as Arg1 do respond to IL-4 challenge (Table 3-1), while other DC2 genes remain silenced. In the future, this could be addressed using *in vitro* TNF α-trained DC1s and untrained DC2s for ATAC-seq to first determine whether DC2 genes are found in open chromatin or not. If DC2 genes are decreased in open chromatin, we could then perform ChIP-PCR using antibodies against selected common repressive histone modification marks, such as H3K27me3, or performing sodium bisulfate sequencing to assess whether there is increased DNA methylation at DC2 gene regions. Upon determining which repressive modifications are involved in TNF α-mediated DC2 gene repression, we could then screen for which predicted enzymes of epigenetic modification machinery are upregulated at the transcriptional level, increased at the protein level, and finally pharmacologically inhibit candidate enzymes to assess whether inhibition of their biological activity ablates TNF α-mediated DC2 gene repression upon IL-4 challenge. This work would be complementary to our findings that TNF α epigenetically activates DC1 genes by MLL1, and may be necessary for the

optimal function of the proposed immunotherapies that might target epigenetic memory of DCs and/or their myeloid precursors in the bone marrow. Activation of DC1 genes in TNFα-trained DCs by MLL1 is only half of the picture, while the concurrent repression of DC2 genes is likely equally important in generation of the robust and stable DC1 polarization. We need to figure out and better understand how epigenetic modifications to DCs result in priming and maintenance of protective T cell-mediated immune responses to *C.neo in vivo.*

Unanswered questions and future directions: epigenetic modifications to DCs during *C.neoformans* infection in the absence of TNFα

In the absence of TNFα during *C.neo* infection *in vivo*, we found that DCs are alternatively activated, and they prime and restimulate Th2/Treg responses throughout 4 weeks of infection (Chapter 3). These DCs do not bear the high H3K4me3 signature that we see in TNFα-trained DCs, nor do they upregulate MLL1. However, we show that DCs matured *ex vivo* from TNFα-depleted, *C.neo*-infected mice are resistant to changing polarization upon cytokine challenge, similar to the TNFα-trained DCs but opposite in the direction of their gene expression. While TNFα-trained DCs matured *ex vivo* from infected hosts were uniformly programmed to be DC1 and resist changes in polarization from pro-DC2 cytokines, untrained DCs matured *ex vivo* from TNFα-deficient infected hosts were uniformly programmed to be DC2, resisting changes in polarization from pro-DC1 cytokines (Figure 4-7B). It is unclear if this is a directed activation and epigenetic stabilization of DC2 genes, or whether the

DC2 polarization could be thought of as the default polarization, and epigenetic modifications solidify and perpetuate this programming. We can see that untrained DCs from TNF α-depleted infected mice had a decrease in H3K4me3 association with the DC1 gene promoters iNOS and IL-12b relative to control mice (Figure 4-2A and B), which implies active demethylation at H3K4me3 in these regions. Furthermore, untrained DC2 have a trend towards increased H3K4me3 association with the Fizz1 promoter region relative to controls, which suggests active methylation in this region. Taken together, these data support the epigenetic suppression of DC1 genes and epigenetic activation of DC2 genes in untrained DC2s *in vivo*. We know from Figure 3-7C and D that TNF α is not a stabilizing factor for DC2 programming *in vitro*, but it remains unclear what may be acting as a stabilizing factor *in vivo*. Continued *in vitro* modeling using other dominant cytokines found during the afferent phase of the immune response to *C.neo* in the absence of TNF α may help address this question. Additionally, cryptococcal antigen may be responsible for inducing– alone or synergistically with other cytokines– epigenetic or other transcriptional programming changes to DCs and their bone marrow precursor populations. We have limited evidence for increased EZH2 activity and H3K27me3 in DC2 cells, both *in vitro* and *in vivo*, but these studies are ongoing. Similarly, we have found that JMJD3 is differentially expressed in TNF α-trained DC1 and DC2 *in vitro* and between DC1 and DC2 *in vivo*. This dissertation has addressed the mechanism by which afferent phase TNF α perpetuates protective immunity to persistent *C.neo* infection, but it is beyond its scope to determine mechanistically how DCs in the absence of TNF α during *C.neo* infection perpetuate their DC2 polarization.

Final thoughts

In this doctoral dissertation, I have shown that while the afferent immune response can dramatically and permanently affect the developing efferent immune response to *C.neo*, perturbations to the afferent response do not necessarily result in concomitant efferent changes. Phagocytes can control *C.neo* to a greater and lesser extent early during infection, but the actions of DCs that prime the T cell response ultimately control the outcome of infection. If DCs are unaffected by a particular virulence factor, its absence doesn't necessarily ultimately correlate to increased protection (see: Ssa1). However, if DCs are activated towards DC2, or remain immature (84), or if cryptococcal virulence factors suppress crucial early host cytokine production (88), the result is generation and perpetuation of a non-protective immune response that ultimately results in persistence and, typically, eventual progressive extrapulmonary dissemination of *C.neo*. Thus, afferent-phase cytokine (i.e. TNF α) modulation of DC polarization (i.e. via epigenetic mechanisms) can control the development of anticryptococcal CD4 T cell-mediated immunity, and is likely an important mechanism in a broad range of host-pathogen interactions.

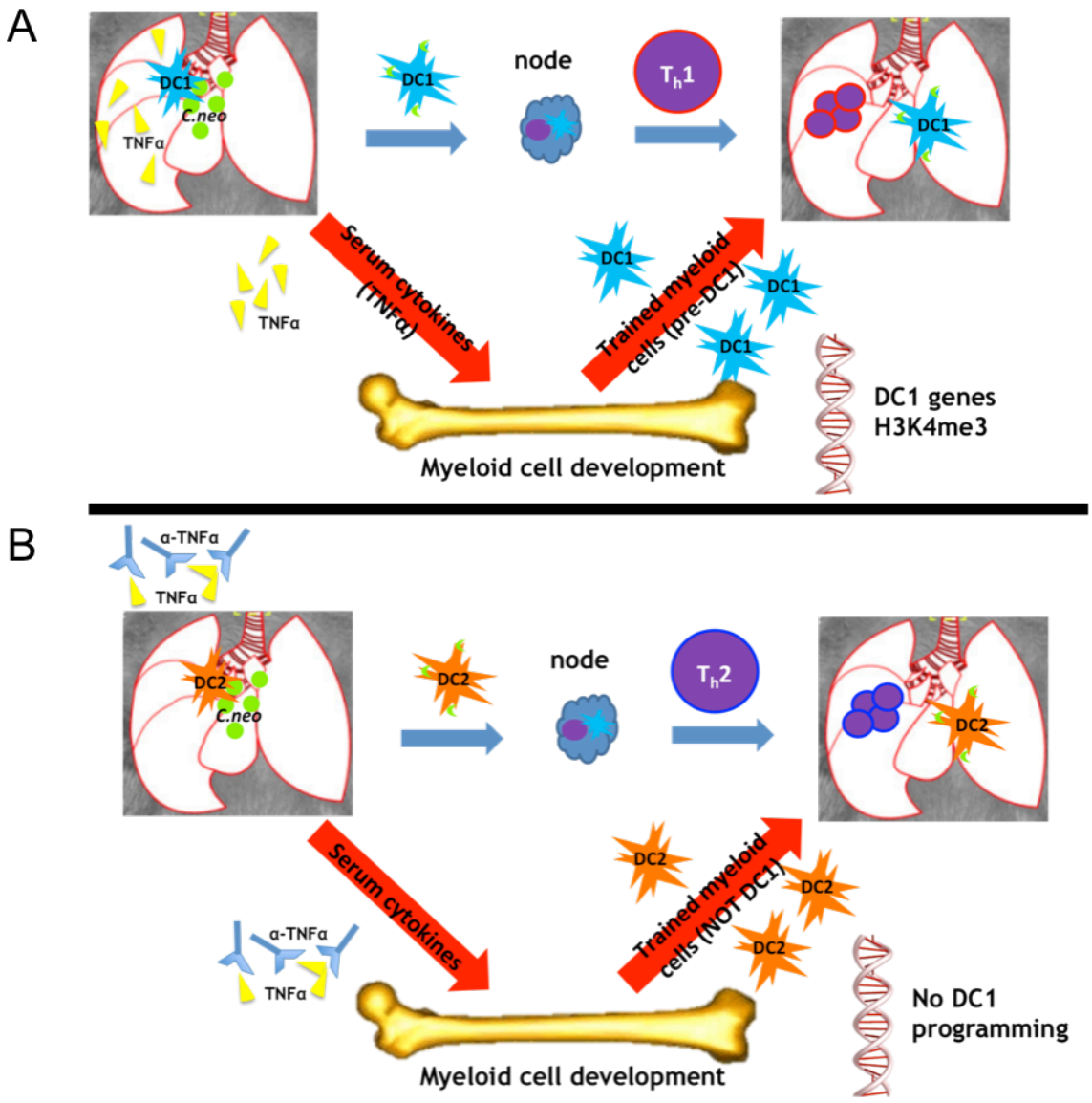

Figure 5-1 A final model: TNFα is necessary for generating robust and stable DC1 expression during *C.neo* infection, thus priming and perpetuating Th1/Th17 protective T cell-mediated immunity.

TNFα– in combination with the inflammatory milieu of the *C.neo*-infected lung– primes DCs to adopt DC1 polarization. TNFα signaling activates MLL1, which adds activating methyl groups to H3K4 at promoter regions of DC1 genes. These robust and stable DC1s traffic to the lung-draining lymph node where they prime Th1/Th17 immune responses, while remaining and recruited pulmonary DC1s restimulate the Th1/Th17 T cells in the lung throughout infection. Pulmonary DC1s are replenished via DC recruitment from the bone marrow, where the TNFα signaling and other inflammatory mediators have modified the

proliferating bone marrow DC precursor population, resulting in recruitment of pre-polarized DC1s to the infected lung. In the absence of TNF α during the afferent response to *C.neo* infection, DCs don't receive epigenetic stabilization to DC1 genes through TNF α and MLL1. Due to the lack of epigenetic stabilization of DC1 genes, and the immunomodulatory effect of cryptococcal antigen (known to promote DC2 activation), DCs polarize to DC2, traffic to the lymph node, prime non-protective Th2 responses, and remaining/recruited pulmonary DC2s restimulate the Th2 T cells in the lung throughout infection. The lack of TNF α in combination with other inflammatory mediators during *C.neo* infection modifies the proliferating bone marrow DC precursor population, resulting in recruitment of pre-polarized DC2s to the infected lung and the perpetuation of non-protective T cell-mediated immunity.

Chapter 6 Materials and Methods

Methods common to all chapters

Intratracheal inoculation of C. neoformans

Mice were anesthetized with intraperitoneal injection of ketamine/xylazine (100/6.8 mg/kg body weight) and were secured onto a clean foam board. Hair was removed from over the trachea and skin was sterilized with iodine and ethanol. A small incision was made over the trachea, and the underlying muscle and glands were separated to expose the trachea. A 30-gauge needle was inserted into the trachea and 30 μl (10^4 CFU) of the washed yeast (3.3×10^5 yeast cells/ml in sterile non-pyrogenic saline) were injected intratracheally from a 1-ml tuberculin syringe fitted to a stepper pipette. After inoculation, the incision was closed with cyanoacrylate adhesive, and mice were kept warm and monitored during recovery from anesthesia.

Serum preparation

Mice were humanely euthanized by CO_2 asphyxiation, then exsanguinated to confirm death. Whole blood was collected in eppendorf tubes, spun down to consolidate blood, allowed to rest at room temperature for 20 minutes. Blood was then incubated at 4°C for 20 minutes, then centrifuged at 5000 RPM to separate serum from erythrocytes. The top serum layer was collected and frozen at -80°C until ELISA or cytometric bead array for cytokine analysis.

Lung leukocyte isolation

At the time of data collection, lungs were perfused with 3 ml sterile nonpyrogenic saline, removed, washed in RPMI 1640, and enzymatically dispersed as previously described (176, 251). Briefly, excised lungs from each mouse were minced with scissors and digested enzymatically at 37°C for 30 min in 5 ml/mouse digestion buffer (RPMI 1640, 5% FBS, penicillin and streptomycin [Invitrogen, Grand Island, NY]; 1 mg/ml collagenase A [Roche Diagnostics, Indianapolis, IN]; and 30 mg/ml DNase [Sigma]). The cell suspension and tissue fragments were further dispersed by repeated aspiration through the bore of a 10-ml syringe and centrifuged. Erythrocytes in the cell pellets were lysed by addition of 3 ml NH_4Cl buffer (0.829% NH_4Cl, 0.1% $KHCO_3$, and 0.0372% Na_2EDTA, pH 7.4) for 3 min followed by a 10-fold excess of RPMI 1640. Cells were resuspended and a second cycle of syringe dispersion and filtration through a sterile 100-mm nylon screen (Nitex, Kansas City, MO) was performed. The filtrate was centrifuged for 25 min at 1500 × g in the presence of 40% Percoll (Sigma) in complete RPMI 1640 (RPMI 1640, 5% FBS, 10 U/ml penicillin and streptomycin [Invitrogen, Grand Island, NY], 1X sodium pyruvate, 1X glutamax, 1X non-essential amino acids, 2-mercaptoethanol) with no brake to separate leukocytes from cell debris and epithelial cells. Leukocyte pellets were resuspended in 5 ml complete RPMI 1640 media and enumerated on a hemocytometer after dilution in trypan blue (Sigma).

CFU assay

For determination of fungal burden in the lungs, 100 μl was removed from the enzymatically dispersed lungs prior to centrifugation and 10-fold dilutions were

plated in duplicate on Sabouraud dextrose agar plates. For determination of brain CFU, brains from mice in the survival study were removed at the time of death and homogenized in 2 ml sterile mili-Q water. 10-fold dilutions were then plated in duplicate on Sabouraud dextrose agar plates. Colonies were counted after 48 h of growth at room temperature, and CFU was calculated on a per-organ basis. For determination of spleen CFU, spleens were removed at the time of death and homogenized in sterile mili-Q water. 10-fold dilutions were then plated in duplicate on Sabouraud dextrose agar plates. Colonies were counted after 48 h of growth at room temperature, and CFU was calculated on a per-organ basis.

Preparation and enumeration of lung leukocytes

Following enzymatic dispersal of the lungs, 50,000 cells were cytospun onto glass slides, fixed, stained with Wright-Giemsa stain, and dried. Monocytes, eosinophils, neutrophils and lymphocytes were counted as described previously (252).

Flow cytometry

Enzymatically dispersed lungs were counted and stained extracellularly, then fixed, permeabilized, and stained intracellularly as previously described (49), then run on an LSR II flow cytometer using FACSDiva software (BD Biosciences, San Jose, CA) and analyzed further using FlowJo software (Tree star, San Carlos, CA). Gating for lung myeloid cells proceeded as follows: the $CD45^+$ cells were identified, lymphocytes were removed ($CD19^+/CD3^+$), neutrophils were

removed ($Ly6G^+/CD11b^+$), eosinophils were excluded ($SSC^{high}/CD11c^{int}$), and then $CD11c^+$ (myeloid cells) or $CD11b^+/CD11c^+$ (DCs) cells were analyzed for expression of activation markers. Gating for lung CD4 T cells proceeded as follows: the $CD45^+$ cells were identified, cells were selected on $CD3^+$, and $CD19/CD11b/CD11c^+$ cells were excluded. T cells were then gated on CD4 vs CD8 expression, and the CD4 single positive population was analyzed for surface activation marker expression and intracellular expression of Th polarization cytokines. Intracellular and intranuclear staining was performed using the FoxP3/Transcription Factor Staining Buffer kit from eBiosciences (San Diego, CA, USA). For specific antibodies, see each respective methods section.

Real-Time PCR

Cells were spun down and directly resuspended in 1 ml Trizol reagent (Life Technologies, Inc., Gaithersburg, MD) in polypropylene tubes. Samples were allowed to incubate at room temperature, and 200 μl chloroform per 1 ml Trizol was added to them. Samples were spun at 10,000 rpm for 15 min, the aqueous phase was transferred into fresh tubes, and equal volumes of isopropanol were added. Samples were then incubated at -20°C for 90 minutes to precipitate the RNA and centrifuged again as described above. Pellets were washed with 1 ml of 70% ethanol and centrifuged. RNA was resuspended in nuclease-free water. The yield and purity of the RNA were determined spectrophotometrically at 260 and 280 nm. cDNA was synthesized using QuantiTect Reverse Transcription Kit (Qiagen, Valencia, CA) using 1 μg RNA according to the manufacturer's instructions. cDNA was quantified with SYBR Green– based detection using an

MX 3000P system (Stratagene, La Jolla, CA) according to the manufacturer's protocols. Forty cycles of PCR (94°C for 15 seconds followed by 60°C for 30 seconds and 72°C for 30 seconds) were performed on a cDNA template.

Statistical analysis

All values are reported as means ± SEM. Continuous ratio scale data were evaluated by unpaired Student's t-test (for comparison between two samples) or by ANOVA (for multiple comparisons) with post hoc analysis using Student's t-test with Bonferroni adjustments. Non-parametric analysis was performed using the Kruskal-Wallis, Kolmogorov-Smirnov, or Mann-Whitney tests. Survival study comparisons were performed using Kaplan-Meier analysis. Statistical calculations were performed on a PC computer using GraphPad Prism version 6.00 for Windows (GraphPad Software, San Diego, CA). Statistical difference was accepted at $p < 0.05$.

Methods for experiments from Chapter 2

Mice

6-8 week old female Balb/c mice were obtained from Jackson Labs and were housed at the Veterinary Medicine Unit at the Ann Arbor Veterans Administration Hospital. Mice were aged to 8-10 weeks old at the time of infection. At the time of data collection, mice were humanely euthanized by CO_2 inhalation followed by severance of the portal vein. All experiments were approved by the University Committee on the Use and Care of Animals and the Veterans Administration Institutional Animal Care and Use Committee.

C. neoformans

C. neoformans serotype A strain H99 (ATCC 208821) was recovered from 10% glycerol frozen stocks stored at -80°C. *C. neoformans* mutants H99-*Δssa1* and H99-*Δssa1::SSA1* were recovered from 10% glycerol frozen stocks stored at -80°C for experiments. Cultures were grown at 37°C in Sabouraud dextrose broth (1% Neopeptone, 2% dextrose, Difco, Detroit, MI) on a shaker. When cultures reached mid-log phase growth (day 3 for H99, day 5 for H99-*Δssa1* and H99-*Δssa1*::SSA1 when cultured from freezer stocks, at which point all strains had similar growth kinetics), an aliquot of culture was washed in sterile non-pyrogenic saline (Travenol, Deerfield, IL), counted on a hemocytometer, and diluted to 3.3×10^5 yeast cells/ml in sterile non-pyrogenic saline.

Generation of serotype A Δssa1 mutant and Δssa1::SSA1 complement strain

To make the deletion construct, a pair of PCR primers, which correspond to an internal sequence within the ORF of *SSA1* (5′-TTCCATCACTCGTGCCCGA-3′ and 5-′TATACAT GTCGTGTCACAGAC-3′), was used to amplify a 1.3 kb *SSA1* genomic fragment. The PCR fragment was cloned into the pCR2.1 TA cloning vector (Invitrogen), and a 1.3 kb fragment of the cryptococcal selection marker *URA5* was PCR amplified from plasmid pURA5g2 as described (129), and inserted into a unique AgeI site. The recovered plasmid (pSSA1URA5-1) was digested with EcoRI, and the deletion construct was gel purified and transformed into a C. neoformans H99 *ura5* strain described previously (253) by electroporation (BioRad). Transformants were screened by PCR, and disruption

of *SSA1* was confirmed by Southern blot using the indicated restriction enzymes and the product was hybridized with a ^{32}P-labelled 1.5 kb PCR-amplified fragment of *SSA1* that was used above to produce the *SSA1* deletion construct. For complementation of the *Δssa1* mutant, a 4.5 kb *SSA1* PCR fragment of wild-type DNA was amplified using 5′-GCCGCCCTGCAGTGAGGTTGATGTGCCTTTCC-3′ and 5′-GCCGCCATCGATATGTCCGAAAGACTATCCGGA-3′, digested with the appropriate restriction enzymes and ligated into compatible sites of pBS-Hyg (pBluscript containing the hygromycin B-resistant gene (254)). The plasmid (pSSA1Hyg-2) was digested with NotI and transformed into the *Δssa1* mutant by electroporation and inoculated onto asparagine agar plates containing hygromycin. The transformant was characterized by Southern blot for *SSA1* and Western blot for Ssa1 and laccase expression analysis. Retention of the *SSA1* deletion in the complemented strain was also confirmed by Southern blot. Furthermore, genomic insertion of the wild-type SSA1-HgR construct was confirmed by Southern blot of uncut DNA hybridized with the HgR gene (data not shown).

Survival study

6-7 mice were infected intratracheally with 10^4 CFU of the wild type H99, H99-*Δssa1* or H99-*Δssa1::SSA1* strains as described above. Mice were monitored daily for survival, and moribund animals were humanely euthanized and survival data recorded.

Assessment of laccase expression

Cryptococcus neoformans strains H99 or H99-*Δssa1* were isolated from the brains of infected mice at the time of death. The brain isolates and the original inoculum were plated on asparagine salts agar (40 g Bacto agar, 4 g Asparagine, 2 g $MgSO_4$, 12 g KH_2PO_4, 12 g glucose, 4 mg thiamine, 4 mM polyphenol per liter in ddH_2O). Melanin production, indicative of laccase expression, results in brown to black-colored colonies, while deficiency in laccase expression results in pale colonies when incubated for 3-7 days at room temperature.

Flow cytometry

For flow cytometry experiments, Abs were purchased from BioLegend (San Diego, CA), including rat anti-murine CD16/CD32 (Fc block), rat anti-murine CD45 conjugated to allophycocyanin, hamster anti-murine CD11c conjugated to Pacific blue, rat anti-murine CD11b conjugated to allophycocyanin-Cy7, rat anti-murine Ly6G conjugated to PE-Cy7, rat anti-murine CD3 or CD19 conjugated to PerCPCy5.5, rat anti-murine CD206 conjugated to FITC, and rat anti-mouse Galectin-3 or MHC class II (2A/IE) conjugated to PE.

RT-qPCR

The primers used are described in Table 6-1. The mRNA levels were normalized to glyceraldehyde-3-phosphate dehydrogenase (GAPDH) mRNA levels and relative expression shown as % of GAPDH.

Gene	Forward/Sense Primer (5′-3′)	Reverse/Anti-Sense Primer (5′-3′)
GAPDH	TATGTCGTGGAGTCTACTGGT	GAGTTGTCATATTTCTCGTGG
IFN-γ	CTACCTCAGACTCTTTGAAGTCT	CAGCGACTCCTTTTCCGCTT
TNF-α	CCTGTAGCCCACGTCGTAGC	AGCAATGACTCCAAAGTAGACC
IL-4	CTGACGGCACAGAGCTATTGA	TATGCGAAGCACCTTGGAAGC
IL-13	GCCAGCCCACAGTTCTACAGC	GAGATGTTGCTCAGCTCCTCA
iNOS	TTTGCTTCCATGCTAATGCGAAAG	GCTCTGTTGAGGTCTAAAGGCTCCG
Fizz1	GGTCCCAGTGCATATGGATGAGACCATAGA	CACCTCTTCACTCGAGGGACAGTTGGCAGC
Arg1	CAGAAGAATGGAAGAGTCAG	CAGATATGCAGGGAGTCACC
CD206	CTCTGTTCAGCTATTGGACGC	CGGAATTTCTGGGATTCAGCTTC
Gal3	TTTCAGGAGAGGGAATGATGTT	TCTTCATCCGATGGTGTGACTG

Table 6-1: Primers used in Chapter 2.

Histology

Lungs were instilled with 1 ml of 10% neutral buffered formalin, excised, immersed 10% in neutral buffered formalin and embedded in paraffin as described previously (46). 5 μm sections were cut and stained with H&E and mucicarmine counterstain. Sections were analyzed with light microscopy and microphotographs were taken using Digital Microphotography system DFX1200 with ACT-1 software (Nikon, Tokyo, Japan).

Fluorescence microscopy

Lungs were inflated and prepared as previously described (71). Sectioning and staining were performed as follows: Serial frozen tissue sections were cut at a thickness of 10 μm and fixed at −20°C in acetone for 10 min. Tissue sections were rehydrated in 70% ethanol for 5 min and washed in PBS for 3 min. Sections were blocked in normal rabbit or rat serum, depending on the species in which the primary staining antibodies used were generated. Antibodies used were rabbit anti-mouse Arg-1 (Santa Cruz Biotechnology, Santa Cruz, CA), rat anti-mouse CD206 (macrophage mannose receptor, AbD Serotec, Raleigh, NC), and rabbit anti-mouse inducible nitric oxide synthase (iNOS, Axxora, San Diego, CA). Primary antibodies were detected using Alexa 488-conjugated goat anti-rat IgG

or goat anti-rabbit IgG secondary antibodies (Invitrogen, Carlsbad, CA). Tissue sections were incubated overnight at 4°C with primary Abs diluted in species-specific serum (3% in PBS) at pre-optimized concentrations. Subsequently, the sections were washed five times in Tris-NaCl-Tween 20 (TNT) buffer solution for 3 min each. Sections were then incubated with secondary Abs for 30 min at room temperature. Slides were washed five times in TNT buffer for 3 min each, once in PBS containing 1% Triton X-100 to minimize background fluorescence (5 min), and given a final wash in TNT buffer (3 min). Sections were then mounted with FluorSave reagent (Calbiochem, La Jolla, CA) containing 0.3 μM DAPI (Molecular Probes, Eugene, OR). Fluorescence was visualized with a Leica DMR epifluorescence microscope (Leica Microsystems, Wetzlar, Germany). Images were acquired using a cooled Spot RT charge-coupled device camera (Diagnostic Instruments, Sterling Heights, MI). Imaging acquisition was done using the auto exposure setting within the software package and evaluating each specimen using these consistent conditions, and imaging analysis was performed using IPLab v4.08 (BD Biosciences).

Methods for experiments from Chapters 3 and 4

Mice

6-8 week old female CBA/J mice were obtained from Jackson Labs and were housed at the Veterinary Medicine Unit at the Ann Arbor Veterans Administration Hospital. Mice were aged to 8-10 weeks old at the time of infection. At the time of data collection, mice were humanely euthanized by CO_2 inhalation followed by severance of the portal vein. All experiments were

approved by the University Committee on the Use and Care of Animals and the Veterans Administration Institutional Animal Care and Use Committee.

C. neoformans

C. neoformans strain 52D (ATCC 24067)was recovered from 10% glycerol frozen stocks stored at -80° C. Cultures were grown at 37°C in Sabouraud dextrose broth (1% Neopeptone, 2% dextrose, Difco, Detroit, MI) on a shaker. When cultures reached mid-log phase growth (day 3 for 52D), an aliquot of culture was washed in sterile non-pyrogenic saline (Travenol, Deerfield, IL), counted on a hemocytometer, and diluted to 3.3×10^5 yeast cells/ml in sterile non-pyrogenic saline.

Cytometric bead array

Cytokine levels were analyzed by LegendPLEX T helper cytokine and Inflammation panels. Serum from whole blood and standard curve was diluted in Matrix C reagent and stained as per manufacturers instructions (BioLegend, San Diego, CA). Bead-antibody-protein complexes were fixed and run on an LSRII flow cytometer using FACSDiva acquisition software. Results were analyzed using software included with LegendPLEX kits.

Magnetic cell separation

From enzymatically digested lungs, lung leukocytes were first labeled with anti-CD4 antibody and magnetically sorted per manufacturers instructions (Stemcell Technologies, Vancouver, BC, Canada). Recovered CD4 cells were pelleted and lysed in Trizol. Flow-through from CD4 sorting was saved, and flow-through

was re-labeled with anti-CD11c antibody and magnetically sorted again. Recovered CD11c cells were pelleted and lysed in Trizol.

Generation of Bone Marrow-derived DCs

Uninfected mice were humanely euthanized and death confirmed by exsanguination. Two femurs and two tibias were isolated from each mouse, washed in 70% ethanol, then epiphyses were removed and marrow flushed with D20 media (DMEM + 20% FBS, 1 U/ml penicillin and streptomycin [Invitrogen, Grand Island, NY], 1X sodium pyruvate, 1X glutamax, 1X non-essential amino acids, 2-mercaptoethanol, 20 nM GM-CSF) using 26 gauge needles. Cells were pelleted, resuspended in D20, and grown in sterile, non-tissue-culture-treated 150mm petri dishes for 7 days. Media was replenished with D20 on day 3. After 7 days, the loosely adherent fraction was harvested in PBS, pelleted, counted, and plated in non-tissue-culture-treated 6-well dishes at a concentration of 2×10^6 cells/well. For an experimental schematic, see Figure 6-1. For the training phase, IFNγ was used at a concentration of 100 ng/ml, TNFα was used at a concentration of 20 ng/ml, and cells were incubated for 24 hours. For the challenge phase, training phase media was aspirated and wells were washed with sterile PBS, and challenge media containing IL-4 was used at a concentration of 20 ng/ml, while IFNγ control-challenge media was at the same concentration as above. For experiments using heat-killed *C.neo*, cultures of strain 52D were counted, diluted to 2×10^8 CFU/mL, and heat killed by incubating at 65°C for 6 hours. Heat-killed cultures were added to the BMDCs at an MOI of 10 during the training phase for 24 hours, and washed out prior to the

challenge phase. For experiments utilizing TNFR1 and/or TNFR2 blockade, sterile validated LEAF-purified blocking antibodies for TNFR1 and TNFR2 were purchased from BioLegend and used at a concentration of 10 μg/ml for 24 hours during the training phase and washed out prior to the challenge phase. For experiments utilizing MM102 (Tocris, Bristol, UK), the inhibitor of MLL1, it was used at a concentration of 50 μM during the training phase for 24 hours and washed out prior to challenge. For media-only and TNFα-only control wells (utilizing same TNFα concentration as above), cells were incubated 24 hours in their respective media, washed identically to experimental wells, and further incubated 24 hours in plain media.

For *ex vivo* BMDC experiments utilizing marrow from infected or uninfected control or TNFα-depleted mice, 4 femurs from each group were isolated and marrow was prepared as above at 7 dpi, taking care to keep each condition separate. Cytokine cycling experiments were performed exactly as above.

In each condition, after the 24 hour challenge phase, media was aspirated and cells were either lysed in 1ml Trizol or incubated with cold PBS on ice and gently scraped from the bottom of the well and stained as above for flow cytometric analysis.

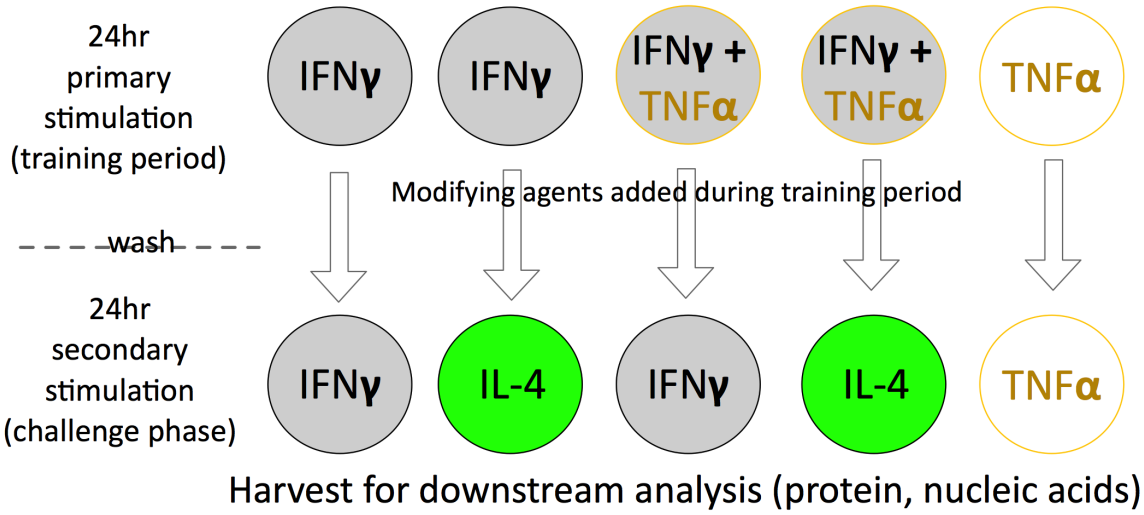

Figure 6-1 Schematic detailing training and challenge phase for *in vitro* experiments from chapters 3 and 4.

qPCR

For CD4 cells, T helper differentiation qPCR arrays with 96 genes per sample were purchased from SA Biosciences (Qiagen) and used initially, while individual RT-qPCR reactions were performed later to confirm and expand analyzed genes. For CD11c cells, custom qPCR arrays with 48 genes per sample were used initially, while individual RT-qPCR reactions were performed later to confirm and expand analyzed genes. RNA was converted to cDNA as described above and mixed with nuclease-free water and master mix according to manufacturer's instructions. Data was analyzed using the 2^{-ddct} method using β-actin as housekeeping control gene and each sample normalized to uninfected control. Data and heatmaps were prepared using Excel (Microsoft, Redmond, WA, USA).

For BMDC experiments, RT-qPCR was performed as described above using the primers listed below in Table 6-2. Each sample was run in duplicate and ct values were averaged before performing calculations. 18s was used as the housekeeping control gene and each sample was normalized to media only-treated BMDCs.

Gene	Sense primer	Antisense primer
18s	GAGGCCCTGTAATTGGAATGAG	GCAGCAACTTTAATATCCGCTATTGG
iNOS	TTTGCTTCCATGCTAATGCGAAAG	GCTCTGTTGAGGTCTAAAGGCTCCG
Arginase	CAGAAGAATGGAAGAGTCAG	CAGATATGCAGGGAGTCACC
Fizz1	GGTCCCAGTGCATATGGATGAGACCATAGA	CACCTCTTCACTCGAGGGACAGTTGGCAGC
MHCII	GCGACGTGGGCGAGTACC	CATTCCGGAACCAGCGCA
CD206	CTCTGTTCAGCTATTGGACGC	CGGAATTTCTGGGATTCAGCTTC
IL-12b	GGAAGCACGGGGAGCAGAATA	AACTTGAGGGAGAAGTAGGAATGG
IL-13	GCCAGCCCACAGTTCTACAGC	GAGATGTTGCTCAGCTCCTCA
iNOS (promoter)	TCCCTAGTGAGTCCCAGTTTTGA	CTGGTCGCCCGTCCAAGG
IL-12b (promoter)	TTCCCCCAGAATGTTTTGACA	TGATGGAAACCCAAAGTAGAAACTG
β-actin (promoter)	AAGGACTCCTATGTGGGTGACGA	ATCTTCTCCATGTCGTCCCAGTTC
Fizz1 (promoter)	TGCAATTCTTTGATGCTGTGTCT	AGCACCCTCAACCCAAAGTG
KDM5c	GACCCATCGCCGAGAAGTC	TCGGGGAGTAAACCTGAAGTT
MLL1	ATCCTCTCAGACCCATCTGTGT	GTAGGAGGTCTTCCTCTCTTC

Table 6-2 Primers used in Chapters 3 and 4.

Flow Cytometry

Antibody	Clone	Vendor
IFNγ	XGM1.2	Biolegend
IL-17	TC11-18H10.1	Biolegend
IL-13	eBio13A	eBiosciences
TNFα	MP6-XT22	Biolegend
MHCII	11-5.2	BD Biosciences
CD86	GL-1	Biolegend
CD206	C068C2	Biolegend
Gal3	eBioM3/38	Biolegend
H3K4me3	MABI 0304	Active Motif
CD45	30-F11	Biolegend
CD3ε	145-2C11	Biolegend
CD19	6D5	Biolegend
CD11b	M1/70	Biolegend
CD11c	N418	Biolegend
Ly6C	HK1.4	Biolegend
Ly6G	1A8	Biolegend
Lin (CD3/Gr-1/CD11b/B220/Ter-119)	N/A	Biolegend
SCA-1	D7	Biolegend
Flt-3	A2F10	Biolegend
c-kit	2B8	Biolegend
CD115	AFS98	Biolegend
CD4	GK1.5	Biolegend
CD8	53-6.7	Biolegend

Table 6-3 Flow cytometry antibodies used in chapters 3 and 4.

Antibodies for intranuclear staining of H3K4me3 were conjugated in house using PE-Cy7 conjugation kit according to the manufacturer's protocol (Abcam, Cambridge, UK). Gating schemes can be seen for pulmonary CD4 T cells (Figure 6-2), pulmonary DCs (Figure 6-3), and bone marrow myeloid precursor cells and pre-DCs (Figure 6-4) below.

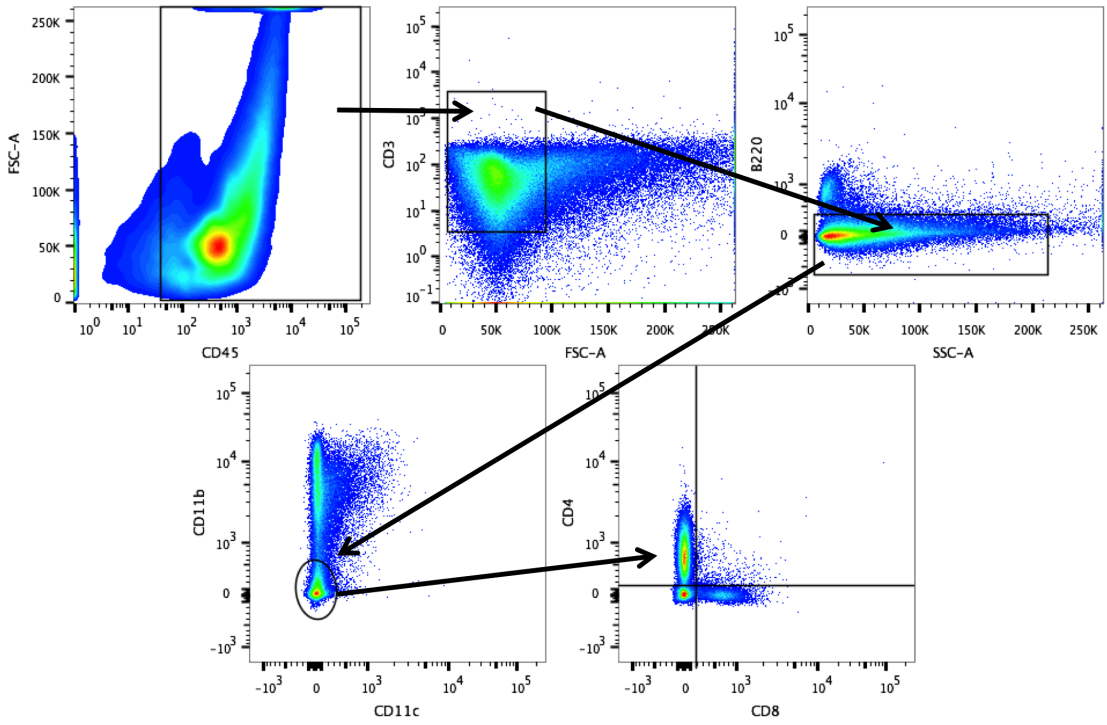

Figure 6-2 Gating scheme for pulmonary CD4 T cells: CD45$^+$/CD3$^+$/B220/CD11b/CD11c/CD4$^+$.

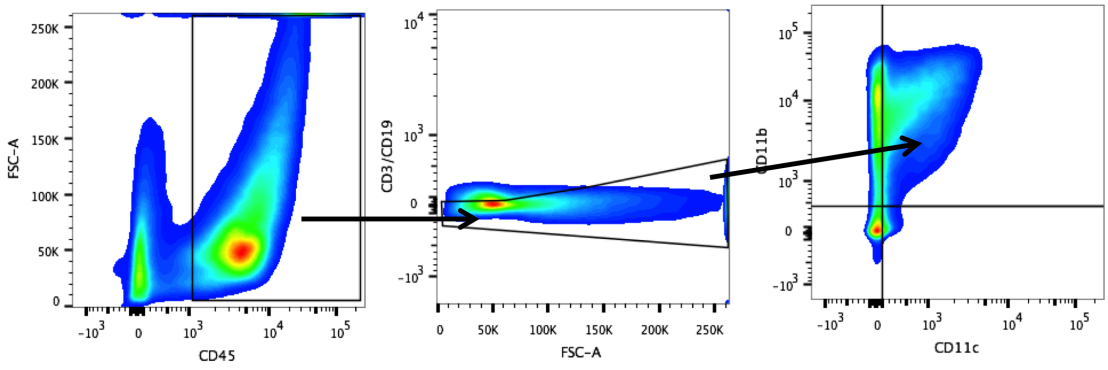

Figure 6-3 Gating scheme for lung dendritic cells: CD45$^+$/Fsc^{high}/CD3/CD19/CD11b$^+$/CD11c^{high}.

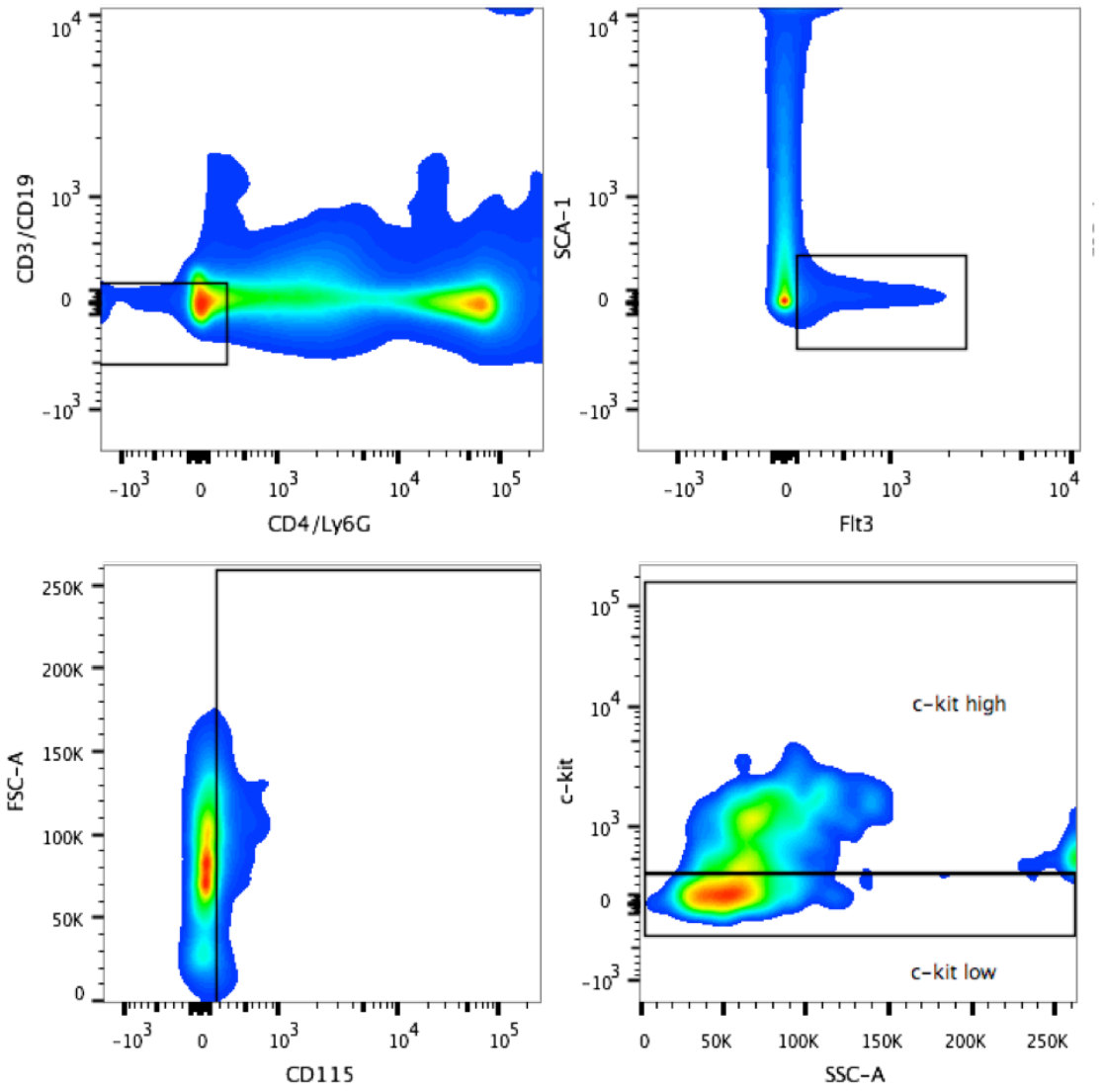

Figure 6-4 Gating scheme for bone marrow myeloid precursor cells and pre-DCs: CD3/CD19/CD4/Ly6G$^-$/SCA-1/Flt3$^-$/CD115$^-$; pre-DCs were further gated on c-kit^{low}.

Adoptive transfer

At day -7, BMDCs were generated as described above, differentiated over 7 days, and on day 0, the loosely-adherent fraction was plated as described above and stimulated for 24 hours with TNF α and IFN γ in combination (γ α) to generate TNF α -trained DC1s, or with IFN γ alone (γ -alone) to generate untrained DC1s.

On day 0, CBA/J mice were inoculated i.t. as above with *C.neo* 52D and TNF α-depleted by i.p. injection of TNF α-blocking antibody. On day 0, another set of BMDCs were generated and differentiated as described above for 7 days. On day 1, 1 million γ α DCs or γ-only DCs in plain PBS were injected i.v. through the retro-orbital route into the *C.neo*-infected, TNF α-depleted mice. On day 7, the loosely-adherent fraction of the second set of BMDCs were harvested, plated, and stimulated for 24 hours with γ α or γ-alone. On day 8, a second retro-orbital injection of 1 million γ α or γ-alone DCs were transferred as described above (for schematic, see Figure 3-12A). Mice were harvested at 14 dpi and the CD4 T cells assessed for Th polarization by intracellular flow cytometry.

Chromatin immunoprecipitation and qPCR

ChIP was performed using the protocol from the laboratory of Dr. Yali Dou at the University of Michigan Department of Pathology. Briefly, magnetically separated $CD11c^+$ cells were isolated from the lungs of mice at 14 dpi and fixed in formaldehyde at a final concentration of 1%. The fixation was stopped with 5M glycine, and cells were pelleted, the supernatant aspirated, and pellets frozen at -80°C until 25-30 x 10^6 cells per treatment were accumulated. Cells were thawed and lysed in SDS lysis buffer (1% SDS, 10mM EDTA, 50mM Tris pH 8.0, 1x complete protease inhibitor cocktail), homogenized by aspiration through a 27-gauge needle twice. Cells were sonicated on ice in a Bioruptor using the highest setting for 15 minutes with 30 sec on/30 sec off cycles. Sonication efficiency and chromatin shearing was assessed by running a small aliquot of

sample on 1% agarose gel before proceeding. Reactions were centrifuged to pellet debris, and supernatant removed and diluted in ChIP dilution buffer (0.01% SDS, 1.1% TritonX-100, 1.2mM EDTA, 16.7mM Tris-HCL pH 7.5, 167mM NaCl, 1x complete protease inhibitor cocktail). 1% input fraction was removed here, then diluted lysate was aliquotted to eppendorf tubes and antibodies were added at a concentration of 2.5 ug. Reactions were incubated over night rotating at 4°C. For immunoprecipitation, 30 ul protein G Dynabeads (Life technologies, Carlsbad, CA, USA) were used for each reaction. Reactions were washed with increasingly stringent washes: low salt wash buffer (0.1% SDS, 1% TritonX-100, 2mM EDTA, 20mM Tris-HCL pH 7.5, 150 mM NaCl), high salt wash buffer (0.1% SDS, 1% TritonX-100, 2mM EDTA, 20mM Tris-HCL pH 7.5, 500 mM NaCl), LiCl wash buffer (0.25M LiCl, 1% NP-40, 1% deoxycholic acid, 1mM EDTA, 10mM Tris-HCK pH 7.5), and TE wash buffer (10mM Tris0-HCL pH 7.5, 1 mM EDTA). Finally, antibody-protein-DNA complexes were eluted using elution buffer (1% SDS, 0.5mM $NaHCO_3$) and heated at 37°C for 1 hour. Crosslinking was reversed by addition of 5M NaCl and incubated overnight at 65°C. DNA was purified using phenol chloroform extraction and isopropanol precipitation. qPCR was performed as described above, using recovered genomic DNA as the template, and primers specific to the promoter regions of β-actin, Fizz, iNOS, and IL-12b.

Fluorescence microscopy

$CD11b^+$ pre-DCs were isolated from the bone marrow of isotype or TNFα-depleted infected and control mice by magnetic bead separation as described above according to the manufacturer's protocol. Cells were washed and counted, then 20,000 cells were cytospun onto charged glass microscope slides, fixed, and

stained with primary antibodies against H3K4me3 (Active Motif, Carlsbad, CA) and Fizz1 (R&D Systems, Minneapolis, MN) or control IgG (R&D Systems), and then stained using anti-rabbit AlexaFluor 594 or anti- goat AlexaFluor 488 secondary antibodies, and mounted with VECTASHIELD mounting media plus DAPI (Vector laboratories, Burlingame, CA, USA). Slides were visualized by confocal microscopy using a spinning disk confocal microscope (Olympus America Inc., Center Valley, PA) with a digital CCD camera (Hamamatsu Photonics, Hamamatsu, Japan) for image capture and an arc lamp illumination source providing excitation wavelengths of 350 to 700 nm and three-color emission analyses. The acquired digital images were processed and analyzed using Stereo Investigator software version 9 (MBF Bioscience, Williston, VT).

References

1. Huffnagle GB, Lipscomb MF, Lovchik JA, Hoag KA, Street NE. The role of CD4+ and CD8+ T cells in the protective inflammatory response to a pulmonary cryptococcal infection. Journal of leukocyte biology. 1994;55(1):35-42. PubMed PMID: 7904293.

2. Vecchiarelli A, Pietrella D, Dottorini M, Monari C, Retini C, Todisco T, Bistoni F. Encapsulation of Cryptococcus neoformans regulates fungicidal activity and the antigen presentation process in human alveolar macrophages. Clin Exp Immunol. 1994;98(2):217-23. PubMed PMID: 7955525; PubMed Central PMCID: PMC1534403.

3. Arora S, Hernandez Y, Erb-Downward JR, McDonald RA, Toews GB, Huffnagle GB. Role of IFN-gamma in regulating T2 immunity and the development of alternatively activated macrophages during allergic bronchopulmonary mycosis. J Immunol. 2005;174(10):6346-56. PubMed PMID: 15879135.

4. Abe K, Kadota J, Ishimatsu Y, Iwashita T, Tomono K, Kawakami K, Kohno S. Th1-Th2 cytokine kinetics in the bronchoalveolar lavage fluid of mice infected with Cryptococcus neoformans of different virulences. Microbiology and immunology. 2000;44(10):849-55. PubMed PMID: 11128069.

5. Guillot L, Carroll SF, Homer R, Qureshi ST. Enhanced innate immune responsiveness to pulmonary Cryptococcus neoformans infection is associated with resistance to progressive infection. Infect Immun. 2008;76(10):4745-56. Epub 2008/08/06. doi: 10.1128/IAI.00341-08. PubMed PMID: 18678664; PubMed Central PMCID: PMC2546841.

6. Snelgrove RJ, Edwards L, Williams AE, Rae AJ, Hussell T. In the absence of reactive oxygen species, T cells default to a Th1 phenotype and mediate protection against pulmonary Cryptococcus neoformans infection. J Immunol. 2006;177(8):5509-16. PubMed PMID: 17015737.

7. Kawakami K, Tohyama M, Qifeng X, Saito A. Expression of cytokines and inducible nitric oxide synthase mRNA in the lungs of mice infected with Cryptococcus neoformans: effects of interleukin-12. Infect Immun. 1997;65(4):1307-12. PubMed PMID: 9119466; PubMed Central PMCID: PMC175132.

8. Merad M, Sathe P, Helft J, Miller J, Mortha A. The dendritic cell lineage: ontogeny and function of dendritic cells and their subsets in the steady state and the inflamed setting. Annu Rev Immunol. 2013;31:563-604. doi: 10.1146/annurev-immunol-020711-074950. PubMed PMID: 23516985; PubMed Central PMCID: PMC3853342.

9. Lindell DM, Moore TA, McDonald RA, Toews GB, Huffnagle GB. Distinct compartmentalization of CD4+ T-cell effector function versus proliferative capacity during pulmonary cryptococcosis. Am J Pathol. 2006;168(3):847-55. PubMed PMID: 16507900.

10. Syme RM, Spurrell JC, Amankwah EK, Green FH, Mody CH. Primary dendritic cells phagocytose Cryptococcus neoformans via mannose receptors and

Fcgamma receptor II for presentation to T lymphocytes. Infect Immun. 2002;70(11):5972-81. PubMed PMID: 12379672; PubMed Central PMCID: PMC130340.

11. Wozniak KL, Levitz SM. Cryptococcus neoformans enters the endolysosomal pathway of dendritic cells and is killed by lysosomal components. Infect Immun. 2008;76(10):4764-71. doi: 10.1128/IAI.00660-08. PubMed PMID: 18678670; PubMed Central PMCID: PMC2546838.

12. Park BJ, Wannemuehler KA, Marston BJ, Govender N, Pappas PG, Chiller TM. Estimation of the current global burden of cryptococcal meningitis among persons living with HIV/AIDS. AIDS. 2009;23(4):525-30. doi: 10.1097/QAD.0b013e328322ffac. PubMed PMID: 19182676.

13. Giles SS, Dagenais TR, Botts MR, Keller NP, Hull CM. Elucidating the pathogenesis of spores from the human fungal pathogen Cryptococcus neoformans. Infect Immun. 2009;77(8):3491-500. doi: 10.1128/IAI.00334-09. PubMed PMID: 19451235; PubMed Central PMCID: PMC2715683.

14. Velagapudi R, Hsueh YP, Geunes-Boyer S, Wright JR, Heitman J. Spores as infectious propagules of Cryptococcus neoformans. Infect Immun. 2009;77(10):4345-55. doi: 10.1128/IAI.00542-09. PubMed PMID: 19620339; PubMed Central PMCID: PMC2747963.

15. Cassone A, Simonetti N, Strippoli V. Wall structure and bud formation inCryptococcus neoformans. Arch Microbiol. 1974;95(1):205-12. doi: 10.1007/BF02451762.

16. Feldmesser M, Kress Y, Casadevall A. Dynamic changes in the morphology of Cryptococcus neoformans during murine pulmonary infection. Microbiology. 2001;147(Pt 8):2355-65. PubMed PMID: 11496012.

17. Chuck SL, Sande MA. Infections with Cryptococcus neoformans in the acquired immunodeficiency syndrome. The New England journal of medicine. 1989;321(12):794-9. doi: 10.1056/NEJM198909213211205. PubMed PMID: 2671735.

18. Pappas PG, Perfect JR, Cloud GA, Larsen RA, Pankey GA, Lancaster DJ, Henderson H, Kauffman CA, Haas DW, Saccente M, Hamill RJ, Holloway MS, Warren RM, Dismukes WE. Cryptococcosis in human immunodeficiency virus-negative patients in the era of effective azole therapy. Clin Infect Dis. 2001;33(5):690-9. doi: 10.1086/322597. PubMed PMID: 11477526.

19. Baddley JW, Perfect JR, Oster RA, Larsen RA, Pankey GA, Henderson H, Haas DW, Kauffman CA, Patel R, Zaas AK, Pappas PG. Pulmonary cryptococcosis in patients without HIV infection: factors associated with disseminated disease. European journal of clinical microbiology & infectious diseases : official publication of the European Society of Clinical Microbiology. 2008;27(10):937-43. doi: 10.1007/s10096-008-0529-z. PubMed PMID: 18449582.

20. Hoang LM, Maguire JA, Doyle P, Fyfe M, Roscoe DL. Cryptococcus neoformans infections at Vancouver Hospital and Health Sciences Centre (1997-2002): epidemiology, microbiology and histopathology. Journal of medical microbiology. 2004;53(Pt 9):935-40. PubMed PMID: 15314203.

21. Kidd SE, Hagen F, Tscharke RL, Huynh M, Bartlett KH, Fyfe M, Macdougall L, Boekhout T, Kwon-Chung KJ, Meyer W. A rare genotype of Cryptococcus gattii caused the cryptococcosis outbreak on Vancouver Island (British Columbia, Canada). Proceedings of the National Academy of Sciences of the United States of America. 2004;101(49):17258-63. doi: 10.1073/pnas.0402981101. PubMed PMID: 15572442; PubMed Central PMCID: PMC535360.

22. Dixit A, Carroll SF, Qureshi ST. Cryptococcus gattii: An Emerging Cause of Fungal Disease in North America. Interdisciplinary perspectives on infectious diseases. 2009;2009:840452. doi: 10.1155/2009/840452. PubMed PMID: 19503836; PubMed Central PMCID: PMC2686104.

23. Rosen LB, Freeman AF, Yang LM, Jutivorakool K, Olivier KN, Angkasekwinai N, Suputtamongkol Y, Bennett JE, Pyrgos V, Williamson PR, Ding L, Holland SM, Browne SK. Anti-GM-CSF autoantibodies in patients with cryptococcal meningitis. J Immunol. 2013;190(8):3959-66. doi: 10.4049/jimmunol.1202526. PubMed PMID: 23509356; PubMed Central PMCID: PMC3675663.

24. Saijo T, Chen J, Chen SC, Rosen LB, Yi J, Sorrell TC, Bennett JE, Holland SM, Browne SK, Kwon-Chung KJ. Anti-granulocyte-macrophage colony-stimulating factor autoantibodies are a risk factor for central nervous system infection by Cryptococcus gattii in otherwise immunocompetent patients. mBio. 2014;5(2):e00912-14. doi: 10.1128/mBio.00912-14. PubMed PMID: 24643864; PubMed Central PMCID: PMC3967522.

25. Chen GH, Olszewski MA, McDonald RA, Wells JC, Paine R, 3rd, Huffnagle GB, Toews GB. Role of granulocyte macrophage colony-stimulating factor in host defense against pulmonary Cryptococcus neoformans infection during murine allergic bronchopulmonary mycosis. Am J Pathol. 2007;170(3):1028-40. PubMed PMID: 17322386.

26. Browne SK. Anticytokine autoantibody-associated immunodeficiency. Annu Rev Immunol. 2014;32:635-57. doi: 10.1146/annurev-immunol-032713-120222. PubMed PMID: 24499273.

27. Ordonez ME, Farraye FA, Di Palma JA. Endemic Fungal Infections in Inflammatory Bowel Disease Associated with Anti-TNF Antibody Therapy. Inflammatory bowel diseases. 2013. doi: 10.1097/MIB.0b013e31828f1fba. PubMed PMID: 23694943.

28. Osawa R, Singh N. Colitis as a manifestation of infliximab-associated disseminated cryptococcosis. International journal of infectious diseases : IJID : official publication of the International Society for Infectious Diseases. 2010;14(5):e436-40. doi: 10.1016/j.ijid.2009.05.019. PubMed PMID: 19660974.

29. Wilson ML, Sewell LD, Mowad CM. Primary cutaneous Cryptococcosis during therapy with methotrexate and adalimumab. Journal of drugs in dermatology : JDD. 2008;7(1):53-4. PubMed PMID: 18246698.

30. Hage CA, Wood KL, Winer-Muram HT, Wilson SJ, Sarosi G, Knox KS. Pulmonary cryptococcosis after initiation of anti-tumor necrosis factor-alpha therapy. Chest. 2003;124(6):2395-7. PubMed PMID: 14665529.

31. Perez-Zafrilla B, Carmona L, Gomez-Reino JJ. Infections in patients with rheumatic diseases treated with TNF antagonists. Current pharmaceutical biotechnology. 2012;13(8):1418-25. PubMed PMID: 22339219.

32. Huffnagle GB, Boyd MB, Street NE, Lipscomb MF. IL-5 is required for eosinophil recruitment, crystal deposition, and mononuclear cell recruitment during a pulmonary Cryptococcus neoformans infection in genetically susceptible mice (C57BL/6). J Immunol. 1998;160(5):2393-400. PubMed PMID: 9498782.

33. Hoag KA, Street NE, Huffnagle GB, Lipscomb MF. Early cytokine production in pulmonary Cryptococcus neoformans infections distinguishes

susceptible and resistant mice. American journal of respiratory cell and molecular biology. 1995;13(4):487-95. PubMed PMID: 7546779.

34. Kobayashi M, Murata K, Hiroshi HO, Tokura Y. Cryptococcosis: long-lasting presence of fungi after successful treatment. Acta dermato-venereologica. 2004;84(4):320-1. PubMed PMID: 15339084.

35. Spitzer ED, Spitzer SG, Freundlich LF, Casadevall A. Persistence of initial infection in recurrent Cryptococcus neoformans meningitis. Lancet. 1993;341(8845):595-6. PubMed PMID: 8094831.

36. Kozel TR, Wilson MA, Pfrommer GS, Schlageter AM. Activation and binding of opsonic fragments of C3 on encapsulated Cryptococcus neoformans by using an alternative complement pathway reconstituted from six isolated proteins. Infect Immun. 1989;57(7):1922-7. PubMed PMID: 2525113; PubMed Central PMCID: PMC313821.

37. Davis MJ, Tsang TM, Qiu Y, Dayrit JK, Freij JB, Huffnagle GB, Olszewski MA. Macrophage M1/M2 polarization dynamically adapts to changes in cytokine microenvironments in Cryptococcus neoformans infection. mBio. 2013;4(3):e00264-13. Epub 2013/06/20. doi: 10.1128/mBio.00264-13. PubMed PMID: 23781069; PubMed Central PMCID: PMC3684832.

38. Wozniak KL, Vyas JM, Levitz SM. In vivo role of dendritic cells in a murine model of pulmonary cryptococcosis. Infect Immun. 2006;74(7):3817-24. doi: 10.1128/IAI.00317-06. PubMed PMID: 16790753; PubMed Central PMCID: PMC1489690.

39. Syme RM, Spurrell JC, Ma LL, Green FH, Mody CH. Phagocytosis and protein processing are required for presentation of Cryptococcus neoformans

mitogen to T lymphocytes. Infect Immun. 2000;68(11):6147-53. PubMed PMID: 11035718; PubMed Central PMCID: PMC97692.

40. Bauman SK, Nichols KL, Murphy JW. Dendritic cells in the induction of protective and nonprotective anticryptococcal cell-mediated immune responses. J Immunol. 2000;165(1):158-67. PubMed PMID: 10861048.

41. Osterholzer JJ, Milam JE, Chen GH, Toews GB, Huffnagle GB, Olszewski MA. Role of dendritic cells and alveolar macrophages in regulating early host defense against pulmonary infection with Cryptococcus neoformans. Infect Immun. 2009;77(9):3749-58. Epub 2009/07/01. doi: 10.1128/IAI.00454-09. PubMed PMID: 19564388; PubMed Central PMCID: PMC2737986.

42. Pericolini E, Cenci E, Gabrielli E, Perito S, Mosci P, Bistoni F, Vecchiarelli A. Indinavir influences biological function of dendritic cells and stimulates antifungal immunity. Journal of leukocyte biology. 2008;83(5):1286-94. doi: 10.1189/jlb.0707454. PubMed PMID: 18252869.

43. Osterholzer JJ, Curtis JL, Polak T, Ames T, Chen GH, McDonald R, Huffnagle GB, Toews GB. CCR2 Mediates Conventional Dendritic Cell Recruitment and the Formation of Bronchovascular Mononuclear Cell Infiltrates in the Lungs of Mice Infected with Cryptococcus neoformans. J Immunol. 2008;181(1):610-20. PubMed PMID: 18566428.

44. Osterholzer JJ, Chen GH, Olszewski MA, Curtis JL, Huffnagle GB, Toews GB. Accumulation of CD11b+ lung dendritic cells in response to fungal infection results from the CCR2-mediated recruitment and differentiation of Ly-6Chigh monocytes. J Immunol. 2009;183(12):8044-53. Epub 2009/11/26. doi: 10.4049/jimmunol.0902823. PubMed PMID: 19933856.

45. Huffnagle GB, Toews GB, Burdick MD, Boyd MB, McAllister KS, McDonald RA, Kunkel SL, Strieter RM. Afferent phase production of TNF-alpha is required for the development of protective T cell immunity to Cryptococcus neoformans. J Immunol. 1996;157(10):4529-36. PubMed PMID: 8906831.

46. Zhang Y, Wang F, Tompkins KC, McNamara A, Jain AV, Moore BB, Toews GB, Huffnagle GB, Olszewski MA. Robust Th1 and Th17 immunity supports pulmonary clearance but cannot prevent systemic dissemination of highly virulent Cryptococcus neoformans H99. Am J Pathol. 2009;175(6):2489-500. Epub 2009/11/07. doi: 10.2353/ajpath.2009.090530. PubMed PMID: 19893050; PubMed Central PMCID: PMC2789623.

47. Chen GH, McNamara DA, Hernandez Y, Huffnagle GB, Toews GB, Olszewski MA. Inheritance of immune polarization patterns is linked to resistance versus susceptibility to Cryptococcus neoformans in a mouse model. Infect Immun. 2008;76(6):2379-91. Epub 2008/04/09. doi: 10.1128/IAI.01143-07. PubMed PMID: 18391002; PubMed Central PMCID: PMC2423067.

48. Hardison SE, Ravi S, Wozniak KL, Young ML, Olszewski MA, Wormley FL, Jr. Pulmonary infection with an interferon-gamma-producing Cryptococcus neoformans strain results in classical macrophage activation and protection. Am J Pathol. 2010;176(2):774-85. doi: 10.2353/ajpath.2010.090634. PubMed PMID: 20056835; PubMed Central PMCID: PMC2808084.

49. Osterholzer JJ, Surana R, Milam JE, Montano GT, Chen GH, Sonstein J, Curtis JL, Huffnagle GB, Toews GB, Olszewski MA. Cryptococcal urease promotes the accumulation of immature dendritic cells and a non-protective T2 immune response within the lung. Am J Pathol. 2009;174(3):932-43. Epub

2009/02/17. doi: 10.2353/ajpath.2009.080673. PubMed PMID: 19218345; PubMed Central PMCID: PMC2665753.

50. Murphy JW. Clearance of Cryptococcus neoformans from immunologically suppressed mice. Infect Immun. 1989;57(7):1946-52. PubMed PMID: 2499541; PubMed Central PMCID: PMC313825.

51. Mody CH, Lipscomb MF, Street NE, Toews GB. Depletion of CD4+ (L3T4+) lymphocytes in vivo impairs murine host defense to Cryptococcus neoformans. J Immunol. 1990;144(4):1472-7. PubMed PMID: 1968080.

52. Huffnagle GB, Yates JL, Lipscomb MF. T cell-mediated immunity in the lung: a *Cryptococcus neoformans* pulmonary infection model using SCID and athymic nude mice. Infect Immun. 1991;59(4):1423-33.

53. Huffnagle GB, Yates JL, Lipscomb MF. Immunity to a pulmonary *Cryptococcus neoformans* infection requires both CD4+ and CD8+ T cells. J Exp Med. 1991;173(4):793-800.

54. Jarvis JN, Harrison TS. HIV-associated cryptococcal meningitis. AIDS. 2007;21(16):2119-29. doi: 10.1097/QAD.0b013e3282a4a64d. PubMed PMID: 18090038.

55. Kovacs JA, Kovacs AA, Polis M, Wright WC, Gill VJ, Tuazon CU, Gelmann EP, Lane HC, Longfield R, Overturf G, et al. Cryptococcosis in the acquired immunodeficiency syndrome. Annals of internal medicine. 1985;103(4):533-8. PubMed PMID: 3898951.

56. Huffnagle GB, Lipscomb MF. Pulmonary cryptococcosis. Am J Pathol. 1992;141(6):1517-20. PubMed PMID: 1466407; PubMed Central PMCID: PMC1886780.

57. Mody CH, Tyler CL, Sitrin RG, Jackson C, Toews GB. Interferon-gamma activates rat alveolar macrophages for anticryptococcal activity. American journal of respiratory cell and molecular biology. 1991;5(1):19-26. PubMed PMID: 1908686.

58. Lim TS, Murphy JW. Transfer of immunity to cryptococcosis by T-enriched splenic lymphocytes from Cryptococcus neoformans-sensitized mice. Infect Immun. 1980;30(1):5-11. PubMed PMID: 7002791; PubMed Central PMCID: PMC551268.

59. Mody CH, Chen GH, Jackson C, Curtis JL, Toews GB. Depletion of murine CD8+ T cells in vivo decreases pulmonary clearance of a moderately virulent strain of Cryptococcus neoformans. J Lab Clin Med. 1993;121(6):765-73. PubMed PMID: 7685044.

60. Steinman RM. Decisions about dendritic cells: past, present, and future. Annu Rev Immunol. 2012;30:1-22. doi: 10.1146/annurev-immunol-100311-102839. PubMed PMID: 22136168.

61. Ma H, May RC. Virulence in Cryptococcus species. Advances in applied microbiology. 2009;67:131-90. doi: 10.1016/S0065-2164(08)01005-8. PubMed PMID: 19245939.

62. Hill JO, Dunn PL. A T cell-independent protective host response against Cryptococcus neoformans expressed at the primary site of infection in the lung. Infect Immun. 1993;61(12):5302-8. PubMed PMID: 7901167; PubMed Central PMCID: PMC281315.

63. Mody CH, Chen GH, Jackson C, Curtis JL, Toews GB. In vivo depletion of murine CD8 positive T cells impairs survival during infection with a highly

virulent strain of Cryptococcus neoformans. Mycopathologia. 1994;125(1):7-17. PubMed PMID: 8028643.

64. Chen GH, McDonald RA, Wells JC, Huffnagle GB, Lukacs NW, Toews GB. The gamma interferon receptor is required for the protective pulmonary inflammatory response to Cryptococcus neoformans. Infect Immun. 2005;73(3):1788-96. PubMed PMID: 15731080.

65. Qiu Y, Zeltzer S, Zhang Y, Wang F, Chen GH, Dayrit J, Murdock BJ, Bhan U, Toews GB, Osterholzer JJ, Standiford TJ, Olszewski MA. Early induction of CCL7 downstream of TLR9 signaling promotes the development of robust immunity to cryptococcal infection. J Immunol. 2012;188(8):3940-8. Epub 2012/03/17. doi: 10.4049/jimmunol.1103053. PubMed PMID: 22422883; PubMed Central PMCID: PMC3324623.

66. Aguirre K, Havell EA, Gibson GW, Johnson LL. Role of tumor necrosis factor and gamma interferon in acquired resistance to Cryptococcus neoformans in the central nervous system of mice. Infect Immun. 1995;63(5):1725-31. PubMed PMID: 7729878; PubMed Central PMCID: PMC173216.

67. Zhang Y, Wang F, Bhan U, Huffnagle GB, Toews GB, Standiford TJ, Olszewski MA. TLR9 signaling is required for generation of the adaptive immune protection in Cryptococcus neoformans-infected lungs. Am J Pathol. 2010;177(2):754-65. Epub 2010/06/29. doi: 10.2353/ajpath.2010.091104. PubMed PMID: 20581055; PubMed Central PMCID: PMC2913381.

68. Nakamura K, Miyazato A, Xiao G, Hatta M, Inden K, Aoyagi T, Shiratori K, Takeda K, Akira S, Saijo S, Iwakura Y, Adachi Y, Ohno N, Suzuki K, Fujita J, Kaku M, Kawakami K. Deoxynucleic acids from Cryptococcus neoformans

activate myeloid dendritic cells via a TLR9-dependent pathway. J Immunol. 2008;180(6):4067-74. PubMed PMID: 18322216.

69. Axton PJ, Bancroft GJ. In vivo analysis of immune responses to Cryptococcus neoformans--role of interferon-gamma in host resistance. Biochemical Society transactions. 1997;25(2):276S. PubMed PMID: 9191320.

70. Flesch IE, Schwamberger G, Kaufmann SH. Fungicidal activity of IFN-gamma-activated macrophages. Extracellular killing of Cryptococcus neoformans. J Immunol. 1989;142(9):3219-24. PubMed PMID: 2496162.

71. Hardison SE, Herrera G, Young ML, Hole CR, Wozniak KL, Wormley FL, Jr. Protective immunity against pulmonary cryptococcosis is associated with STAT1-mediated classical macrophage activation. J Immunol. 2012;189(8):4060-8. doi: 10.4049/jimmunol.1103455. PubMed PMID: 22984078; PubMed Central PMCID: PMC3466339.

72. Murdock BJ, Huffnagle GB, Olszewski MA, Osterholzer JJ. Interleukin-17A enhances host defense against cryptococcal lung infection through effects mediated by leukocyte recruitment, activation, and gamma interferon production. Infect Immun. 2014;82(3):937-48. doi: 10.1128/IAI.01477-13. PubMed PMID: 24324191; PubMed Central PMCID: PMC3957981.

73. Kawakami K, Qifeng X, Tohyama M, Qureshi MH, Saito A. Contribution of tumour necrosis factor-alpha (TNF-alpha) in host defence mechanism against Cryptococcus neoformans. Clin Exp Immunol. 1996;106(3):468-74. PubMed PMID: 8973614; PubMed Central PMCID: PMC2200622.

74. Kawakami K, Tohyama M, Teruya K, Kudeken N, Xie Q, Saito A. Contribution of interferon-gamma in protecting mice during pulmonary and disseminated infection with Cryptococcus neoformans. FEMS immunology and

medical microbiology. 1996;13(2):123-30. doi: 10.1016/0928-8244(95)00093-3. PubMed PMID: 8731020.

75. Kleinschek MA, Muller U, Brodie SJ, Stenzel W, Kohler G, Blumenschein WM, Straubinger RK, McClanahan T, Kastelein RA, Alber G. IL-23 enhances the inflammatory cell response in Cryptococcus neoformans infection and induces a cytokine pattern distinct from IL-12. J Immunol. 2006;176(2):1098-106. PubMed PMID: 16393998.

76. Zaragoza O, Alvarez M, Telzak A, Rivera J, Casadevall A. The relative susceptibility of mouse strains to pulmonary Cryptococcus neoformans infection is associated with pleiotropic differences in the immune response. Infect Immun. 2007;75(6):2729-39. doi: 10.1128/IAI.00094-07. PubMed PMID: 17371865; PubMed Central PMCID: PMC1932903.

77. Szymczak WA, Sellers RS, Pirofski LA. IL-23 dampens the allergic response to Cryptococcus neoformans through IL-17-independent and -dependent mechanisms. Am J Pathol. 2012;180(4):1547-59. doi: 10.1016/j.ajpath.2011.12.038. PubMed PMID: 22342846; PubMed Central PMCID: PMC3349902.

78. Piehler D, Stenzel W, Grahnert A, Held J, Richter L, Kohler G, Richter T, Eschke M, Alber G, Muller U. Eosinophils contribute to IL-4 production and shape the T-helper cytokine profile and inflammatory response in pulmonary cryptococcosis. Am J Pathol. 2011;179(2):733-44. doi: 10.1016/j.ajpath.2011.04.025. PubMed PMID: 21699881; PubMed Central PMCID: PMC3157286.

79. Muller U, Stenzel W, Kohler G, Werner C, Polte T, Hansen G, Schutze N, Straubinger RK, Blessing M, McKenzie AN, Brombacher F, Alber G. IL-13 induces disease-promoting type 2 cytokines, alternatively activated macrophages

and allergic inflammation during pulmonary infection of mice with Cryptococcus neoformans. J Immunol. 2007;179(8):5367-77. PubMed PMID: 17911623.

80. Hernandez Y, Arora S, Erb-Downward JR, McDonald RA, Toews GB, Huffnagle GB. Distinct roles for IL-4 and IL-10 in regulating T2 immunity during allergic bronchopulmonary mycosis. J Immunol. 2005;174(2):1027-36. PubMed PMID: 15634927.

81. Boulware DR, Meya DB, Bergemann TL, Wiesner DL, Rhein J, Musubire A, Lee SJ, Kambugu A, Janoff EN, Bohjanen PR. Clinical features and serum biomarkers in HIV immune reconstitution inflammatory syndrome after cryptococcal meningitis: a prospective cohort study. PLoS medicine. 2010;7(12):e1000384. Epub 2011/01/22. doi: 10.1371/journal.pmed.1000384. PubMed PMID: 21253011; PubMed Central PMCID: PMC3014618.

82. Jarvis JN, Casazza JP, Stone HH, Meintjes G, Lawn SD, Levitz SM, Harrison TS, Koup RA. The phenotype of the Cryptococcus-specific CD4+ memory T-cell response is associated with disease severity and outcome in HIV-associated cryptococcal meningitis. The Journal of infectious diseases. 2013;207(12):1817-28. Epub 2013/03/16. doi: 10.1093/infdis/jit099. PubMed PMID: 23493728; PubMed Central PMCID: PMC3654748.

83. Bauman SK, Huffnagle GB, Murphy JW. Effects of tumor necrosis factor alpha on dendritic cell accumulation in lymph nodes draining the immunization site and the impact on the anticryptococcal cell-mediated immune response. Infect Immun. 2003;71(1):68-74. PubMed PMID: 12496150; PubMed Central PMCID: PMC143367.

84. Herring AC, Falkowski NR, Chen GH, McDonald RA, Toews GB, Huffnagle GB. Transient neutralization of tumor necrosis factor alpha can produce a chronic fungal infection in an immunocompetent host: potential role of immature dendritic cells. Infect Immun. 2005;73(1):39-49. PubMed PMID: 15618139.

85. Herring AC, Lee J, McDonald RA, Toews GB, Huffnagle GB. Induction of interleukin-12 and gamma interferon requires tumor necrosis factor alpha for protective T1-cell-mediated immunity to pulmonary Cryptococcus neoformans infection. Infect Immun. 2002;70(6):2959-64. PubMed PMID: 12010985.

86. Marwaha RK, Trehan A, Jayashree K, Vasishta RK. Hypereosinophilia in disseminated cryptococcal disease. The Pediatric infectious disease journal. 1995;14(12):1102-3. PubMed PMID: 8745027.

87. Yamaguchi H, Komase Y, Ikehara M, Yamamoto T, Shinagawa T. Disseminated cryptococcal infection with eosinophilia in a healthy person. Journal of infection and chemotherapy : official journal of the Japan Society of Chemotherapy. 2008;14(4):319-24. doi: 10.1007/s10156-008-0618-z. PubMed PMID: 18709538.

88. Huston SM, Li SS, Stack D, Timm-McCann M, Jones GJ, Islam A, Berenger BM, Xiang RF, Colarusso P, Mody CH. Cryptococcus gattii is killed by dendritic cells, but evades adaptive immunity by failing to induce dendritic cell maturation. J Immunol. 2013;191(1):249-61. doi: 10.4049/jimmunol.1202707. PubMed PMID: 23740956.

89. von Garnier C, Filgueira L, Wikstrom M, Smith M, Thomas JA, Strickland DH, Holt PG, Stumbles PA. Anatomical location determines the distribution and

function of dendritic cells and other APCs in the respiratory tract. J Immunol. 2005;175(3):1609-18. PubMed PMID: 16034100.

90. Lin KL, Suzuki Y, Nakano H, Ramsburg E, Gunn MD. CCR2+ monocyte-derived dendritic cells and exudate macrophages produce influenza-induced pulmonary immune pathology and mortality. J Immunol. 2008;180(4):2562-72. PubMed PMID: 18250467.

91. Collin M, McGovern N, Haniffa M. Human dendritic cell subsets. Immunology. 2013;140(1):22-30. doi: 10.1111/imm.12117. PubMed PMID: 23621371; PubMed Central PMCID: PMC3809702.

92. Osterholzer JJ, Chen GH, Olszewski MA, Zhang YM, Curtis JL, Huffnagle GB, Toews GB. Chemokine receptor 2-mediated accumulation of fungicidal exudate macrophages in mice that clear cryptococcal lung infection. Am J Pathol. 2011;178(1):198-211. Epub 2011/01/13. doi: 10.1016/j.ajpath.2010.11.006. PubMed PMID: 21224057; PubMed Central PMCID: PMC3069860.

93. Shao X, Mednick A, Alvarez M, van Rooijen N, Casadevall A, Goldman DL. An innate immune system cell is a major determinant of species-related susceptibility differences to fungal pneumonia. J Immunol. 2005;175(5):3244-51. PubMed PMID: 16116215.

94. Jambo KC, Banda DH, Kankwatira AM, Sukumar N, Allain TJ, Heyderman RS, Russell DG, Mwandumba HC. Small alveolar macrophages are infected preferentially by HIV and exhibit impaired phagocytic function. Mucosal immunology. 2014;7(5):1116-26. doi: 10.1038/mi.2013.127. PubMed PMID: 24472847; PubMed Central PMCID: PMC4009066.

95. Kawakami K, Qureshi MH, Koguchi Y, Zhang T, Okamura H, Kurimoto M, Saito A. Role of TNF-alpha in the induction of fungicidal activity of mouse

peritoneal exudate cells against Cryptococcus neoformans by IL-12 and IL-18. Cellular immunology. 1999;193(1):9-16. doi: 10.1006/cimm.1999.1460. PubMed PMID: 10202108.

96. Serbina NV, Salazar-Mather TP, Biron CA, Kuziel WA, Pamer EG. TNF/iNOS-producing dendritic cells mediate innate immune defense against bacterial infection. Immunity. 2003;19(1):59-70. Epub 2003/07/23. doi: S1074761303001717 [pii]. PubMed PMID: 12871639.

97. Szymczak WA, Deepe GS, Jr. The CCL7-CCL2-CCR2 axis regulates IL-4 production in lungs and fungal immunity. J Immunol. 2009;183(3):1964-74. doi: 10.4049/jimmunol.0901316. PubMed PMID: 19587014; PubMed Central PMCID: PMC2743878.

98. Traynor TR, Kuziel WA, Toews GB, Huffnagle GB. CCR2 expression determines T1 versus T2 polarization during pulmonary Cryptococcus neoformans infection. J Immunol. 2000;164(4):2021-7. PubMed PMID: 10657654.

99. Traynor TR, Herring AC, Dorf ME, Kuziel WA, Toews GB, Huffnagle GB. Differential roles of CC chemokine ligand 2/monocyte chemotactic protein-1 and CCR2 in the development of T1 immunity. J Immunol. 2002;168(9):4659-66. PubMed PMID: 11971015.

100. Boltjes A, van Wijk F. Human dendritic cell functional specialization in steady-state and inflammation. Frontiers in immunology. 2014;5:131. doi: 10.3389/fimmu.2014.00131. PubMed PMID: 24744755; PubMed Central PMCID: PMC3978316.

101. Henri S, Vremec D, Kamath A, Waithman J, Williams S, Benoist C, Burnham K, Saeland S, Handman E, Shortman K. The dendritic cell populations of mouse lymph nodes. J Immunol. 2001;167(2):741-8. PubMed PMID: 11441078.

102. Shortman K, Liu YJ. Mouse and human dendritic cell subtypes. Nat Rev Immunol. 2002;2(3):151-61. doi: 10.1038/nri746. PubMed PMID: 11913066.

103. Olszewski MA, Zhang Y, Huffnagle GB. Mechanisms of cryptococcal virulence and persistence. Future microbiology. 2010;5(8):1269-88. doi: 10.2217/fmb.10.93. PubMed PMID: 20722603.

104. Dong ZM, Murphy JW. Cryptococcal polysaccharides bind to CD18 on human neutrophils. Infect Immun. 1997;65(2):557-63. PubMed PMID: 9009313; PubMed Central PMCID: PMC176096.

105. Shoham S, Huang C, Chen JM, Golenbock DT, Levitz SM. Toll-like receptor 4 mediates intracellular signaling without TNF-alpha release in response to Cryptococcus neoformans polysaccharide capsule. J Immunol. 2001;166(7):4620-6. PubMed PMID: 11254720.

106. Vecchiarelli A, Pericolini E, Gabrielli E, Kenno S, Perito S, Cenci E, Monari C. Elucidating the immunological function of the Cryptococcus neoformans capsule. Future microbiology. 2013;8(9):1107-16. doi: 10.2217/fmb.13.84. PubMed PMID: 24020739.

107. Yauch LE, Mansour MK, Shoham S, Rottman JB, Levitz SM. Involvement of CD14, toll-like receptors 2 and 4, and MyD88 in the host response to the fungal pathogen Cryptococcus neoformans in vivo. Infect Immun. 2004;72(9):5373-82. doi: 10.1128/IAI.72.9.5373-5382.2004. PubMed PMID: 15322035; PubMed Central PMCID: PMC517466.

108. Nakamura K, Miyagi K, Koguchi Y, Kinjo Y, Uezu K, Kinjo T, Akamine M, Fujita J, Kawamura I, Mitsuyama M, Adachi Y, Ohno N, Takeda K, Akira S, Miyazato A, Kaku M, Kawakami K. Limited contribution of Toll-like receptor 2 and 4 to the host response to a fungal infectious pathogen, Cryptococcus

neoformans. FEMS immunology and medical microbiology. 2006;47(1):148-54. doi: 10.1111/j.1574-695X.2006.00078.x. PubMed PMID: 16706798.

109. Biondo C, Midiri A, Messina L, Tomasello F, Garufi G, Catania MR, Bombaci M, Beninati C, Teti G, Mancuso G. MyD88 and TLR2, but not TLR4, are required for host defense against Cryptococcus neoformans. European journal of immunology. 2005;35(3):870-8. doi: 10.1002/eji.200425799. PubMed PMID: 15714580.

110. Edwards L, Williams AE, Krieg AM, Rae AJ, Snelgrove RJ, Hussell T. Stimulation via Toll-like receptor 9 reduces Cryptococcus neoformans-induced pulmonary inflammation in an IL-12-dependent manner. European journal of immunology. 2005;35(1):273-81. doi: 10.1002/eji.200425640. PubMed PMID: 15597328.

111. Wang JP, Lee CK, Akalin A, Finberg RW, Levitz SM. Contributions of the MyD88-dependent receptors IL-18R, IL-1R, and TLR9 to host defenses following pulmonary challenge with Cryptococcus neoformans. PloS one. 2011;6(10):e26232. doi: 10.1371/journal.pone.0026232. PubMed PMID: 22039448; PubMed Central PMCID: PMC3198470.

112. Tanaka M, Ishii K, Nakamura Y, Miyazato A, Maki A, Abe Y, Miyasaka T, Yamamoto H, Akahori Y, Fue M, Takahashi Y, Kanno E, Maruyama R, Kawakami K. Toll-like receptor 9-dependent activation of bone marrow-derived dendritic cells by URA5 DNA from Cryptococcus neoformans. Infect Immun. 2012;80(2):778-86. doi: 10.1128/IAI.05570-11. PubMed PMID: 22104112; PubMed Central PMCID: PMC3264295.

113. Latz E, Schoenemeyer A, Visintin A, Fitzgerald KA, Monks BG, Knetter CF, Lien E, Nilsen NJ, Espevik T, Golenbock DT. TLR9 signals after translocating

from the ER to CpG DNA in the lysosome. Nat Immunol. 2004;5(2):190-8. doi: 10.1038/ni1028. PubMed PMID: 14716310.

114. Wesche H, Henzel WJ, Shillinglaw W, Li S, Cao Z. MyD88: an adapter that recruits IRAK to the IL-1 receptor complex. Immunity. 1997;7(6):837-47. PubMed PMID: 9430229.

115. Burns K, Martinon F, Esslinger C, Pahl H, Schneider P, Bodmer JL, Di Marco F, French L, Tschopp J. MyD88, an adapter protein involved in interleukin-1 signaling. The Journal of biological chemistry. 1998;273(20):12203-9. PubMed PMID: 9575168.

116. Medzhitov R, Preston-Hurlburt P, Kopp E, Stadlen A, Chen C, Ghosh S, Janeway CA, Jr. MyD88 is an adaptor protein in the hToll/IL-1 receptor family signaling pathways. Molecular cell. 1998;2(2):253-8. PubMed PMID: 9734363.

117. Bürgel PHM, Saavedra P. H., Magalhaes K. G., Cordero R. J., Zamboni D. S., Tavares A. H., Albuquerque P., Casadevall A., Bocca A. L. Differences between acapsular and encapsulated strain of Cryptococcus neoformans in NLRP3 inflammasome dependent activation. Mycoses. 2014;57:33-108. doi: 10.1111/myc.12196.

118. Nakamura K, Kinjo T, Saijo S, Miyazato A, Adachi Y, Ohno N, Fujita J, Kaku M, Iwakura Y, Kawakami K. Dectin-1 is not required for the host defense to Cryptococcus neoformans. Microbiology and immunology. 2007;51(11):1115-9. PubMed PMID: 18037789.

119. Nakamura Y, Sato K, Yamamoto H, Matsumura K, Matsumoto I, Nomura T, Miyasaka T, Ishii K, Kanno E, Tachi M, Yamasaki S, Saijo S, Iwakura Y, Kawakami K. Dectin-2 deficiency promotes Th2 response and mucin production

in the lungs after pulmonary infection with Cryptococcus neoformans. Infect Immun. 2014. doi: 10.1128/IAI.02835-14. PubMed PMID: 25422263.

120. Means TK, Mylonakis E, Tampakakis E, Colvin RA, Seung E, Puckett L, Tai MF, Stewart CR, Pukkila-Worley R, Hickman SE, Moore KJ, Calderwood SB, Hacohen N, Luster AD, El Khoury J. Evolutionarily conserved recognition and innate immunity to fungal pathogens by the scavenger receptors SCARF1 and CD36. J Exp Med. 2009;206(3):637-53. doi: 10.1084/jem.20082109. PubMed PMID: 19237602; PubMed Central PMCID: PMC2699123.

121. Qiu Y, Dayrit JK, Davis MJ, Carolan JF, Osterholzer JJ, Curtis JL, Olszewski MA. Scavenger receptor A modulates the immune response to pulmonary Cryptococcus neoformans infection. J Immunol. 2013;191(1):238-48. Epub 2013/06/05. doi: 10.4049/jimmunol.1203435. PubMed PMID: 23733871.

122. Dan JM, Kelly RM, Lee CK, Levitz SM. Role of the mannose receptor in a murine model of Cryptococcus neoformans infection. Infect Immun. 2008;76(6):2362-7. doi: 10.1128/IAI.00095-08. PubMed PMID: 18391001; PubMed Central PMCID: PMC2423054.

123. Gordon S. Alternative activation of macrophages. Nat Rev Immunol. 2003;3(1):23-35. doi: 10.1038/nri978. PubMed PMID: 12511873.

124. Cross CE, Bancroft GJ. Ingestion of acapsular Cryptococcus neoformans occurs via mannose and beta-glucan receptors, resulting in cytokine production and increased phagocytosis of the encapsulated form. Infect Immun. 1995;63(7):2604-11. PubMed PMID: 7790075; PubMed Central PMCID: PMC173349.

125. Chieppa M, Bianchi G, Doni A, Del Prete A, Sironi M, Laskarin G, Monti P, Piemonti L, Biondi A, Mantovani A, Introna M, Allavena P. Cross-linking of

the mannose receptor on monocyte-derived dendritic cells activates an anti-inflammatory immunosuppressive program. J Immunol. 2003;171(9):4552-60. PubMed PMID: 14568928.

126. Nigou J, Zelle-Rieser C, Gilleron M, Thurnher M, Puzo G. Mannosylated lipoarabinomannans inhibit IL-12 production by human dendritic cells: evidence for a negative signal delivered through the mannose receptor. J Immunol. 2001;166(12):7477-85. PubMed PMID: 11390501.

127. Feldmesser M, Tucker S, Casadevall A. Intracellular parasitism of macrophages by Cryptococcus neoformans. Trends in microbiology. 2001;9(6):273-8. PubMed PMID: 11390242.

128. Noverr MC, Williamson PR, Fajardo RS, Huffnagle GB. CNLAC1 is required for extrapulmonary dissemination of Cryptococcus neoformans but not pulmonary persistence. Infect Immun. 2004;72(3):1693-9. PubMed PMID: 14977977; PubMed Central PMCID: PMC356011.

129. Salas SD, Bennett JE, Kwon-Chung KJ, Perfect JR, Williamson PR. Effect of the laccase gene CNLAC1, on virulence of Cryptococcus neoformans. J Exp Med. 1996;184(2):377-86. PubMed PMID: 8760791; PubMed Central PMCID: PMC2192698.

130. Qiu Y, Davis MJ, Dayrit JK, Hadd Z, Meister DL, Osterholzer JJ, Williamson PR, Olszewski MA. Immune modulation mediated by cryptococcal laccase promotes pulmonary growth and brain dissemination of virulent Cryptococcus neoformans in mice. PloS one. 2012;7(10):e47853. doi: 10.1371/journal.pone.0047853. PubMed PMID: 23110112; PubMed Central PMCID: PMC3478276.

131. Panepinto J, Liu L, Ramos J, Zhu X, Valyi-Nagy T, Eksi S, Fu J, Jaffe HA, Wickes B, Williamson PR. The DEAD-box RNA helicase Vad1 regulates multiple virulence-associated genes in Cryptococcus neoformans. J Clin Invest. 2005;115(3):632-41. doi: 10.1172/JCI23048. PubMed PMID: 15765146; PubMed Central PMCID: PMC1051994.

132. Qiu J, Olszewski MA, Williamson PR. Cryptococcus neoformans growth and protection from innate immunity are dependent on expression of a virulence-associated DEAD-box protein, Vad1. Infect Immun. 2013;81(3):777-88. doi: 10.1128/IAI.00821-12. PubMed PMID: 23264050; PubMed Central PMCID: PMC3584887.

133. Eastman AJ, He X, Qiu Y, Davis MJ, Vedula P, Lyons DM, Park YD, Hardison SE, Malachowski AN, Osterholzer JJ, Wormley FL, Jr., Williamson PR, Olszewski MA. Cryptococcal Heat Shock Protein 70 Homolog Ssa1 Contributes to Pulmonary Expansion of Cryptococcus neoformans during the Afferent Phase of the Immune Response by Promoting Macrophage M2 Polarization. J Immunol. 2015;194(12):5999-6010. doi: 10.4049/jimmunol.1402719. PubMed PMID: 25972480; PubMed Central PMCID: PMC4458402.

134. He X, Lyons DM, Toffaletti DL, Wang F, Qiu Y, Davis MJ, Meister DL, Dayrit JK, Lee A, Osterholzer JJ, Perfect JR, Olszewski MA. Virulence factors identified by Cryptococcus neoformans mutant screen differentially modulate lung immune responses and brain dissemination. Am J Pathol. 2012;181(4):1356-66. Epub 2012/08/01. doi: 10.1016/j.ajpath.2012.06.012. PubMed PMID: 22846723; PubMed Central PMCID: PMC3463625.

135. Bulmer GS, Sans MD. Cryptococcus neoformans. II. Phagocytosis by human leukocytes. Journal of bacteriology. 1967;94(5):1480-3. PubMed PMID: 4862192; PubMed Central PMCID: PMC276851.

136. Bulmer GS, Sans MD, Gunn CM. Cryptococcus neoformans. I. Nonencapsulated mutants. Journal of bacteriology. 1967;94(5):1475-9. PubMed PMID: 6057803; PubMed Central PMCID: PMC276850.

137. Feldmesser M, Casadevall A. Mechanism of action of antibody to capsular polysaccharide in Cryptococcus neoformans infection. Frontiers in bioscience : a journal and virtual library. 1998;3:d136-51. PubMed PMID: 9445465.

138. Vecchiarelli A. The cellular responses induced by the capsular polysaccharide of Cryptococcus neoformans differ depending on the presence or absence of specific protective antibodies. Current molecular medicine. 2005;5(4):413-20. PubMed PMID: 15977997.

139. Bulmer GS, Sans MD. Cryptococcus neoformans. 3. Inhibition of phagocytosis. Journal of bacteriology. 1968;95(1):5-8. PubMed PMID: 4866104; PubMed Central PMCID: PMC251963.

140. Bhattacharjee AK, Kwon-Chung KJ, Glaudemans CP. On the structure of the capsular polysaccharide from Cryptococcus neoformans serotype C. Immunochemistry. 1978;15(9):673-9. PubMed PMID: 367954.

141. Bhattacharjee AK, Kwon-Chung KJ, Glaudemans CP. On the structure of the capsular polysaccharide from Cryptococcus neoformans serotype C--II. Molecular immunology. 1979;16(7):531-2. PubMed PMID: 387576.

142. Bhattacharjee AK, Kwon-Chung KJ, Glaudemans CP. The structure of the capsular polysaccharide from Cryptococcus neoformans serotype D. Carbohydrate research. 1979;73:183-92. PubMed PMID: 113098.

143. Bhattacharjee AK, Kwon-Chung KJ, Glaudemans CP. Structural studies on the major, capsular polysaccharide from Cryptococcus bacillisporus serotype B. Carbohydrate research. 1980;82(1):103-11. PubMed PMID: 6772300.

144. Bhattacharjee AK, Kwon-Chung KJ, Glaudemans CP. Capsular polysaccharides from a parent strain and from a possible, mutant strain of Cryptococcus neoformans serotype A. Carbohydrate research. 1981;95(2):237-48. PubMed PMID: 7028261.

145. Todaro-Luck F, Reiss E, Cherniak R, Kaufman L. Characterization of Cryptococcus neoformans capsular glucuronoxylomannan polysaccharide with monoclonal antibodies. Infect Immun. 1989;57(12):3882-7. PubMed PMID: 2680986; PubMed Central PMCID: PMC259921.

146. Cherniak R, Reiss E, Slodki ME, Plattner RD, Blumer SO. Structure and antigenic activity of the capsular polysaccharide of Cryptococcus neoformans serotype A. Molecular immunology. 1980;17(8):1025-32. PubMed PMID: 6777664.

147. Merrifield EH, Stephen AM. Structural investigations of two capsular polysaccharides from cryptococcus neoformans. Carbohydrate research. 1980;86(1):69-76. doi: http://dx.doi.org/10.1016/S0008-6215(00)84582-6.

148. Lupo P, Chang YC, Kelsall BL, Farber JM, Pietrella D, Vecchiarelli A, Leon F, Kwon-Chung KJ. The presence of capsule in Cryptococcus neoformans influences the gene expression profile in dendritic cells during interaction with the fungus. Infect Immun. 2008;76(4):1581-9. doi: 10.1128/IAI.01184-07. PubMed PMID: 18250173; PubMed Central PMCID: PMC2292858.

149. Vecchiarelli A, Monari C, Retini C, Pietrella D, Palazzetti B, Pitzurra L, Casadevall A. Cryptococcus neoformans differently regulates B7-1 (CD80) and B7-2 (CD86) expression on human monocytes. European journal of immunology.

1998;28(1):114-21. doi: 10.1002/(SICI)1521-4141(199801)28:01<114::AID-IMMU114>3.0.CO;2-B. PubMed PMID: 9485191.

150. Vecchiarelli A, Retini C, Monari C, Tascini C, Bistoni F, Kozel TR. Purified capsular polysaccharide of Cryptococcus neoformans induces interleukin-10 secretion by human monocytes. Infect Immun. 1996;64(7):2846-9. PubMed PMID: 8698522; PubMed Central PMCID: PMC174153.

151. Vecchiarelli A, Pietrella D, Lupo P, Bistoni F, McFadden DC, Casadevall A. The polysaccharide capsule of Cryptococcus neoformans interferes with human dendritic cell maturation and activation. Journal of leukocyte biology. 2003;74(3):370-8. PubMed PMID: 12949240.

152. Vecchiarelli A, Retini C, Pietrella D, Monari C, Tascini C, Beccari T, Kozel TR. Downregulation by cryptococcal polysaccharide of tumor necrosis factor alpha and interleukin-1 beta secretion from human monocytes. Infect Immun. 1995;63(8):2919-23. PubMed PMID: 7622213; PubMed Central PMCID: PMC173397.

153. Levitz SM, Nong S, Mansour MK, Huang C, Specht CA. Molecular characterization of a mannoprotein with homology to chitin deacetylases that stimulates T cell responses to Cryptococcus neoformans. Proceedings of the National Academy of Sciences of the United States of America. 2001;98(18):10422-7. doi: 10.1073/pnas.181331398. PubMed PMID: 11504924; PubMed Central PMCID: PMC56976.

154. Mansour MK, Schlesinger LS, Levitz SM. Optimal T cell responses to Cryptococcus neoformans mannoprotein are dependent on recognition of conjugated carbohydrates by mannose receptors. J Immunol. 2002;168(6):2872-9. PubMed PMID: 11884457.

155. Orendi JM, Verheul AF, De Vos NM, Visser MR, Snippe H, Cherniak R, Vaishnav VV, Rijkers GT, Verhoef J. Mannoproteins of Cryptococcus neoformans induce proliferative response in human peripheral blood mononuclear cells (PBMC) and enhance HIV-1 replication. Clin Exp Immunol. 1997;107(2):293-9. PubMed PMID: 9030866.

156. Pitzurra L, Cherniak R, Giammarioli M, Perito S, Bistoni F, Vecchiarelli A. Early induction of interleukin-12 by human monocytes exposed to Cryptococcus neoformans mannoproteins. Infect Immun. 2000;68(2):558-63. PubMed PMID: 10639417; PubMed Central PMCID: PMC97176.

157. Pietrella D, Corbucci C, Perito S, Bistoni G, Vecchiarelli A. Mannoproteins from Cryptococcus neoformans promote dendritic cell maturation and activation. Infect Immun. 2005;73(2):820-7. doi: 10.1128/IAI.73.2.820-827.2005. PubMed PMID: 15664921; PubMed Central PMCID: PMC547028.

158. Mansour MK, Latz E, Levitz SM. Cryptococcus neoformans glycoantigens are captured by multiple lectin receptors and presented by dendritic cells. J Immunol. 2006;176(5):3053-61. PubMed PMID: 16493064.

159. Levitz SM, Specht CA. The molecular basis for the immunogenicity of Cryptococcus neoformans mannoproteins. FEMS yeast research. 2006;6(4):513-24. doi: 10.1111/j.1567-1364.2006.00071.x. PubMed PMID: 16696647.

160. Dan JM, Wang JP, Lee CK, Levitz SM. Cooperative stimulation of dendritic cells by Cryptococcus neoformans mannoproteins and CpG oligodeoxynucleotides. PloS one. 2008;3(4):e2046. doi: 10.1371/journal.pone.0002046. PubMed PMID: 18446192; PubMed Central PMCID: PMC2297515.

161. Olszewski MA, Noverr MC, Chen GH, Toews GB, Cox GM, Perfect JR, Huffnagle GB. Urease expression by Cryptococcus neoformans promotes microvascular sequestration, thereby enhancing central nervous system invasion. Am J Pathol. 2004;164(5):1761-71. doi: 10.1016/S0002-9440(10)63734-0. PubMed PMID: 15111322; PubMed Central PMCID: PMC1615675.

162. Eisenman HC, Mues M, Weber SE, Frases S, Chaskes S, Gerfen G, Casadevall A. Cryptococcus neoformans laccase catalyses melanin synthesis from both D- and L-DOPA. Microbiology. 2007;153(Pt 12):3954-62. doi: 10.1099/mic.0.2007/011049-0. PubMed PMID: 18048910.

163. Williamson PR. Biochemical and molecular characterization of the diphenol oxidase of Cryptococcus neoformans: identification as a laccase. J Bacteriol. 1994;176(3):656-64. PubMed PMID: 8300520; PubMed Central PMCID: PMC205102.

164. Zhu X, Gibbons J, Garcia-Rivera J, Casadevall A, Williamson PR. Laccase of Cryptococcus neoformans is a cell wall-associated virulence factor. Infect Immun. 2001;69(9):5589-96. PubMed PMID: 11500433; PubMed Central PMCID: PMC98673.

165. Zhang S, Hacham M, Panepinto J, Hu G, Shin S, Zhu X, Williamson PR. The Hsp70 member, Ssa1, acts as a DNA-binding transcriptional co-activator of laccase in Cryptococcus neoformans. Molecular microbiology. 2006;62(4):1090-101. Epub 2006/10/17. doi: 10.1111/j.1365-2958.2006.05422.x. PubMed PMID: 17040492.

166. Kapsenberg ML. Dendritic-cell control of pathogen-driven T-cell polarization. Nat Rev Immunol. 2003;3(12):984-93. PubMed PMID: 14647480.

167. Cook PC, Jones LH, Jenkins SJ, Wynn TA, Allen JE, MacDonald AS. Alternatively activated dendritic cells regulate CD4+ T-cell polarization in vitro and in vivo. Proceedings of the National Academy of Sciences of the United States of America. 2012;109(25):9977-82. doi: 10.1073/pnas.1121231109. PubMed PMID: 22660926; PubMed Central PMCID: PMC3382483.

168. Athie-Morales V, Smits HH, Cantrell DA, Hilkens CM. Sustained IL-12 signaling is required for Th1 development. J Immunol. 2004;172(1):61-9. PubMed PMID: 14688310.

169. Wormley FL, Jr., Perfect JR, Steele C, Cox GM. Protection against cryptococcosis by using a murine gamma interferon-producing Cryptococcus neoformans strain. Infect Immun. 2007;75(3):1453-62. doi: 10.1128/IAI.00274-06. PubMed PMID: 17210668; PubMed Central PMCID: PMC1828544.

170. Arora S, Olszewski MA, Tsang TM, McDonald RA, Toews GB, Huffnagle GB. Effect of cytokine interplay on macrophage polarization during chronic pulmonary infection with Cryptococcus neoformans. Infect Immun. 2011;79(5):1915-26. Epub 2011/03/09. doi: 10.1128/IAI.01270-10. PubMed PMID: 21383052; PubMed Central PMCID: PMC3088136.

171. Grahnert A, Richter T, Piehler D, Eschke M, Schulze B, Muller U, Protschka M, Kohler G, Sabat R, Brombacher F, Alber G. IL-4 receptor-alpha-dependent control of Cryptococcus neoformans in the early phase of pulmonary infection. PloS one. 2014;9(1):e87341. doi: 10.1371/journal.pone.0087341. PubMed PMID: 24475277; PubMed Central PMCID: PMC3903725.

172. Hamilton TA, Zhao C, Pavicic PG, Jr., Datta S. Myeloid colony-stimulating factors as regulators of macrophage polarization. Frontiers in immunology.

2014;5:554. doi: 10.3389/fimmu.2014.00554. PubMed PMID: 25484881; PubMed Central PMCID: PMC4240161.

173. Chen GH, Curtis JL, Mody CH, Christensen PJ, Armstrong LR, Toews GB. Effect of granulocyte-macrophage colony-stimulating factor on rat alveolar macrophage anticryptococcal activity in vitro. J Immunol. 1994;152(2):724-34. PubMed PMID: 8283047.

174. Milam JE, Herring-Palmer AC, Pandrangi R, McDonald RA, Huffnagle GB, Toews GB. Modulation of the pulmonary type 2 T-cell response to Cryptococcus neoformans by intratracheal delivery of a tumor necrosis factor alpha-expressing adenoviral vector. Infect Immun. 2007;75(10):4951-8. PubMed PMID: 17646355.

175. Huffnagle GB, Chen GH, Curtis JL, McDonald RA, Strieter RM, Toews GB. Down-regulation of the afferent phase of T cell-mediated pulmonary inflammation and immunity by a high melanin-producing strain of Cryptococcus neoformans. J Immunol. 1995;155(7):3507-16. PubMed PMID: 7561046.

176. Olszewski MA, Huffnagle GB, Traynor TR, McDonald RA, Cook DN, Toews GB. Regulatory effects of macrophage inflammatory protein 1alpha/CCL3 on the development of immunity to Cryptococcus neoformans depend on expression of early inflammatory cytokines. Infect Immun. 2001;69(10):6256-63. Epub 2001/09/13. doi: 10.1128/IAI.69.10.6256-6263.2001. PubMed PMID: 11553568; PubMed Central PMCID: PMC98759.

177. Angkasekwinai P, Sringkarin N, Supasorn O, Fungkrajai M, Wang YH, Chayakulkeeree M, Ngamskulrungroj P, Angkasekwinai N, Pattanapanyasat K. Cryptococcus gattii infection dampens Th1 and Th17 responses by attenuating dendritic cell function and pulmonary chemokine expression in the

immunocompetent hosts. Infect Immun. 2014;82(9):3880-90. doi: 10.1128/IAI.01773-14. PubMed PMID: 24980974; PubMed Central PMCID: PMC4187835.

178. Takeuch O, Akira S. Epigenetic control of macrophage polarization. European journal of immunology. 2011;41(9):2490-3. doi: 10.1002/eji.201141792. PubMed PMID: 21952803.

179. Conaway JW. Introduction to theme "Chromatin, epigenetics, and transcription". Annual review of biochemistry. 2012;81:61-4. doi: 10.1146/annurev-biochem-090711-093103. PubMed PMID: 22404631.

180. Cedar H, Bergman Y. Programming of DNA methylation patterns. Annual review of biochemistry. 2012;81:97-117. doi: 10.1146/annurev-biochem-052610-091920. PubMed PMID: 22404632.

181. Kohli RM, Zhang Y. TET enzymes, TDG and the dynamics of DNA demethylation. Nature. 2013;502(7472):472-9. doi: 10.1038/nature12750. PubMed PMID: 24153300; PubMed Central PMCID: PMC4046508.

182. Sabio G, Davis RJ. TNF and MAP kinase signalling pathways. Seminars in immunology. 2014;26(3):237-45. doi: 10.1016/j.smim.2014.02.009. PubMed PMID: 24647229; PubMed Central PMCID: PMC4099309.

183. Palacios D, Mozzetta C, Consalvi S, Caretti G, Saccone V, Proserpio V, Marquez VE, Valente S, Mai A, Forcales SV, Sartorelli V, Puri PL. TNF/p38alpha/polycomb signaling to Pax7 locus in satellite cells links inflammation to the epigenetic control of muscle regeneration. Cell stem cell. 2010;7(4):455-69. doi: 10.1016/j.stem.2010.08.013. PubMed PMID: 20887952; PubMed Central PMCID: PMC2951277.

184. Neves BM, Cruz MT, Francisco V, Garcia-Rodriguez C, Silvestre R, Cordeiro-da-Silva A, Dinis AM, Batista MT, Duarte CB, Lopes MC. Differential roles of PI3-Kinase, MAPKs and NF-kappaB on the manipulation of dendritic cell T(h)1/T(h)2 cytokine/chemokine polarizing profile. Molecular immunology. 2009;46(13):2481-92. doi: 10.1016/j.molimm.2009.05.021. PubMed PMID: 19520433.

185. Nie M, Knox AJ, Pang L. beta2-Adrenoceptor agonists, like glucocorticoids, repress eotaxin gene transcription by selective inhibition of histone H4 acetylation. J Immunol. 2005;175(1):478-86. PubMed PMID: 15972682.

186. Diermeier S, Kolovos P, Heizinger L, Schwartz U, Georgomanolis T, Zirkel A, Wedemann G, Grosveld F, Knoch TA, Merkl R, Cook PR, Langst G, Papantonis A. TNFalpha signalling primes chromatin for NF-kappaB binding and induces rapid and widespread nucleosome repositioning. Genome biology. 2014;15(12):536. doi: 10.1186/s13059-014-0536-6. PubMed PMID: 25608606; PubMed Central PMCID: PMC4268828.

187. Chang YC, Chen TC, Lee CT, Yang CY, Wang HW, Wang CC, Hsieh SL. Epigenetic control of MHC class II expression in tumor-associated macrophages by decoy receptor 3. Blood. 2008;111(10):5054-63. doi: 10.1182/blood-2007-12-130609. PubMed PMID: 18349319.

188. Wen H, Dou Y, Hogaboam CM, Kunkel SL. Epigenetic regulation of dendritic cell-derived interleukin-12 facilitates immunosuppression after a severe innate immune response. Blood. 2008;111(4):1797-804. doi: 10.1182/blood-2007-08-106443. PubMed PMID: 18055863; PubMed Central PMCID: PMC2234040.

189. Kuo HP, Wang Z, Lee DF, Iwasaki M, Duque-Afonso J, Wong SH, Lin CH, Figueroa ME, Su J, Lemischka IR, Cleary ML. Epigenetic roles of MLL

oncoproteins are dependent on NF-kappaB. Cancer cell. 2013;24(4):423-37. doi: 10.1016/j.ccr.2013.08.019. PubMed PMID: 24054986; PubMed Central PMCID: PMC3816582.

190. Foster SL, Hargreaves DC, Medzhitov R. Gene-specific control of inflammation by TLR-induced chromatin modifications. Nature. 2007;447(7147):972-8. doi: 10.1038/nature05836. PubMed PMID: 17538624.

191. Xie L, Liu C, Wang L, Gunawardena HP, Yu Y, Du R, Taxman DJ, Dai P, Yan Z, Yu J, Holly SP, Parise LV, Wan YY, Ting JP, Chen X. Protein phosphatase 2A catalytic subunit alpha plays a MyD88-dependent, central role in the gene-specific regulation of endotoxin tolerance. Cell reports. 2013;3(3):678-88. doi: 10.1016/j.celrep.2013.01.029. PubMed PMID: 23434512; PubMed Central PMCID: PMC4060247.

192. Lyn-Kew K, Rich E, Zeng X, Wen H, Kunkel SL, Newstead MW, Bhan U, Standiford TJ. IRAK-M regulates chromatin remodeling in lung macrophages during experimental sepsis. PloS one. 2010;5(6):e11145. doi: 10.1371/journal.pone.0011145. PubMed PMID: 20585389; PubMed Central PMCID: PMC2886833.

193. Weinmann AS, Plevy SE, Smale ST. Rapid and selective remodeling of a positioned nucleosome during the induction of IL-12 p40 transcription. Immunity. 1999;11(6):665-75. PubMed PMID: 10626889.

194. Weinmann AS, Mitchell DM, Sanjabi S, Bradley MN, Hoffmann A, Liou HC, Smale ST. Nucleosome remodeling at the IL-12 p40 promoter is a TLR-dependent, Rel-independent event. Nat Immunol. 2001;2(1):51-7. doi: 10.1038/83168. PubMed PMID: 11135578.

195. Pompei L, Jang S, Zamlynny B, Ravikumar S, McBride A, Hickman SP, Salgame P. Disparity in IL-12 release in dendritic cells and macrophages in response to Mycobacterium tuberculosis is due to use of distinct TLRs. J Immunol. 2007;178(8):5192-9. PubMed PMID: 17404302.

196. Cox GM, Mukherjee J, Cole GT, Casadevall A, Perfect JR. Urease as a virulence factor in experimental cryptococcosis. Infection and immunity. 2000;68(2):443-8. PubMed PMID: 10639402; PubMed Central PMCID: PMC97161.

197. Motta A, Schmitz C, Rodrigues L, Ribeiro F, Teixeira C, Detanico T, Bonan C, Zwickey H, Bonorino C. Mycobacterium tuberculosis heat-shock protein 70 impairs maturation of dendritic cells from bone marrow precursors, induces interleukin-10 production and inhibits T-cell proliferation in vitro. Immunology. 2007;121(4):462-72. doi: 10.1111/j.1365-2567.2007.02564.x. PubMed PMID: 17346283; PubMed Central PMCID: PMC2265970.

198. Lopez-Ribot JL, Alloush HM, Masten BJ, Chaffin WL. Evidence for presence in the cell wall of Candida albicans of a protein related to the hsp70 family. Infection and immunity. 1996;64(8):3333-40. PubMed PMID: 8757872; PubMed Central PMCID: PMC174226.

199. Sun JN, Solis NV, Phan QT, Bajwa JS, Kashleva H, Thompson A, Liu Y, Dongari-Bagtzoglou A, Edgerton M, Filler SG. Host cell invasion and virulence mediated by Candida albicans Ssa1. PLoS pathogens. 2010;6(11):e1001181. doi: 10.1371/journal.ppat.1001181. PubMed PMID: 21085601; PubMed Central PMCID: PMC2978716.

200. Rodrigues ML, Nimrichter L, Oliveira DL, Nosanchuk JD, Casadevall A. Vesicular Trans-Cell Wall Transport in Fungi: A Mechanism for the Delivery of

Virulence-Associated Macromolecules? Lipid insights. 2008;2:27-40. PubMed PMID: 20617119; PubMed Central PMCID: PMC2898286.

201. Kakeya H, Udono H, Ikuno N, Yamamoto Y, Mitsutake K, Miyazaki T, Tomono K, Koga H, Tashiro T, Nakayama E, Kohno S. A 77-kilodalton protein of Cryptococcus neoformans, a member of the heat shock protein 70 family, is a major antigen detected in the sera of mice with pulmonary cryptococcosis. Infection and immunity. 1997;65(5):1653-8. PubMed PMID: 9125543; PubMed Central PMCID: PMC175192.

202. Kakeya H, Udono H, Maesaki S, Sasaki E, Kawamura S, Hossain MA, Yamamoto Y, Sawai T, Fukuda M, Mitsutake K, Miyazaki Y, Tomono K, Tashiro T, Nakayama E, Kohno S. Heat shock protein 70 (hsp70) as a major target of the antibody response in patients with pulmonary cryptococcosis. Clinical and experimental immunology. 1999;115(3):485-90. PubMed PMID: 10193422; PubMed Central PMCID: PMC1905239.

203. Chaturvedi AK, Weintraub ST, Lopez-Ribot JL, Wormley FL, Jr. Identification and characterization of Cryptococcus neoformans protein fractions that induce protective immune responses. Proteomics. 2013;13(23-24):3429-41. doi: 10.1002/pmic.201300213. PubMed PMID: 24170628; PubMed Central PMCID: PMC3916089.

204. Young M, Macias S, Thomas D, Wormley FL, Jr. A proteomic-based approach for the identification of immunodominant Cryptococcus neoformans proteins. Proteomics. 2009;9(9):2578-88. doi: 10.1002/pmic.200800713. PubMed PMID: 19343717; PubMed Central PMCID: PMC2754056.

205. Toffaletti DL, Del Poeta M, Rude TH, Dietrich F, Perfect JR. Regulation of cytochrome c oxidase subunit 1 (COX1) expression in Cryptococcus neoformans

by temperature and host environment. Microbiology. 2003;149(Pt 4):1041-9. PubMed PMID: 12686646.

206. Ngamskulrungroj P, Chang Y, Roh J, Kwon-Chung KJ. Differences in nitrogen metabolism between Cryptococcus neoformans and C. gattii, the two etiologic agents of cryptococcosis. PloS one. 2012;7(3):e34258. doi: 10.1371/journal.pone.0034258. PubMed PMID: 22479580; PubMed Central PMCID: PMC3313984.

207. Cox GM, McDade HC, Chen SC, Tucker SC, Gottfredsson M, Wright LC, Sorrell TC, Leidich SD, Casadevall A, Ghannoum MA, Perfect JR. Extracellular phospholipase activity is a virulence factor for Cryptococcus neoformans. Molecular microbiology. 2001;39(1):166-75. PubMed PMID: 11123698.

208. Schoffelen T, Illnait-Zaragozi MT, Joosten LA, Netea MG, Boekhout T, Meis JF, Sprong T. Cryptococcus gattii induces a cytokine pattern that is distinct from other cryptococcal species. PloS one. 2013;8(1):e55579. doi: 10.1371/journal.pone.0055579. PubMed PMID: 23383232; PubMed Central PMCID: PMC3561320.

209. Retzlaff C, Yamamoto Y, Hoffman PS, Friedman H, Klein TW. Bacterial heat shock proteins directly induce cytokine mRNA and interleukin-1 secretion in macrophage cultures. Infection and immunity. 1994;62(12):5689-93. PubMed PMID: 7960155; PubMed Central PMCID: PMC303322.

210. Weiss LM, Ma YF, Takvorian PM, Tanowitz HB, Wittner M. Bradyzoite development in Toxoplasma gondii and the hsp70 stress response. Infection and immunity. 1998;66(7):3295-302. PubMed PMID: 9632598; PubMed Central PMCID: PMC108345.

211. Mun HS, Aosai F, Norose K, Chen M, Hata H, Tagawa YI, Iwakura Y, Byun DS, Yano A. Toxoplasma gondii Hsp70 as a danger signal in toxoplasma gondii-infected mice. Cell stress & chaperones. 2000;5(4):328-35. PubMed PMID: 11048655; PubMed Central PMCID: PMC312862.

212. Eastman AJ, Osterholzer JJ, Olszewski MA. Role of dendritic cell-pathogen interactions in the immune response to pulmonary cryptococcal infection. Future microbiology. 2015;10(11):1837-57. doi: 10.2217/fmb.15.92. PubMed PMID: 26597428.

213. Van Ginderachter JA, Movahedi K, Hassanzadeh Ghassabeh G, Meerschaut S, Beschin A, Raes G, De Baetselier P. Classical and alternative activation of mononuclear phagocytes: picking the best of both worlds for tumor promotion. Immunobiology. 2006;211(6-8):487-501. doi: 10.1016/j.imbio.2006.06.002. PubMed PMID: 16920488.

214. Fotin-Mleczek M, Henkler F, Samel D, Reichwein M, Hausser A, Parmryd I, Scheurich P, Schmid JA, Wajant H. Apoptotic crosstalk of TNF receptors: TNF-R2-induces depletion of TRAF2 and IAP proteins and accelerates TNF-R1-dependent activation of caspase-8. Journal of cell science. 2002;115(Pt 13):2757-70. PubMed PMID: 12077366.

215. Hijdra D, Vorselaars AD, Grutters JC, Claessen AM, Rijkers GT. Differential expression of TNFR1 (CD120a) and TNFR2 (CD120b) on subpopulations of human monocytes. Journal of inflammation. 2012;9(1):38. doi: 10.1186/1476-9255-9-38. PubMed PMID: 23039818; PubMed Central PMCID: PMC3542013.

216. Sundquist M, Wick MJ. TNF-alpha-dependent and -independent maturation of dendritic cells and recruited CD11c(int)CD11b+ Cells during oral Salmonella infection. J Immunol. 2005;175(5):3287-98. PubMed PMID: 16116221.

217. Maney NJ, Reynolds G, Krippner-Heidenreich A, Hilkens CM. Dendritic cell maturation and survival are differentially regulated by TNFR1 and TNFR2. J Immunol. 2014;193(10):4914-23. doi: 10.4049/jimmunol.1302929. PubMed PMID: 25288570.

218. Quintin J, Saeed S, Martens JH, Giamarellos-Bourboulis EJ, Ifrim DC, Logie C, Jacobs L, Jansen T, Kullberg BJ, Wijmenga C, Joosten LA, Xavier RJ, van der Meer JW, Stunnenberg HG, Netea MG. Candida albicans infection affords protection against reinfection via functional reprogramming of monocytes. Cell host & microbe. 2012;12(2):223-32. doi: 10.1016/j.chom.2012.06.006. PubMed PMID: 22901542.

219. Netea MG, Quintin J, van der Meer JW. Trained immunity: a memory for innate host defense. Cell host & microbe. 2011;9(5):355-61. doi: 10.1016/j.chom.2011.04.006. PubMed PMID: 21575907.

220. Carson WF, Cavassani KA, Dou Y, Kunkel SL. Epigenetic regulation of immune cell functions during post-septic immunosuppression. Epigenetics : official journal of the DNA Methylation Society. 2011;6(3):273-83. PubMed PMID: 21048427; PubMed Central PMCID: PMC3092675.

221. Ishii M, Wen H, Corsa CA, Liu T, Coelho AL, Allen RM, Carson WFt, Cavassani KA, Li X, Lukacs NW, Hogaboam CM, Dou Y, Kunkel SL. Epigenetic regulation of the alternatively activated macrophage phenotype. Blood. 2009;114(15):3244-54. Epub 2009/07/02. doi: 10.1182/blood-2009-04-217620. PubMed PMID: 19567879; PubMed Central PMCID: PMC2759649.

222. Cheng SC, Quintin J, Cramer RA, Shepardson KM, Saeed S, Kumar V, Giamarellos-Bourboulis EJ, Martens JH, Rao NA, Aghajanirefah A, Manjeri GR, Li Y, Ifrim DC, Arts RJ, van der Meer BM, Deen PM, Logie C, O'Neill LA, Willems P, van de Veerdonk FL, van der Meer JW, Ng A, Joosten LA, Wijmenga C, Stunnenberg HG, Xavier RJ, Netea MG. mTOR- and HIF-1alpha-mediated aerobic glycolysis as metabolic basis for trained immunity. Science. 2014;345(6204):1250684. doi: 10.1126/science.1250684. PubMed PMID: 25258083.

223. Kleinnijenhuis J, Quintin J, Preijers F, Joosten LA, Ifrim DC, Saeed S, Jacobs C, van Loenhout J, de Jong D, Stunnenberg HG, Xavier RJ, van der Meer JW, van Crevel R, Netea MG. Bacille Calmette-Guerin induces NOD2-dependent nonspecific protection from reinfection via epigenetic reprogramming of monocytes. Proceedings of the National Academy of Sciences of the United States of America. 2012;109(43):17537-42. doi: 10.1073/pnas.1202870109. PubMed PMID: 22988082; PubMed Central PMCID: PMC3491454.

224. Dong ZM, Murphy JW. Cryptococcal polysaccharides induce L-selectin shedding and tumor necrosis factor receptor loss from the surface of human neutrophils. J Clin Invest. 1996;97(3):689-98. doi: 10.1172/JCI118466. PubMed PMID: 8609224; PubMed Central PMCID: PMC507105.

225. Lortholary O, Dromer F, Mathoulin-Pelissier S, Fitting C, Improvisi L, Cavaillon JM, Dupont B, French Cryptococcosis Study G. Immune mediators in cerebrospinal fluid during cryptococcosis are influenced by meningeal involvement and human immunodeficiency virus serostatus. The Journal of infectious diseases. 2001;183(2):294-302. doi: 10.1086/317937. PubMed PMID: 11110651.

226. Pastille E, Didovic S, Brauckmann D, Rani M, Agrawal H, Schade FU, Zhang Y, Flohe SB. Modulation of dendritic cell differentiation in the bone marrow mediates sustained immunosuppression after polymicrobial sepsis. J Immunol. 2011;186(2):977-86. doi: 10.4049/jimmunol.1001147. PubMed PMID: 21160046.

227. Garly ML, Martins CL, Bale C, Balde MA, Hedegaard KL, Gustafson P, Lisse IM, Whittle HC, Aaby P. BCG scar and positive tuberculin reaction associated with reduced child mortality in West Africa. A non-specific beneficial effect of BCG? Vaccine. 2003;21(21-22):2782-90. PubMed PMID: 12798618.

228. van 't Wout JW, Poell R, van Furth R. The role of BCG/PPD-activated macrophages in resistance against systemic candidiasis in mice. Scandinavian journal of immunology. 1992;36(5):713-9. PubMed PMID: 1439583.

229. Klose RJ, Kallin EM, Zhang Y. JmjC-domain-containing proteins and histone demethylation. Nature reviews Genetics. 2006;7(9):715-27. doi: 10.1038/nrg1945. PubMed PMID: 16983801.

230. Yokoyama A, Wang Z, Wysocka J, Sanyal M, Aufiero DJ, Kitabayashi I, Herr W, Cleary ML. Leukemia proto-oncoprotein MLL forms a SET1-like histone methyltransferase complex with menin to regulate Hox gene expression. Molecular and cellular biology. 2004;24(13):5639-49. doi: 10.1128/MCB.24.13.5639-5649.2004. PubMed PMID: 15199122; PubMed Central PMCID: PMC480881.

231. Karatas H, Townsend EC, Cao F, Chen Y, Bernard D, Liu L, Lei M, Dou Y, Wang S. High-affinity, small-molecule peptidomimetic inhibitors of MLL1/WDR5 protein-protein interaction. Journal of the American Chemical Society. 2013;135(2):669-82. doi: 10.1021/ja306028q. PubMed PMID: 23210835.

232. Wissmann G, Morilla R, Martin-Garrido I, Friaza V, Respaldiza N, Povedano J, Praena-Fernandez JM, Montes-Cano MA, Medrano FJ, Goldani LZ, de la Horra C, Varela JM, Calderon EJ. Pneumocystis jirovecii colonization in patients treated with infliximab. European journal of clinical investigation. 2011;41(3):343-8. doi: 10.1111/j.1365-2362.2010.02415.x. PubMed PMID: 21299548.

233. Wood KL, Hage CA, Knox KS, Kleiman MB, Sannuti A, Day RB, Wheat LJ, Twigg HL, 3rd. Histoplasmosis after treatment with anti-tumor necrosis factor-alpha therapy. American journal of respiratory and critical care medicine. 2003;167(9):1279-82. doi: 10.1164/rccm.200206-563OC. PubMed PMID: 12615627.

234. Clarke DL, Clifford RL, Jindarat S, Proud D, Pang L, Belvisi M, Knox AJ. TNFalpha and IFNgamma synergistically enhance transcriptional activation of CXCL10 in human airway smooth muscle cells via STAT-1, NF-kappaB, and the transcriptional coactivator CREB-binding protein. The Journal of biological chemistry. 2010;285(38):29101-10. doi: 10.1074/jbc.M109.0999952. PubMed PMID: 20833730; PubMed Central PMCID: PMC2937941.

235. Ohmori Y, Schreiber RD, Hamilton TA. Synergy between interferon-gamma and tumor necrosis factor-alpha in transcriptional activation is mediated by cooperation between signal transducer and activator of transcription 1 and nuclear factor kappaB. The Journal of biological chemistry. 1997;272(23):14899-907. PubMed PMID: 9169460.

236. Robinson CM, Hale PT, Carlin JM. NF-kappa B activation contributes to indoleamine dioxygenase transcriptional synergy induced by IFN-gamma and tumor necrosis factor-alpha. Cytokine. 2006;35(1-2):53-61. doi: 10.1016/j.cyto.2006.07.007. PubMed PMID: 16931033.

237. Schlitzer A, Sivakamasundari V, Chen J, Sumatoh HR, Schreuder J, Lum J, Malleret B, Zhang S, Larbi A, Zolezzi F, Renia L, Poidinger M, Naik S, Newell EW, Robson P, Ginhoux F. Identification of cDC1- and cDC2-committed DC progenitors reveals early lineage priming at the common DC progenitor stage in the bone marrow. Nat Immunol. 2015;16(7):718-28. doi: 10.1038/ni.3200. PubMed PMID: 26054720.

238. Li Y, Han J, Zhang Y, Cao F, Liu Z, Li S, Wu J, Hu C, Wang Y, Shuai J, Chen J, Cao L, Li D, Shi P, Tian C, Zhang J, Dou Y, Li G, Chen Y, Lei M. Structural basis for activity regulation of MLL family methyltransferases. Nature. 2016;530(7591):447-52. doi: 10.1038/nature16952. PubMed PMID: 26886794.

239. Brenner D, Blaser H, Mak TW. Regulation of tumour necrosis factor signalling: live or let die. Nat Rev Immunol. 2015;15(6):362-74. doi: 10.1038/nri3834. PubMed PMID: 26008591.

240. Feldmesser M, Kress Y, Novikoff P, Casadevall A. Cryptococcus neoformans is a facultative intracellular pathogen in murine pulmonary infection. Infect Immun. 2000;68(7):4225-37. PubMed PMID: 10858240; PubMed Central PMCID: PMC101732.

241. Chen GH, Osterholzer JJ, Choe MY, McDonald RA, Olszewski MA, Huffnagle GB, Toews GB. Dual roles of CD40 on microbial containment and the development of immunopathology in response to persistent fungal infection in the lung. Am J Pathol. 2010;177(5):2459-71. Epub 2010/09/25. doi: 10.2353/ajpath.2010.100141. PubMed PMID: 20864680; PubMed Central PMCID: PMC2966803.

242. Lindell DM, Moore TA, McDonald RA, Toews GB, Huffnagle GB. Generation of antifungal effector CD8+ T cells in the absence of CD4+ T cells

during Cryptococcus neoformans infection. J Immunol. 2005;174(12):7920-8. PubMed PMID: 15944298.

243. Lapierre LA, Fiers W, Pober JS. Three distinct classes of regulatory cytokines control endothelial cell MHC antigen expression. Interactions with immune gamma interferon differentiate the effects of tumor necrosis factor and lymphotoxin from those of leukocyte alpha and fibroblast beta interferons. J Exp Med. 1988;167(3):794-804. PubMed PMID: 2450953; PubMed Central PMCID: PMC2188900.

244. Johnson DR, Pober JS. Tumor necrosis factor and immune interferon synergistically increase transcription of HLA class I heavy- and light-chain genes in vascular endothelium. Proceedings of the National Academy of Sciences of the United States of America. 1990;87(13):5183-7. PubMed PMID: 2164225; PubMed Central PMCID: PMC54286.

245. Huang Y, Krein PM, Muruve DA, Winston BW. Complement factor B gene regulation: synergistic effects of TNF-alpha and IFN-gamma in macrophages. J Immunol. 2002;169(5):2627-35. PubMed PMID: 12193734.

246. Huang Y, Krein PM, Winston BW. Characterization of IFN-gamma regulation of the complement factor B gene in macrophages. European journal of immunology. 2001;31(12):3676-86. PubMed PMID: 11745388.

247. Qiao Y, Giannopoulou EG, Chan CH, Park SH, Gong S, Chen J, Hu X, Elemento O, Ivashkiv LB. Synergistic activation of inflammatory cytokine genes by interferon-gamma-induced chromatin remodeling and toll-like receptor signaling. Immunity. 2013;39(3):454-69. doi: 10.1016/j.immuni.2013.08.009. PubMed PMID: 24012417; PubMed Central PMCID: PMC3857147.

248. Delano MJ, Ward PA. Sepsis-induced immune dysfunction: can immune therapies reduce mortality? J Clin Invest. 2016;126(1):23-31. doi: 10.1172/JCI82224. PubMed PMID: 26727230; PubMed Central PMCID: PMC4701539.

249. Burgess SL, Buonomo E, Carey M, Cowardin C, Naylor C, Noor Z, Wills-Karp M, Petri WA, Jr. Bone marrow dendritic cells from mice with an altered microbiota provide interleukin 17A-dependent protection against Entamoeba histolytica colitis. mBio. 2014;5(6):e01817. doi: 10.1128/mBio.01817-14. PubMed PMID: 25370489; PubMed Central PMCID: PMC4222101.

250. Bernal CE, Zorro MM, Sierra J, Gilchrist K, Botero JH, Baena A, Ramirez-Pineda JR. Encephalitozoon intestinalis Inhibits Dendritic Cell Differentiation through an IL-6-Dependent Mechanism. Frontiers in cellular and infection microbiology. 2016;6:4. doi: 10.3389/fcimb.2016.00004. PubMed PMID: 26870700; PubMed Central PMCID: PMC4735406.

251. Olszewski MA, Huffnagle GB, McDonald RA, Lindell DM, Moore BB, Cook DN, Toews GB. The role of macrophage inflammatory protein-1 alpha/CCL3 in regulation of T cell-mediated immunity to Cryptococcus neoformans infection. J Immunol. 2000;165(11):6429-36. Epub 2000/11/22. PubMed PMID: 11086082.

252. Jain AV, Zhang Y, Fields WB, McNamara DA, Choe MY, Chen GH, Erb-Downward J, Osterholzer JJ, Toews GB, Huffnagle GB, Olszewski MA. Th2 but not Th1 immune bias results in altered lung functions in a murine model of pulmonary Cryptococcus neoformans infection. Infect Immun. 2009;77(12):5389-99. Epub 2009/09/16. doi: 10.1128/IAI.00809-09. PubMed PMID: 19752036; PubMed Central PMCID: PMC2786439.

253. Erickson T, Liu L, Gueyikian A, Zhu X, Gibbons J, Williamson PR. Multiple virulence factors of Cryptococcus neoformans are dependent on VPH1. Molecular microbiology. 2001;42(4):1121-31. PubMed PMID: 11737651.

254. Cox GM, Toffaletti DL, Perfect JR. Dominant selection system for use in Cryptococcus neoformans. Journal of medical and veterinary mycology : bi-monthly publication of the International Society for Human and Animal Mycology. 1996;34(6):385-91. PubMed PMID: 8971627.